044133 (SSP8)

RECLAIM

REsolving CLimAtic IMpacts on fish stocks

Specific Targeted Research Project on "Modernisation and sustainability of fisheries, including aquaculture-based production systems"

Start date of project: 1st of January 2007 Duration: 3 years

3.5 The relative roles of fishing (top-down) and climate-driven changes in productivity (bottom-up) on changes in the structure of the food web in the North sea

Due date of deliverable:	June 2009
Actual submission date:	July 2009

Mike Heath
(Partner 2, Marine Scotland, Marine Laboratory Aberdeen , UK)

John Steele
Woods Hole Oceanographic Institute, USA

Project co-funded by the European Commission within the Sixth Framework Programme (2002-2006)		
Dissemination Level		
PU	Public	
PP	Restricted to other programme participants (including the Commission Services)	
RE	Restricted to a group specified by the consortium (including the Commission Services)	
CO	Confidential, only for members of the consortium (including the Commission Services)	X

Summary

We developed an ecosystem model for the North Sea to simulate the flow of nutrient up the food web from dissolved inorganic matter to fisheries yield and production of birds and mammals, and the dependence for this flux on environmental conditions. The key environmental drivers were temperature, vertical mixing, advection by ocean inflow and the concentrations of dissolved inorganic and particulate organic nutrient in inflow waters, freshwater discharges and dissolved nutrient concentrations in iver waters, and atmospheric deposition of nutrients. We identified four distinght regimes of environmental conditions in the North Sea between 1960 and 2005, and analysed the changes in fisheries yield and the maximum sustainable yields that these have caused. Finally, we subjected the model to projected future environmental forcing based on climate change expected to occur by 2100 and analysed the changes in yield and ecosystem fluxes that these were likely to cause.

The four most important conclusions from the study are that:

- The North Sea is a net sink for dissolved inorganic nitrogen and a net exporter of particulate organic nitrogen.
- Fisheries for pelagic and demersal fish and benthic species cannot be considered as independent of each other. Food web interactions may cause production and landings of pelagic fish and shellfish to vary by up to 15% in a constant environment and with constant pelagic harvesting rates, solely as a result of varying demersal harvesting rates. Similarly, demersal production and landings may vary by up to 10% solely as a result of varying pelagic harvesting rates. Hence advice on maximum fisheries yield for pelagic fish, for example, can only be given in the context of a given level of abundance of demersal fish, and vice versa.
- Shifts in the nutrient supply to the ecosystem caused by combinations of environmental factors propagate up the food web to cause large changes in fish production and potential yield from fisheries. The difference between maximum and minimum fish production since 1960 has been a factor of 1.7, easily within the range of demersal fish annual landing rates which have been observed over the same period.
- The expected change in climate before 2100 is predicted to cause an increase in nutrient supply and primary production, but not necessarily similar increases in fish production.

Introduction

Scientific advice feeds into the fisheries management process in three main ways – a) estimates of the history and current state of fish stocks, b) forecasts of the short term future state of stocks under different exploitation scenarios given the current state, and c) strategic advice on the fishing effort and mortality rates likely to produce sustainable yields and ensure the long-term persistence of healthy stocks. In the past these types of advice have all been provided from single species population models which assume time-independent productivity, and natural (non-fishing related) mortality rates which are independent of multi-species interactions and changes in underlying primary production. It is well recognized that these assumptions are only approximations of reality and that some systematic variation is likely due to other harvestable components of the food web, but operational models for taking these into account have proved extremely problematic. Also, it has been argued that the failure to take account of these factors has probably not led to dramatic departures from the likely outcomes for individual species, based on analyses in which the uncertainty has been parameterized as variability in probabilistic Monte-Carlo type analyses. Nevertheless, it seems intrinsically unlikely that, for example, that the sum of maximum sustainable yields for all of the assessed species in the North Sea, as currently estimated, could be a sustainable objective at the system level. This was certainly the conclusion of a recent study on fisheries yield in the Eastern Bering Sea (Mueter and Megrey 2006). Such concerns becomes increasingly important as EU nations are required to demonstrate Good Environmental Status for marine waters under the Marine Strategy Framework Directive. There are likely to be important trade-offs between fishing sectors and other users of the marine environment, all of which need to be seen in the context of, and climate related fluctuations in, underlying primary production which must ultimately set a limit to the amount of biomass that can he sustainably harvested from the system (Perry and Schweigert 2008).

Delivering whole-ecosystem advice on, for example maximum sustainable fishery yields and the levels of exploitation producing such yields, is clearly exceptionally challenging. Models which resolve individual species and their predator-prey interactions sufficiently to be capable of simulating fishing yields are typically incompatible with simulation of primary and zooplankton production processes and their forcing by oceanographic variability, and vice versa. For example, ECOPATH (, Pauly et al. 2000, Pitcher and Cochrane 2002, Walters et al 1997) is essentially a mass balance budgeting system consisting of a network of 'top-down' formulated equations (i.e. the abundance, growth rate and measured diet of a species is used to calculate its requirement for food consumption) and hence intrinsically incapable of interpreting the 'bottom-up' consequences of fluctuations in primary production. The bottom-up formulated version ECOSIM (Pauly 1988, Walters et al. 2000) includes only sparse representation of nutrient-phytoplankton processes, but can at least in principle be used to simulate the effects of known changes in primary production on higher trophic levels at a spatially aggregated scale. Models incorporating sophisticated representations of physics-nutrient-phytoplankton processes rarely extend their trophic range beyond meso-zooplankton (Lenhart et al. 2004, Moll 1997, Radach and Moll 2006, Skogen et al. 1995). It is likely that the solution lies not in one single model, but a variety of models, differing in their extent of trophic focus and resolution, perhaps linked or nested in some way.

In this paper, we describe an ecosystem model which makes many difficult compromises on spatial and taxonomic resolution, in order to reflect the flux of material from inorganic nutrient through the food web to fisheries yield. The aim was to compare the effects of variations in fisheries exploitation rates on yields at a coarse functional group level, with the effects on yields of recent fluctuations in climatic forcing. Key to defining the structure of such a model was identification of the minimum set of processes at the lowest trophic levels which need to be represented in order that the model caricatures the essential production dynamics of the system. The enterprise is part of an effort working towards improving strategic advice on the fishing effort and mortality rates likely to produce sustainable yields and ensure the long-term persistence of healthy stocks.

Necessary detail in the representation of primary production

The literature abounds with descriptions of the complexity of processes affecting primary production in the sea and the diversity of functionality among algal taxa (e.g. Williams et al. 2002). Our task was to identify the minimum set of processes which captured the essential dynamics of availability of material to be passed up the food web. Our starting point was the synthesis of primary production in the nitrogen limited regions of the open ocean encapsulated in the 'f-ratio' concept (Dugdale and Goering 1967, Eppley and Peterson 1979, Garside and Garside 1993).

The water column in the open ocean may be several km deep, but there is sufficient light for photosynthesis in only a thin layer (50-100m) at the surface (down to 0.1-1% of the sea surface irradiance). We refer to this as the photic zone. Dissolved inorganic nitrogen that is present as nitrate in the photic zone at the end of the winter is converted into living, and then dead particulate form as a result of photosynthesis, grazing and predation. Dead particulate matter sinks out of the photic zone. The depletion of nitrate in the photic zone sets up a vertical concentration gradient and nitrate diffuses from the underlying waters into the photic zone, supporting additional particulate matter production and export to the deep ocean, until declining irradiance in the autumn curtails photosynthesis. During the winter, vertical mixing recharges the photic zone with nitrate from the underlying waters. If the annual cycle of nitrogen in the photic zone is stationary, then the annual integrated vertical mixing and diffusion flux of nitrate into the photic zone from deep water must equal the sinking flux of detritus to the deep ocean. We refer to the primary production equivalent to the annual vertical mixing and diffusion flux as annual new production (ANP). However, ANP does not equal total annual primary production (TAPP), because in the process of metabolizing the algal biomass equivalent to ANP, the grazer and predator community in the photic zone excretes ammonia, which is then directly available to support additional primary production, or indirectly through short-term nitrification of ammonia to nitrate. We refer to the annual component of TAPP supported by ammonia excreted by the heterotroph community as annual recycled production ARP, so that TAPP = ANP + ARP and the term ANP/TAPP as the annual f-ratio. Note that this is different from the instantaneous f-ratio which is measured by stable isotope ^{15}N incubation techniques:

$$f = NP/TPP = NO_3 \text{ uptake}/((NO_3 + NH_4) \text{ uptake})$$

The instantaneous *f*-ratio in the open ocean increases monotonically with the rate of TPP – the greater TPP the greater the fraction that is new production, providing the basis for "global" relations between the *f*-ratio, temperature and TPP (Goes et al. 2000, Laws et al, 2000) which have been used to create global inventories of carbon flux to the deep ocean. The annual f-ratio concept has been considered as a summary of the material available for supporting the food web, and hence is potentially useful in the context of this study (Richardson *et al*, 1998; Bisagni, 2003; Heath and Beare, 2008). However, the main fisheries interest in rates of primary production is in shelf seas rather than the open ocean, and there are a number of key differences between ocean and shelf nutrient cycles.

In the deep ocean, the majority of remineralisation and nitrification of the particulate matter sinking out of the photic zone contributes to the pool of deep ocean nitrate. But, since this pool is large compared to the annual export flux from the photic zone, the effective recycling rate of nutrient back to the surface waters has been assumed to be extremely slow (on the order of hundreds of years) and the space scales correspondingly large. Thus there is a clear disconnection between the very long term cycling of nutrient between the deep ocean and the photic zone, and short term dynamics of nutrient uptake by autotrophs and excretion of ammonia by heterotrophs.

In shallow shelf seas the photic zone may extend to the seabed and hence there is no separation in either space or time of the processes of nitrate uptake, and the mineralization and nitrification of organic nitrogen back to nitrate, such as exists in the ocean. Nitrate production, together with inputs from rivers, atmospheric deposition, anthropogenic discharges and horizontal mixing occur throughout the year in the photic zone. In addition, the process of denitrification which involves the microbial utilization of nitrate as a source of oxygen in anaerobic environments and the release of gaseous nitrogen to the atmosphere, is a potentally significant loss term in shallow waters (Law and Owens 1990, Lohse et al. 1996). In estuarine systems in particular, denitrification is a very significant term in the nitrogen budget (Brion et al. 2004). In the ocean, denitrification must be confined to deep waters where it cannot compete with phytoplankton for the available nitrate. The dynamics of nitrate concentration in the coastal water column will therefore be complicated, and reflect the balance between external inputs, competition between phytoplankton and nitrifying bacteria for the ammonia produced by remineralisation of dead organic matter, and between phytoplankton and denitrifying bacteria for nitrate (Kelly-Gerreyn et al. 2001). However, it is clear that as a first order approximation the depth integrated mass of DIN at the onset of the bloom (predominantly nitrate), effectively sets a limit to the net amount of material that can be transferred up the food web – the equivalent of ANP in the ocean situation (Falkowski et al. 1998, Horne et al. 1998). The availability of nitrate to the photic zone, the amount of recycling activity and nitrification, will all act to modify the extent to which this limitation on the food web flux is achieved in a given gear.

Our model of the food web was designed to represent the essence of the nitrogen cycle in the lower trophic levels, and its control by simple caricatures of the main physical processes in a 1-dimensional (vertical) water column box model. A fundamental assumption was that nitrogen is the primary limiting nutrient in the system. The focus of the study was on ecosystem dynamics in a horizontally averaged representation of the North Sea. Clearly, the North Sea is highly heterogeneous and

encompasses a wide range of hydrobiological conditions. Other models have attempted to represent the spatial heterogeneity of biological dynamics at scales of a few tens of km, by simulating biological processes on a grid of nodes linked by advection and diffusion rates calculated by hydrodynamic models (Radach and Lenhart 1995, Radach and Moll 2006, Radach and Patsch 2007). However, such systems are typically capable of representing in a fully dynamic way only the lower trophic components of the food web (detritus-nutrient-phytoplankton, occasionally a zooplankton component) which can be approximately represented as passively transported by water currents. Retaining spatial resolution becomes increasingly problematic as the model food web is extended to larger zooplankton, fish and higher trophic levels, because these components are certainly not passively transported throughout their life-cycle. Hunting activity, reproductive migrations and aggregation occur at spatial scales which are many times the grid resolution of such models. Unless the spatial behavior of these components can be reasonably represented, a pragmatic compromise is to dispense with spatial resolution (at least for the higher trophic levels) and concentrate on caricaturing the biological processes associated with the more complex demography of higher trophic levels.

An additional consideration for bulk biomass-based ecosystem model studies is the selection of appropriate parameters for the biological rate processes. Selection of parameters on the basis of laboratory scale experiments is rarely successful since the components of the model typically represent taxonomically diverse and variable functional groups of species, and the rate processes encapsulate sub-grid scale spatial and temporal variability in abundance and demography of the constituent species (e.g. Broekhuizen et al. 1995). Most often, parameter values are fixed more-or-less by expert judgment, or manually tuned to achieve a qualitative fit to observed time series. There is an additional constraint for highly resolved spatial models in that the computational demands of simulation runs can be high, so the time cost of conducting large numbers of runs (thousands) in order to quantitatively explore the parameter space becomes prohibitive.

In this study, we optimized the model to fit an extensive observational dataset. Biological parameters of the model for which there was more reliable evidence were fixed, and the values of the parameters for which there was only weak evidence and/or the model displayed high sensitivity were then iteratively optimized partially manually and partially using a simplex algorithm, to minimize an objective function defined by the deviations between simulated and measured values of a wide a range of model components. To make this possible, we dispensed completely with spatial resolution and represented our chosen sea area as a one-dimension (vertical) system. Since the model had no horizontal spatial resolution, each layer in the vertical represented the horizontally averaged conditions in the study sea area. The implicit assumption was that the region was well mixed horizontally, which could be a reasonable approximation for the higher trophic levels, and least reasonable for the lower trophic levels and nutrients.

Once an optimized parameter set had been achieved for a suite of driving data representative of the time period over which the measured values were collected, the model could then be reasonably used prognostically to examine the effects of varying the external forcing and harvesting rates of fish on the dynamics of the system.

Model description

The generic form of the model was a bulk-biomass box representation of detritus-nutrient-phytoplankton-zooplankton-predator dynamics with exchanges between the components described by a series of ordinary differential equations. There are many varieties of such models, at least for lower trophic levels, described in the literature (Soetaert and Herman 2008). The specific form of the model used here was designed to distinguish between production fluxes due to the uptake of annually regenerated nitrate-nitrogen, and those due to within-year recycled nitrogen, under different scenarios of vertical physics and external sources of nutrient and the transfer of nutrient up the food web. The currency of the model was molar nitrogen units. A full description of the model, which was programmed in R (R Development Core Team 2005) is given in Appendix 1, and a schematic summary in Fig. 1.

Non-living components and biogeochemical processes

In the non-living phase, the model resolved the dynamics of detritus, ammonia and nitrate. In the context of this model, detritus refers to both dissolved organic nitrogen and particulate dead organic nitrogen. Exchanges between these constituents as a result of bacterial activity were expressed by the mineralization of detritus to ammonia, nitrification of ammonia to nitrate, and denitrification of nitrate to nitrogen gas, with the latter being a sink term for nitrogen in the model.

Primary producers

Two classes of phytoplankton were represented. Mico-phytoplankton were assumed to utilize only ammonia, so their dynamics were linked to recycling of nutrients. Meso-phytoplankton (archetype: diatoms) utilized both nitrate and ammonia.

Secondary producers

Three classes of zooplankton were represented. Micro-zooplankton were assumed to feed only on micro-phytoplankton. Meso-zooplankton (archetype: copepods) fed on meso-phytoplankton and micro-zooplankton. Carnivorous zooplankton fed on meso-zooplankton.

The benthos was resolved into suspension feeders, deposit feeders (which included meibenthos) and carnivores. The suspension feeders removed suspended detritus and meso-phytoplankton from that part of the water column assigned for them to filter. The deposit feeders processed sediment detritus, and the carnivores fed on suspension and deposit feeders.

Fish and top predators

Fish were resolved into pelagic and demersal, and their demography represented by larvae and adults. Within a set interval of days each year, adult fish shed a percentage of their biomass per day which was transferred directly to larvae. Within a different

set interval of days each year, a percentage of the biomass of larvae per day recruited to the adults.

Fish larvae (of both pelagic and demersal fish) fed on meso-zooplankton, and were preyed upon by carnivorous zooplankton and the adults of pelagic and demersal fish. Adult pelagic fish fed on meso- and carnivorous zooplankton, and fish larvae. Adult demersal fish fed on carnivorous zooplankton, but not meso-zooplankton, all types of benthos and adult pelagic fish. Adult fish were potentially subject to harvesting by fishing, and fishing was the only predation process on demersal fish. For each fishery, a discarding rate was defined as the proportion of fish caught which were not retained for landing. Discards were transferred directly to the sediment detritus pool. Removals of landed fish represented a sink of material for the model.

The birds/mammals class was a demographically unstructured bulk predator group feeding on pelagic fish only.

Bio-geochemical rate processes

The rates of mineralization, nitrification and denitrification were defined by temperature dependent proportions of substrate consumed per day. Temperature dependency was represented by a Q_{10} function:

$$k = \exp\left(\frac{1}{10}(T - T_R).\log_e Q_{10} + \log_e k_{TR}\right)$$

where T_R was the reference temperature and k_{TR} was the value of k at the reference temperature.

Heterotrophic and detritivore uptake functions

An approximation to the Beddington-DeAngelis functional response was assumed for all predator-prey interactions (Huisman and de Boer 1997, Negi and Gakkhar 2007). Below a threshold of predator abundance, the consumption rate (proportion consumed per day) of each prey category was assumed to scale lineally with predator abundance. Hence, weight specific uptake rate of the predator increased lineally with prey abundance as per Lotka-Volterra dynamics (Morin 1999). Above the threshold of predator abundance, the proportion of prey consumed per day remained constant, i.e. weight-specific uptake rate of the predator decreased with predator abundance.

The Beddington-DeAngelis function form involves three parameters as follows:

$$Uptake/unit\ time = \frac{predator * prey * k1}{prey + k2 + k3 * predator}$$

The approximation to this used here, which has fewer parameters but similar properties, was as follows:

$$Uptake/unit\ time = prey * K1 * Min\left\{1.0\ ,\ \frac{predator}{K2}\right\}$$

The parameter K1 (d^{-1}) was assumed to be dependent on sea temperature according to a Q_{10} function for all predators except birds/mammals:

$$K1 = \exp\left(\frac{1}{10}(T - T_R).\log_e Q_{10} + \log_e K1_{TR}\right)$$

where T_R was the reference temperature and $K1_{TR}$ was the value of K1 at the reference temperature. The same value of Q_{10} (2.2) was assumed for all heterotrophic uptake processes. Temperatures were supplied as external driving data for the model. The parameter K2 in each uptake function as assumed to be temperature independent.

Autotrophic uptake functions

Primary production was represented by the light and concentration-dependent uptake rate of nutrients (nitrate and ammonia) by the phytoplankton classes, and restricted to the surface layer. Nutrient uptake kinetics were also assumed to follow the approximation to the Beddington-DeAngelis functional form, scaled by the depth mean daily irradiance in the surface layer, such that uptake was zero at zero irradiance and increasing lineally to a maximum rate at a saturating value of daily depth mean irradiance (L_{max}). Hence:

$$Nutrient\,uptake/unit\,time = Min\left\{1.0\,,\,\frac{L}{L_{\max}}\right\} * nutrient * K1 * Min\left\{1.0\,,\,\frac{phytoplankton}{K2}\right\}$$

As for the heterotrophic uptake processes, the parameter K1 of the autotrophic uptake process was assumed to be temperature dependent whilst K2 was temperature independent. The same value of Q_{10} (2.0) was assumed for all autotrophic uptake processes.

In this version of the model, we disregard the autotrophic fixation of atmospheric nitrogen by cyanobacteria. In some ecosystem, direct nitrogen fixation can be a significant input to the nitrogen budget but the available evidence suggest that this is probably not important in the North Sea (Lipshultz and Owens 1996).
.

Metabolism

Food ingested by heterotrophs was either assimilated and contributed to increase in predator biomass, or was passed to detritus and ammonia. The proportion assimilated was governed by a constant assimilation coefficient. Half of the non-assimilated food was assumed to be lost to detritus and half to ammonia. In addition to this feeding dependent ammonia excretion, heterotrophs excreted a proportion of their biomass per day as ammonia, as a caricature of basal metabolism. The proportion excreted per day was assumed to be temperature dependent with a Q_{10} of 2.4 for all categories of heterotrophs.

Vertical structure

The model had 2 water column layers interconnected by a vertical mixing exchange rate, and underpinned by a sediment layer (Fig.1). In the water column, every component except meso-zooplankton, carnivorous zooplankton, fish and fish larvae, and birds/mammals were resolved to layer. Meso-zooplankton, carnivorous zooplankton, benthos, fish and fish larvae, and birds/mammals were represented as depth integrated populations and hence not subject to vertical mixing.

Meso-zooplankton, though represented by a depth integrated population, distributed their feeding activity between the surface and deep layers in proportion to the vertical distribution of their prey (meso-phytoplankton and micro-zooplankton). Meso- and carnivorous zooplankton, pelagic fish and fish larvae excreted to the surface and deep layer ammonia pools in proportion to layer thicknesses, and defaecated detritus directly to the deep detritus pool. Demersal fish excreted and defaecated only to the deep ammonia and detritus pools. Birds/mammals excreted to the surface layer and defaecated detritus to the deep layer.

Seafloor diagenetic processes are dependent on the porosity (proportion water by volume) and the permeability of the sediment. The porosity depends on the texture, shape, and sorting of the particles in the sediment. Permeability, which is a measure of the ability of water to circulate through the sediment.

The sediment layer in the model was assumed to have a constant thickness and porosity. Pore-water masses of ammonia and nitrate, and the mass of detritus and benthos were resolved in the sediment layer. All classes of benthos were assumed to defaecate to the sediment. However, carnivorous and suspension feeding benthos were assumed to excrete ammonia direct to the deep water column layer, whilst deposit feeding benthos excreted to the sediment pore-water pool.

Dynamics of detritus

Detritus in the system took various forms. Suspended detritus in the surface and deep layers originated from the defaecation of micro-zooplankton and the death of micro-phytoplankton and meso-phytoplankton cells. Suspended detritus had a sinking rate expressed as a proportion per day transferring from the surface to deep layer, and from the deep layer to the sediment, and was also mixed vertically by vertical mixing. For settlement from the deep layer to the sediment the proportion per day was inversely related to the $\log_{10}$ transformed vertical mixing rate so that a smaller proportion settled to the sediment in more strongly mixed systems, as a caricature of the resuspension of sediment in regions of strong tidal flow. The faeces of meso-zooplankton, carnivores, and fish settled directly to the deep layer. Faeces of benthos were added to the sediment detritus and were never suspended.

Detritus in the water column was consumed by bacterial mineralization and converted to ammonia. In the deep layer, filter feeding benthos could feed on suspended detritus in a layer of a given thickness above the seabed. Detritus was assumed to be uniformly distributed through the deep layer, so only a fraction of the deep layer suspended detritus was available to the benthos.

Sediment detritus was consumed by deposit feeding benthos, and mineralised to ammonia. Ammonia produced in the seabed by mineralization, and nitrate produced by nitrification of ammonia, contributed to dissolved pools in the pore-water of a layer of sediment of constant thickness. Exchange of ammonia and nitrate between the sediment pore-waters and the deep water column layer was governed by a sediment-water diffusion coefficient acting on the difference in concentrations. Pore-water concentration were derived by assuming that the dissolved pool was uniformly distributed through the layer of sediment.

Horizontal advection

Horizontal advection was represented by a volume inflow to the surface and deep layer (parameterised as a proportion of layer volume inflowing per day). To conserve volume, a balancing outflow was assumed from each layer. All horizontal inflow to the surface layer was assumed to exit via the surface layer. However, a proportion (between 0 and 1) of the inflow to the deep layer was allowed to upwell vertically into the surface layer, augmenting the surface layer outflow. All components which were subject to vertical diffusion (nitrate, ammonia, suspended detritus, phytoplankton classes and micr-zooplankton) were also eligible to be advected vertically and horizontally. Ocean boundary concentrations (moles N/m^3) in inflows to the system were set as external values.

River inputs

Nutrient and detritus inputs from rivers were confined to the surface layer and represented by a volume inflow (proportion of surface layer volume per day) with given concentration of nutrient load (moles N/m^3). The volume input from rivers generated a corresponding outflow volume from the surface layer, which was added to that generated by horizontal advection.

Atmospheric input of nutrient

Deposition of nitrate and ammonia to the surface layer from the atmosphere was represented by an external driving dataset of fluxes ($moleN/m^2/d$)

Biological parameter optimization

The aim of the optimization process was to identify a parameter set which resulted in the simulated monthly averaged concentrations and biomasses, and annual fluxes of all the components for which target data existed, lying as close as possible to the median of the observed values and within given quantiles. The procedure for optimization was as follows:

- By means of a sensitivity analysis, identify a subset of the parameters to be subjected to optimization, the remainder being fixed on the basis of literature and expert judgment.
- Divide the parameters to be optimized into two groups – those focused on the lower half of the food web (detritus, nutrients, phytoplankton, micro- and meso-zooplankton), and those on the upper half (meso- and carnivorous zooplankton, fish and birds/mammals).

- Assemble target data sets documenting the seasonal dynamics of the concentrations and biomasses of model components, and the annual fluxes between components.
- Assemble driving data sets based on observations from a period of years equivalent to the target data.
- Set initial (default) values for all of the parameters to be optimized based on literature and expert judgment
- Optimize the lower trophic level parameter subset to the average monthly target data on nutrients, chlorophyll and zooplankton (type 1 target data), with the upper level parameters set to default values.
- Optimize the higher trophic level parameter subset to the average annual flux target data on zooplankton, fish and birds/mammals (type 2 target data), with the lower level parameters set to the optimized values.
- Optimize the entire parameter subset to the entire target data set, with initial values set to the outcome of the first and second stages of optimization.

The objective function for the optimization process was defined as the standardized deviation of simulated values from the target observations, integrated over all target observations. For the type 1 target data comprising *i* components of the model and *m* months, this was represented as:

$$T_1 = \sum_{i=1}^{i=I} \left(Q_i \left(\frac{\sum_{m=1}^{m=12} \left(\frac{\sqrt{(\mathrm{mod}\,el_{i,m} - t\arg et_{i,m})^2}}{\left(t\arg et_{i,m=1\,to\,12}\right)} \right)}{12} \right) \right)$$

For type 2 observations where the data were annual integrated values:

$$T_2 = \sum_{i=1}^{i=I} \left(Q_i \left(\frac{\sqrt{(\mathrm{mod}\,el_i - t\arg et_i)^2}}{t\arg et_i} \right) \right)$$

The term Q_i was an importance weighting which could be applied to load the objective function in favor of particular components of the model.

Model setup and driving data

Geographical setting and layer thicknesses

The model was configured to simulate the volume averaged responses of the biological constituents of the North Sea (ICES area IV; Fig. 2) to external environmental driving and fishing rates. However, the driving and where possible the target data sets were assembled separately at the scale of the sub-areas IVa, IVb and IVc. These loosely reflect the summer stratified, frontal and tidally well mixed

regions of the North Sea respectively, and in addition, correspond to significant spatial variations in river discharges of freshwater and nutrients. Seas surface area and volumetric data for each sub-area were derived from the ETOPO5 5 min gridded elevation dataset (National Geophysical Data Centre, www.ngdc.noaa.gov/mgg/global/global.htm), and the sub-area specific driving and target data combined with appropriate volumetric weighting to provide whole-North Sea data sets.

The surface layer of the model was set to a maximum depth of 30m, which is the approximate depth of the seasonal thermocline in the northern North Sea where the maximum seabed depth is deeper than 100m. However, the seabed depth in many parts of the North Sea is shallower than 30m, so to take account of this the mean thickness of the surface layer was derived as (volume shallower then 30m / sea surface area), which was 28m. Similarly, the mean thickness of the deep layer was estimated as 42m (volume below 30m / area at the 30m isobath).

Seabed sediment layer thickness, porosity and diffusion properties

The mass of nitrogen in sediment detritus and pore-water nutrients was assumed to be distributed over a layer of defined thickness to determine the concentration levels which define the uptake rates by benthic detritivores, and the gradients between pore waters and the overlying water column which generate diffusion fluxes into or out of the sediment. By reference to pore-water concentration profiles of nitrate and ammonia this layer thickness was set to 10cm (Law and Owens 1990). In principle, this says that we assume material deeper than 10cm in sediment cores to be buried and unavailable for exchange with the water column.

The porosity of marine sediments decreases with increasing mean grain size (Ruardij & Raaphorst, 1995). North Sea sediments range from soft impermeable muds in the deeper northern areas to highly permeable coarse sands and gravel in the south. Heath et. al. (2002) provide information on the mean porosity of the sediment classes mapped at a resolution of 1° x 1° in the Atlas of the Seas around the British Isles. By area weighting of these types, we estimated the mean porosity of the surficial sediments in the North Sea (0.45). Correspondingly, the mean coefficient of diffusivity for sediment water exchange was estimated to be approximately 10^{-8} $m^2.s^{-1}$, with an effective diffusion length scale (the thickness of the sediment layer over which the concentration gradient is established) of 1cm.

Sea surface irradiance

Sea surface daily irradiance (E m^{-2} d^{-1}) was represented by monthly average of a daily resolution sinusoidal function, varying between a seasonal maximum (day 180) and minimum (day 0 and 360). The seasonal maximum and minimum values were based on records of irradiance collected at Aberdeen (latitude 57º 15'N; Fig.3).

Vertical attenuation of surface irradiance

The vertical attenuation coefficient in the surface layer was parameterized from an external driving data set on the concentration of suspended particulate matter (SPM) in the water (Fig.3). Field observations indicate strong spatial and temporal variability

in SPM loads related particularly to freshwater fluxes from the land, tidal erosion and storm surges. Spatially and temporally resolved data on SMP at a nominal depth of 5m were obtained from an independent model of suspended matter (Puls and Sundermann, 1990; Pohlmann and Puls 1994; 1/5 latitude x 1/3 degree longitude spatial resolution, 5d temporal resolution for a climatological year), calibrated using archived observational data as described by Lenhart *et al*., 1997. The data were averaged by month and ICES sub-area (IVa, IVb and IVc).

A relationship between SMP ($mg.m^{-3}$) and vertical attenuation coefficient of irradiance was derived from a time series of measurements at a location of the east coast of Scotland (57N 2W, water depth 47m; Heath et al. 1999). Turbidity (Formazine Turbidity Units, FTU) and irradiance profiles were measured approximately weekly over a 2-year period (2007-2008) to establish a relationship between the attenuation coefficient and depth averaged turbidity over the upper 10m of the water column:

attenuation coefficient ($\log_e$) = 0.1775 +0.061(FTU); $r^2 = 0.646$, n = 140, $p<0.01$

To relate FTU to the SPM values derived from the suspended matter model, we extracted the modeled SPM in a region centered on the sampling site off the Scottish coast (56.9N – 57.1N, 2.2W – 1.9W), and compared the measured FTU with the SPM values for the corresponding day of the year:

ln(FTU) = -10.547 + 1.567(ln(SPM)); $r^2 = 0.358$, n = 162, $p<0.01$

We assumed that these calibration relationships between SPM, FTU and vertical light attenuation coefficient applied widely across the North Sea.

Vertical diffusivity and mixing length scale

Parameterising vertical diffusivity in vertical box models is a particular challenge. The parameterization must caricature a range of physical processes operating on a range of different time and length scales, including tidally induced turbulence, wind mixing and internal waves. These processes generate vertical exchanges between layers in the water column which we represent as a simple diffusive process in the model. Diffusive processes produce net fluxes of material only when there is a concentration gradient across the interface between neighboring compartments. In our box model, we assume that our compartments are well mixed, so we do not resolve the gradient, only the difference in mean concentration between compartments. Hence, in addition to supplying a diffusion coefficient to caricature the process, we must also assume a length scale over which the diffusion acts.

We obtained time series of vertical diffusivity coefficients for compartments of the North Sea used in the ERSEM model from Lenhart et al. 1995, Pohlmann 1996). We then applied these to the three ICES sub-area with appropriate area weighting, averaged over calendar months, and combined then to produce a horizontally averaged North Sea wide time series of vertical diffusivity (Fig.3). We assumed that the length scale for vertical diffusion varied between a value of 1.0(seabed depth) at

mean winter values of vertical diffusivity ($\log_e$ k = -1.8) and 0.4(seabed depth) at summer values in the northern stratified parts of the North Sea ($\log_e$ k = -3.5).

Temperature

Temperature measurements collected in the North Sea between 1960 and 2000 were obtained from the ICES Environmental Data Centre. The data were first averaged over the ICES sub-areas and depth layers by month and year. For each month, the median and quantiles of the annual values were then calculated. Sub-area medians and quantiles for each layer were then combined to derive North Sea wide values by volumetric weighted averaging (Fig.3).

Ocean boundary transport rates

The North Sea has four open boundaries to the North Atlantic and neighboring shelf area, through which water, dissolved and suspended material is imported and exported by currents (Orkney-Shetland Channel; Shetland-Norway; Entrance to the Skagerrak, and English Channel; Fig.3). Monthly averaged volumes of inflow and outflow to the upper (0 - 30m) and lower (30m – seabed) layers through each of these boundaries were provided for years in the period 1960-2005 from the NORWECOM ocean circulation model (courtesy of Morten Skogen, IMR Norway; Skogen et al 1997, Skogen and Soiland 1998). The median and quantiles of these data were calculated by month to produce an average seasonal cycle of inflow volume to each layer from the four boundaries. The total volume inflow to the North Sea was the sum of the inflows through the boundary sections.

Ocean boundary concentrations of advected components

The model components which were eligible to be advected in and out of each layer were the dissolved nutrients, detritus, phytoplankton and micro-zooplankton. To establish monthly mean boundary concentration data for the inflows along each boundary section, we collated measurements of nitrate, ammonia and chlorophyll from the ICES Environmental Data Centre. We defined surface spatial and depth compartments along each boundary (Fig.4), and averaged all the available measurements in the Data Centre from within each compartment by sampling month for the years 1960-1999.

Boundary concentrations of meso and micro-phytoplankton nitrogen and detritus were estimated by scaling from chlorophyll. Carbon:chlorophyll ($g.g^{-1}$) was assumed to be 40, along with molar Redfield nitrogen:carbon (16:106; Redfield et al. 1963). During January-June, 75% of the chlorophyll was assumed to be attributable to meso-phytoplankton and 25% to micro-phytoplankton, and vice-versa during July-December. As further approximations, micro-zooplankton biomass was assumed to be 10% of meso-phytoplankton, and deep suspended detritus to be 10-times the nitrogen mass of meso- and micro-phytoplankton combined. The surface boundary concentration of suspended detritus was assumed to be zero.

River discharge volumes and nutrient concentrations

Monthly averaged freshwater discharge rates (m^3 d^{-1}) and fluxes of nitrate and ammonia nitrogen (kg d^{-1}) through segments of coastline, each of approximately 75 km length, were assembled for the period 1960-2005 from the data synthesis of Heath (2007). Briefly, the synthesis method involved statistical interpolation of daily catchment discharges of freshwater derived for specific years (1985, 1987 and 1990) from river gauging data and terrain modeling, to monthly averages for all years in the series 1960-2005 using GAMs based on rainfall data, and the equivalent interpolation of river nutrient concentration monitoring data. Long-term monthly freshwater discharge rates and nutrient fluxes were estimated for the three ICES sub-areas separately by summing the relevant segments of coastline, and summed to provide the discharge rate for the whole North Sea (Fig.3). The flow-weighted concentration in all river discharges to the North Sea was then the monthly nutrient flux divided by the monthly freshwater volume (Fig.5).

Atmospheric deposition rates of nutrients

Simulated data on the yearly integrated atmospheric deposition of total oxidized nitrogen and reduced nitrogen (mg N m^{-2} y^{-1}) produced by the Co-operative Programme for Monitoring and Evaluation of the Long-range Transmission of Air pollutants in Europe (EMEP) Unified 50 x 50 km^2 grid model (revision 1.7; Simpson et al. 2003, Tarrasón 2003; www.emep.int/Model_data/yearly_data.html; accessed 11 Jan 2008) were averaged over the ICES sub areas and over the whole North Sea. The EMEP 50 x 50 km^2 grid model represents the current state-of-the-art with respect to synthesis of data on emissions (natural and anthropogenic) to the atmosphere, and simulation of the chemical transformation of compounds, aerial dispersal and deposition. EMEP model data were available for the years 1980, 1985, 1990, 1995 and 2000. For the purposes of our model, was assumed that the deposition rate was constant over the year (Fig.5).

Fish harvesting and discarding rates

The mortality rates of fish and benthos due to fishing was expressed in the model as a proportion of standing stock biomass removed per day. In the case of fisheries for benthic species, this expression is equivalent to the harvesting ratio used to describe the fishing on, for example North Sea *Nephrops* (annual landings/biomass; ~10%). However, for assessed fin-fish species exploitation rates are usually expressed as age-specific per-capita mortality rates, which are less easily related to biomass harvesting rates. For cod, a simulation based on typical von Bertalanffy growth rates, average weight at length, a Ricker stock-recruitment relationship fitted to historical data, and a typical exploitation pattern (distribution of fishing mortality across age classes), indicated that at equilibrium the annual catch for a mean annual fishing mortality rate of 1.0 on ages 3-6, was approximately 232% of the equilibrium spawning stock biomass (SSB). At a fishing mortality rate of 0.65 the annual catch was approximately equivalent to the SSB. The maximum sustainable yield from the stock was achieved at an annual fishing mortality rate of 0.55 (annual catch/SSB = 79%). Given that exploited species represent approximately 40% of the demersal fish biomass, we might expect daily biomass harvesting rates to be of the order of 1-5% of the total community biomass per day.

Discarding rates in the model represented several aspects of the fishing process. Under-size fish that escape through net meshes but are damaged and do not survive, spillage from nets during gear recovery, non-target species which are discarded from the catch, under-size fish of target species which are discarded at sea, were all implicitly included in the discard fraction term in the model. There are few data on which to base an estimate of this fraction at the functional group biomass level, but intuitively we expect the fraction to be higher for demersal fisheries than pelagic because manual selection of marketable species is more prevalent in demersal fisheries than pelagic.

Target data sets for fitting of the model

Data sets for model fitting were of two types. First, data from a combination of the ICES Environmental Data Centre and the Continuous Plankton Recorder (CPR) surveys, were assembled to produce average monthly values of nitrate, ammonia and chlorophyll concentrations in each layer, and meso-zooplankton and carnivorous zooplankton nitrogen biomass, for each of the ICES sub-areas and for the North Sea as a whole. Second, data from a recent analysis of the North Sea food web (Heath, 2005) were assembled to produce estimates of North Sea averaged annual production and fluxes between biological components of the model.

For the first data type, nutrient and chlorophyll observations collected between 1960 and 2000 were first averaged over the ICES sub-areas and depth layers by month and year. For each month, the median, 17^{th} and 83^{rd} quantiles (median, 5^{th} and 95^{th} for chlorophyll for which there was fewer data) of the annual values were then calculated. Sub-area medians and quantiles for each layer were then combined to derive North Sea wide values by volumetric weighted averaging. CPR zooplankton species numbers were converted to biomass and grouped into omnivorous and carnivorous zooplankton categories as described by Heath (2005) for each ICES sub-area, year and month. Then, each month the median, 5^{th} and 95^{rd} quantiles of the annual values were calculated. The second type of data (annual fluxes) were only available as North Sea wide values for the period 1973-2000. In this case, annual values were summarized by the median, 5^{th} and 95th quantiles.

Results

Parameter optimization

The parameters selected for optimization are listed in Table 1. Each stage of the optimization process aimed to produce reductions in the objective function describing the distance between the model results and the available observations, compared to the initial results obtained with the default parameters. It proved extremely difficult to achieve convergence of the simplex optimization algorithm for anything more than one or two of the most sensitive parameters. Hence the automatic process was used for initial range finding, and the final optimization was performed manually. The fits and for the final optimized model are shown in Fig. 6 and 7).

The fitting process was able to match surface dissolved inorganic nutrient concentrations to monthly mean target values more closely than deep concentrations (Table 2, Fig. 6). Meso-zooplankton concentrations were well also matched. However, almost all of the monthly concentration data were contained within the quantiles of target data (Fig. 6).

The fitting process was able to adequately match all of the available annual target data (objective function <0.35) except for the flux due to predation by fish on other fish (Table 3, Fig. 7). In this case the target data were considered uncertain due to the method of calculation and were down weighted in the overall fitting process.

Table 1. Main parameters subjected to optimization, in decreasing order of importance

Parameter	**Reason for selection**
$\mu_{DIN\text{-}mesophyt}$ and $h_{DIN\text{-}mesophyt}$	Dictate the uptake rate of nitrate in the system
$\mu_{DIN\text{-}micophyt}$ and $h_{DIN\text{-}microphyt}$	Dictate the uptake rate of ammonia in the system
$\mu_{mesophyt\text{-}mesozoo}$ and $h_{mesophyt\text{-}mesozoo}$	Dictate the transfer of nitrate driven primary production up the food web
$\mu_{microphyt\text{-}microzoo}$ and $h_{microphyt\text{-}microzoo}$	Dictate the transfer of ammonia driven primary production up the food web
Pelagic harvesting rate and discard rate	Dictate the top-down predation on meso-zooplankton
Demersal harvesting rate and discard rate	Dictate the top-down predation on benthos and pelagic fish
Harvesting rate and discard rate for suspension feeding and carnivorous benthos	Dictate the landings of shellfish

Table 2. Objective function values (scaled by a factor of 10) at the optimized values of parameters.

	Months												
Monthly averaged component	**1**	**2**	**3**	**4**	**5**	**6**	**7**	**8**	**9**	**10**	**11**	**12**	**An. avg**
Surface nitrate	4	1	4	0	1	0	2	2	1	1	1	6	2

$mM.m^{-3}$													
Deep nitrate $mM.m^{-3}$	3	6	6	7	2	5	5	8	4	2	1	2	4
Surface ammonia $mM.m^{-3}$	0	2	2	2	1	4	3	0	4	3	3	2	2
Deep ammonia $mM.m^{-3}$	14	11	8	6	7	11	11	13	10	14	11	16	11
Surface chlorophyll $mg.m^{-3}$	2	8	6	58	56	15	18	15	22	19	2	4	19
Meso-zoo. $mM.m^{-3}$	0	0	0	1	7	13	5	0	1	1	1	0	3
Carniv. zoo. $mM.m^{-3}$	6	11	11	13	15	28	31	3	16	2	9	3	12

Table 3. Simulated and target annual fluxes, and objective function values at the optimized values of parameters.

Annual flux	**Model $gC.m^{-2}.y^{-1}$**	**Target $gC.m^{-2}.y^{-1}$**	**Objective function value**
MMIP	46.98	50.42	0.068
Meso-zooplankton production	39.49	34.07	0.16
Carnivorous zooplankton production	3.55	3.53	0.0058
Pelagic fish production	3.32	3.65	0.092
Demersal fish production	1.66	1.44	0.15
Carnivorous benthos production	1.81	1.36	0.33
Consumption of fish by fish	0.71	2.41	
Consumption of zooplankton by fish	8.59	7.34	0.17
Consumption of meso-zooplankton by carnivorous zooplankton	10.09	11.75	0.14
Consumption of benthos by fish	3.73	2.91	0.28
Landings of pelagic fish	0.42	0.49	0.14
Landings of demersal fish	0.14	0.13	0.098
Landings of benthos	0.0079	0.0068	0.15

The full optimized set of parameter values is listed in Appendix 1 (Tables A1-A5).

Structure and function of the optimized model ecosystem

At the conclusion of a 15-year run with a repeating annual cycle of boundary and driving data, the stationary equilibrium total mass of nitrogen in the system varied during the year between 1135 and 974 $mMN.m^{-2}$. Under these conditions the annual import of nitrogen was 1385.8 $mMN.m^{-2}.y^{-1}$ (82% dissolved inorganic nutrient (DIN)

advected across the open boundaries, 8% particulate organic nitrogen (PON) advected across the open boundaries, 4% atmospheric deposition, and 6% river discharges) which was matched by an equal total export comprising 83% DIN, 13% PON, 2.0% nitrogen gas, and 2% fisheries catch. Hence, at the macro-scale the North Sea appeared to act as a net sink for DIN, and a net source of PON and nitrogen gas.

Equilibrium annual fluxes of material though the simulated food web are listed in Table 4. We summarized the primary production status of the system by 6 measures based on nitrogen fluxes, and their carbon flux equivalents calculated assuming Redfield equivalence between nitrogen and carbon (Table 5):

(1) NIP. The annual integral of the nitrate uptake rate by algae,
(2) PNP. Potential New Production, determined as the sum of the annual vertical flux of nitrate into the photic layer plus the net horizontal flux of nitrate through the photic zone (i.e. horizontal imports less exports). This should be equal to uptake of nitrate in the surface layer by algae and denitrifying bacteria, less the production of nitrate in the surface layer by nitrification of ammonia. This definition of PNP corresponds to that calculated by Bisagni (2003), except that Bisagni disregarded the horizontal flux term.
(3) MMP. Defined as the difference, on an annual basis, between the maximum and minimum values of nitrate concentrations integrated from surface to seabed (Heath and Beare, 2008).
(4) IP. Defined as the annual lateral rate of input of inorganic N (nitrite + ammonia) into the region from rivers, atmospheric deposition and exchange across the shelf edge. Calculated from river and deposition data, and estimates of advection across the shelf edge (Heath and Beare, 2008).
(5) MMIP. Sum of MMP plus that part of IP occurring between the julian dates of maximum and minimum integrated nitrate values (Heath and Beare, 2008)
(6) TAPP. The annually integrated sum of autotrophic uptake rates of nitrate plus ammonia.

Table 4. Equilibrium annual fluxes in nitrogen units and their carbon equivalents assuming Redfield relationship between carbon and nitrogen during the final year of a 6-year run of the model with the optimized parameter set.

	$mMN.m^{-2}.y^{-1}$	Carbon equivalent $gC.m^{-2}.y^{-1}$
Annual DIN advection inflow	1136.83	90.38
Annual DIN advection outflow	1159.12	110.17
Annual PON advection inflow	109.06	8.67
Annual PON advection outflow	189.81	15.09
Annual atmospheric DIN input	55.05	4.38
Annual river DIN input	84.83	6.74
Annual river PON input	0.00	0.00
April-Sept DIN advection inflow	402.55	32.00
April-Sept DIN advection outflow	403.68	32.09
April-Sept PON advection inflow	52.97	4.21
April-Sept PON advection outflow	148.26	11.79
April-Sept river DIN input	30.80	2.45
April-Sept atmospheric DIN input	27.68	2.20

Annual vertical nitrate flux	1182.29	93.99
Annual horizontal surface nitrate flux	73.85	5.87
Total system nitrogen on day 1 January ($mMN.m^{-2}$, C equivalent $gC.m^{-2}$)	1325.07	105.34
Total annual primary production	2013.68	160.09
MMP	533.60	42.42
PNP	1256.32	99.88
Annual nitrate uptake by algae	1338.89	106.44
MMIP	590.95	46.98
Annual fratio based on MMIP	0.29	0.29
Annual fratio based on nitrate uptake	0.66	0.66
Annual micro-phytoplankton production	216.23	17.19
Annual meso-phytoplankton production	1862.32	148.05
Annual micro-zooplankton production	22.33	1.77
Annual meso-zooplankton production	496.78	39.49
Annual carnivorous-zooplankton production	44.61	3.55
Annual suspension-feeding benthos production	95.38	7.58
Annual deposit-feeding benthos production	235.38	18.71
Annual carnivorous-feeding benthos production	22.80	1.81
Annual pelagic fish larvae production	18.98	1.51
Annual demersal fish larvae production	1.15	0.09
Annual pelagic fish production	22.72	1.81
Annual demersal fish production	19.71	1.57
Annual bird/mammal production	0.20	0.02
Total higher trophic level production	980.04	77.91
Higher trophic level production /MMIP	1.66	1.66
Higher trophic level production / total primary production	0.49	0.49
Annual pelagic fish landings	5.30	0.42
Annual demersal fish landings	1.80	0.14
Annual shellfish landings	0.099	0.008
Total landings / MMIP	0.012	0.012
Total catch / total primary production	0.0036	0.0036
Annual detritus mineralization in the water column	262.84	20.90
Annual detritus mineralization in the sediment	682.53	54.26
Annual nitrification in the water column	1201.29	95.50
Annual nitrification in the sediment	49.27	3.92
Annual denitrification in the water column	8.30	0.66
Annual denitrification in the sediment	21.35	1.70
Annual ammonia production in the water column	860.71	68.43
Annual sediment – water ammonia flux	1443.97	114.80
Annual nitrate production in the water column	1201.29	95.50
Annual sediment – water nitrate flux	27.92	2.22
Annual uptake of meso-zooplanton by carniviorous zooplankton	126.90	10.09
Annual uptake of pelagic fish larvae by carniviorous zooplankton	4.21	0.33
Annual uptake of demersal fish larvae by carniviorous zooplankton	0.098	0.008
Annual uptake of suspension-feeding benthos by	19.46	1.55

carniviorous benthos		
Annual uptake of detritus-feeding benthos by carniviorous benthos	47.59	3.78
Annual uptake of meso-zooplankton by pelagic fish larvae	55.82	4.44
Annual uptake of meso-zooplankton by demersal fish larvae	3.38	0.27
Annual uptake of meso-zooplankton by pelagic fish	48.85	3.88
Annual uptake of carnivorous-zooplankton by pelagic fish	11.58	0.92
Annual uptake of pelagic fish larvae by pelagic fish	6.10	0.48
Annual uptake of demersal fish larvae by pelagic fish	0.31	0.02
Annual uptake of carnivorous-zooplankton by demersal fish	8.52	0.68
Annual uptake of suspension-feeding benthos by demersal fish	11.88	0.94
Annual uptake of detritus-feeding benthos by demersal fish	31.34	2.49
Annual uptake of carnivorous-feeding benthos by demersal fish	3.70	0.29
Annual uptake of pelagic fish larvae by demersal fish	1.37	0.11
Annual uptake of demersal fish larvae by demersal fish	0.0060	0.0005
Annual uptake of pelagic fish by demersal fish	1.16	0.09
Annual uptake of pelagic fish by birds/mammals	0.59	0.05
Annual export from secondary producers	345.21	27.44
Annual egg production by pelagic fish	0.51	0.04
Annual recruitment to pelagic fish adults	1.54	0.12
Annual egg production by demersal fish	0.079	0.006
Annual recruitment to demersal fish adults	0.362	0.029

Table 5. Equilibrium values of measures of annual primary production

	$mMN.m^{-2}.y^{-1}$	$gC.m^{-2}.y^{-1}$
NIP	1338.89	106.44
PNP	1256.32	99.88
MMP	533.60	42.42
IP	1385.77	110.17
MMIP	590.95	46.98
TAPP	2013.68	160.09

The equilibrium total annual primary production (160.09 $gC.m^{-2}.y^{-1}$) was slightly higher than the value of 121 S.D. 12 $gC.m^{-2}.y^{-1}$ from fully spatially resolved simulations using the NORWECOM and ECOHAM1 models (Skogen and Moll, 2005), and both were much less than values predicted from analysis of remote sensing sea surface color data (~550 $gC.m^{-2}.y^{-1}$ Chassot et al. 2007). Based on the annual integrated uptake of nitrate by algae, the annual f-ratio was 0.66, and lower (0.29) if

based on MMIP. The total import of new nitrogen to the system (advection + atmospheric deposition + river discharge) did not equate to any of the new production measures.

With regard to recycling processes, 72% of detritus mineralization (945.4 $mMn.m^{-2}.y^{-1}$) took place in the sediment and 28% in the water column. A similar proportion of the annual production of ammonia (2304.7 $mMN.m^{-2}.y^{-1}$) occurred in the sediment (62% due to sediment-water flux, 38% due to ammonia production in the water column by bacterial and heterotrophic metabolism). In contrast, almost all (>96%) of annual nitrification (1250.6 $mMN.m^{-2}.y^{-1}$) occurred in the water column, and 4% in the sediment. This dominance of annual sediment-water nutrient fluxes by ammonia is borne out by experimental observations (Lohse et al. 1996, Law and Owens 1990). Denitrification (29.7 $mMn.m^{-2}.y^{-1}$) was concentrated in the sediment (72%). Total annual denitrification represented 20% annual river and atmospheric inputs, which is of similar magnitude to that estimated by other investigators (Law and Owens, 1990).

The harvesting and discarding rates required to fit the observed production and landing rates of pelagic and demersal fish were 0.030 d^{-1} (harvesting) with 0.70 discarding for pelagic fish, 0.054 d^{-1} (harvesting) and 0.88 (discarding) for demersal fish, and 0.0000083 d^{-1} (harvesting) with 0 discarding for benthic fisheries. Remembering that these rates refer to the entire community not just to the exploited species, a large difference between fin and benthos fisheries seems justifiable since the majority of benthic taxa are not subject to harvesting. However, whilst discarding rates for static gear benthos fisheries (eg. creels) are probably close to zero, it is clear that this is not the case in, for example in trawl fisheries for *Nephrops*. In addition, there is clear evidence of mortality inflicted on benthos by trawl fisheries for demersal fish which could be included in the discarding rate terms as defined for this model. However, the data on which to establish the annual production rates of deposit, suspension and carnivorous feeding benthos are poor or non-existent at the scale of the North Sea, so we considered it preferable to ignore discarding of benthos and establish a harvesting rate to fit the landings assuming no discarding.

Total annual higher trophic level production (all zooplankton, benthos, fish, and birds/mammals combined) amounted to 980.0 $mMN.m^{-2}.y^{-1}$ (equivalent to 77.9 $gC.m^{-2}.y^{-1}$), which represented 166% of MMIP, and 49% of TAPP. Total zooplankton production (miro-, meso- and carnovores combined) represented 29% of TAPP (563.7 $mMN.m^{-2}.y^{-1}$, 44.8 $gC.m^{-2}.y^{-1}$). Similarly, benthos production (suspension and deposit feeders and carnivores) represented 19% of TAPP, and total fish production (pelagic and demersal) 3.3% of TAPP. The fishery landings of pelagic, demersal and shellfish represented 0.35% of TAPP, in line with ratios derived by a variety of means from observational data (Chassot et al. 2007, Nixon 1988).

Simulated fisheries yield from the optimized model ecosystem with long-term average environmental driving data – interaction between sectors

Using the optimized parameter set, we ran sets of simulation to explore the consequences of varying pelagic, demersal and shellfish harvesting rates around the

fitted values. Holding two of the harvesting rates at the optimized value in turn, we varied the remaining rate between zero and approximately 3-times optimized value.

Varying pelagic and demersal harvesting rates between 0 and 20% of biomass per day produced characteristic responses in production and landings, in which production of the targeted group declined from a maximum value in the un-exploited situation to extinction as the harvesting rate was increased. Over the same range, landings varied from zero in the un-exploited situation, through a maximum and back to zero at the point where the resource became extinct. The maximum of the catch response is referred to as the maximum sustainable yield (MSY) from the functional group, and the harvesting rate at which this occurred, as F_{MSY} (Fig. 8a).

In addition to the above patterns, which were entirely consistent with responses in single species stock models, the ecosystem model predicted responses in other components of the system as a result of food web interactions. In the case where only pelagic harvesting rate was varied and other harvesting rates remained constant, the depletion and eventual extinction of pelagic fish in the system caused a response in demersal fish production and yield (Fig. 8a,b). In the early stages of pelagic fish depletion the primary mechanism for this response was an increase in predation on demersal fish larvae by carnivorous zooplankton which were stimulated by reduced predation from pelagic fish. In the later stages of pelagic fish depletion, demersal fish showed increasing production and catch. In this case the mechanism was the disappearance of predation on demersal larvae by pelagic fish. The simulated diet composition of demersal fish became more benthivorous and planktivorous (feeding on carnivorous zooplankton) as pelagic fish became depleted (Fig. 8c). Associated with the indirect stimulation and increased benthivory of demersal fish, production of benthos and catch in shellfish fisheries declined as a result of increased consumption of benthos by demersal fish.

In the case where only demersal harvesting rate was varied and other harvesting rates remained constant, carnivorous zooplankton production increased as demersal fish became depleted and then extinct (Fig. 9a,b). This resulted in an increase in predation on early life stages of pelagic fish and on mesozooplankton. As demersal fish became extinct, the contribution of carnivorous zooplankton to the diet of adult pelagic fish expanded to approximately 25%, having been <5% when demersal fish were only lightly exploited (Fig. 9c). Initial depletion of demersal fish had a detrimental effect on pelagic fish production and catch, changing to a positive impact as demersal fish became futher depleted and then extinct. In the early stages, the detrimental effect was due to increased predation on pelagic fish larvae by carnivorous zooplankton, and in the later stages due to the relaxation and then disappearance of predation on larvae and adults by demersal fish. Depletion and extinction of demersal fish had a positive impact on production of benthos and yield from shell-fisheries.

Optimised harvesting rates on benthos (shell-fisheries) were 4-orders of magnitude lower than on fin-fish. Hence, varying the harvesting rate between 0 and ~3-times the optimized value did not explore the same response range as for pelagic and demersal fish. Increasing selfish harvesting rates merely caused a linear increase in catch and landings which no significant food web impacts on other components of the system.

Effects of climate related changes in environmental regime state on simulated ecosystem function and fisheries yield

Variations in the physical and chemical environmental drivers of the model were expected to be due to the combined effects of climate fluctuations and human activity. Advection, temperature, vertical diffusion and freshwater discharge were presumed to be predominantly affected by climate, whilst the flow weighted concentrations of nutrient in freshwater discharges and atmospheric deposition were probably mainly affected by human activity. The relative contributions of climate and human activity to variability in ocean boundary concentrations of nutrients was less clear. At the northern boundary, climate factors are probably the predominant factor leading to variations in the origins of water entering the North Sea, and hence to variations in boundary nutrient concentrations. In contrast, inflows through the English Channel and Skagerrak presumably include significant loads of nutrient from anthropogenic discharges in the eastern Channel and Kattegat respectively.

We identified regimes of environmental driving conditions based on Principal Components Analysis (PCA) of the major climatic and anthropogenic drivers for which we had detailed data available. These were annual integrals of horizontal advection volume inputs, freshwater volume inputs, annual average temperature, and flow-weighted nitrate concentrations in freshwater. We did not have available any year-resolved data on vertical diffusion rates, irradiance or silt concentrations, these being the other physical, mainly climate related drivers in the model. Atmospheric inputs of DIN, which were presumably principally driven by anthropogenic factors rather than climatic, were available only at 5-yearly intervals from 1980 – 2000. Seawater nutrient and chlorophyll concentrations in the boundary regions were in principle available by year and month, but in reality the data were too sparse to resolve year-specific values of annual average concentrations.

Each data series was first normalized to the long-term (1960-2005) mean ($\left(x-\bar{x}\right)/\bar{x}$) and principal components (PC's) derived using the princop function in R. The first two PC's accounted for 92.4% of the variation (74.4 and 18% respectively). PC1 was highly correlated with the flow-weighted nitrate concentration in freshwater which increased from 1960 to the 1980's and then slowly declined towards the end of the series, whilst PC2 summarized the inflow volume, freshwater volume and temperature data.

The time series of PC2 scores indicated four relatively clear regimes (Fig. 10). During 1960-1975 the PC2 score fluctuated around zero (25% outside the range -0.1 to +0.1). Between 1976 and 1988, 85% of the PC2 scores were negative. Between 1989 and 1995, 83% of the PC2 scores were positive. Finally, from 1996 to the end of the series in 2005 the PC2 scores returned to fluctuating around zero (none outside the range -0.1 to +0.1). The inflow, freshwater and temperature conditions during each of these regimes, summarized by the mean annual deviations from the long-term average, are shown in Table 6. To characterize the four regime, the two extremes were 1976-1988 which was cold with high freshwater discharge and slightly below average inflow, compared with 1989-1995 which was warm with low freshwater discharge and high inflow. The difference between the earlier and later regimes was that 1960-1975 was cool with average freshwater discharge and slightly lower than average inflow, whilst

1996-2005 was warm with average freshwater discharge and average inflow. The regime-specific deviations were applied to the long-term median physical forcing data sets to produce regime-specific physical drivers for the model (Fig. 11).

Table 6. Mean values of annual deviations of environmental drivers over each of the regime periods

	1960-1975	1976-1988	1989-1995	1996-2005
Inflow volume	-0.037	-0.030	0.180	0.002
Freshwater volume	-0.016	0.061	-0.057	-0.014
Temperature	-0.018	-0.043	0.040	0.056

The mean flow weighted concentrations of nitrate and ammonia in river waters during these regime periods are shown in Table 7.

Regime average deviations in atmospheric inputs of oxidized and reduced nitrogen were derived by simply assigning each of the available years of data to a regime and averaging were appropriate. The deviation during 1960-1975 was assumed to be equal to that in 1976-1988.

Estimating regime average deviations in boundary nutrient and chlorophyll concentrations was problematic due to the sparse data. For each boundary zone and depth layer, the deviation from the long term average monthly median value was first calculated for each year and month where data were available. Deviations were then averaged (arithmetic mean) across months for each year, implicitly assuming that interannual effects were applicable equally to all months in a given year. Inspection of these results indicated that there were no discernible differences in annual average deviations between depth layers for a given boundary zone, so the layer-specific data for each zone were averaged. The most comprehensive data coverage was for nitrate, and in this case there was evidence that the time series for the two northern boundary zones (Orkney-Shetland and Shetland-Norway) were indistinguishable from each other, but different from the Skagerrak and English Channel boundary zones, which could also not be distinguished from each other (Fig. 12). Concentrations in the northern boundary zones would be expected to be driven more by climatic factors than anthrogenic inputs, and vice-versa for the more southerly zones. Hence, we averaged the annual deviations for the two northern boundaries, and for the two southern boundaries. No spatial differences in the annual time series of ammonia and chlorophyll deviations could be resolved, so a single time series of annual deviations was calculated for each parameter by averaging the available data across zones for each year. Even so, there were numerous gaps in the 1960-2005 time series which we filled by interpolation. The regime-averaged annual deviations of North Sea-wide boundary nutrient and chlorophyll concentrations are shown in Table 7, and these were applied to the long-term average monthly values to produce regime-specific annual cycles of boundary concentrations of the various components of the model (Fig. 13).

Table 7. Regime averaged deviations in river water nutrient concentrations and boundary nutrient and chlorophyll concentrations.

	1960-1975	1976-1988	1989-1995	1996-2005

Flow-weighted freshwater nitrate and ammonia concentrations	-0.276	0.192	0.179	0.067
Northern boundary nitrate concentration	0.019	0.095	0.092	0.031
Southern and eastern boundary nitrate concentration	-0.113	0.214	0.014	0.040
Boundary ammonia concentrations	1.292	0.510	0.238	-0.417
Boundary chlorophyll concentrations	-0.157	0.826	0.659	0.675

The first stage of analyzing the effects of environmental regimes on the equilibrium fluxes of material though the food web was to independently test the sensitivity to three aspects of regime state – the physical drivers, the anthropogenic nutrient drivers, and the boundary concentration drivers, whilst holding fishery harvesting rates constant (Table 8, sets 1-5).

Table 8. Specifications of model runs to analyse the effects of regime conditions on the North Sea food web.

Set	Fishery harvesting rates	Physical drivers (inflow, freshwater, temperature)	Boundary concentrations	Anthropogenic nutrient drivers (flow weighted river concentrations, atmospheric deposition)	Number of runs
1	Optimised values for each sector	Long-term median	Long-term median	Long-term median	1
2	Optimised values for each sector	Long-term median	Regime specific	Long-term median	4
3	Optimised values for each sector	Long-term median	Long-term median	Regime specific	4
4	Optimised values for each sector	Regime specific	Long-term median	Long-term median	4
5	Optimised values for each sector	Regime specific	Regime specific	Regime specific	4
6	Constant demersal rate, range of values for pelagic rate	Regime specific	Regime specific	Regime specific	40
7	Constant pelagic	Regime specific	Regime specific	Regime specific	40

	rate, range of values for demersal rate				

The results from the first three sets, in which there were no differences between runs in the physical drivers of the model, showed that the annual rate of nitrogen import (boundary inflow plus rivers and atmospheric deposition) dictated the levels of production throughout the model food web. Across all runs, production at every level in the food web was proportional to nitrogen import (Fig.14, 15). However, when regime-specific physical drivers were introduced (sets 4 and 5), the overall relationship between production and nitrogen input was no longer present, although the relationship between levels within the system was preserved. The key factor affecting the relationship between nitrogen import and production when physical factors were introduced was the flushing effect of advection. Although the high volume transport rates during the 1988-1995 regime generated a large influx of nitrogen, it also resulted in a large export flux of living and dead particulate nitrogen produced within the model which removed production from the system. Hence, with long-term median boundary and river concentrations and atmospheric deposition, the advection regime in 1988-1995 caused a 15% increase in nitrogen input, but a small (2%) decrease in total annual primary production. The results indicated that magnitude of temperature variation between the regimes had only a negligible impact on annual production, and certainly much less then the magnitude of variation in advection.

The second stage of the analysis was to run the model with regime-specific physical driving data, boundary and river water concentrations of nutrients, and atmospheric inputs, but with varying rates of fish harvesting. Two sets of runs were performed – one with the harvesting rate of demersal fish fixed at the optimized rate and a range of harvesting rates for pelagic fish, and another with the pelagic harvesting rate fixed and a range of demersal harvesting rates (Table 8, sets 6 and 7).

The large variations in production at all levels of the food web induced by the different environmental regime conditions resulted in equivalent changes in the maximum sustainable yield from both pelagic and demersal fisheries, and also changes in the harvesting rate at which maximum yield might be achieved (F_{MSY}). Maximum sustainable yield of pelagic fish, assuming long-term average demersal harvesting rates, was during the 1976-1988 regime and was 1.4-times higher than the maximum yield during 1996-2005 (Fig. 16a,b, 17a,b).

Comparing the equilibrium biomass and production results for each regime to observational data on production and yield collected during the equivalent periods was problematic because the regime-specific fish harvesting rates were unknown. We therefore ran the model for each regime and fitted the pelagic and demersal fish annual production rates as closely as possible to the regime averaged observations, by adjusting only the harvesting rates. The measured and fitted production rates, the harvesting rates required to achieve these values, and the consequent modeled landings compared to observed landings, are shown in Fig. 18. The results imply that pelagic fish have been exploited at around their maximum sustainable rate since 1960,

except during the 1976-1988 regime when harvesting rates were above F_{MSY}. In contrast, demersal fish appear to have been consistently exploited at rates significantly higher than F_{MSY} since 1960, resulting in lower production and landings than could have been achieved given the underlying rate of production in the system. The model performed particularly well at explaining the declining landings of demersal fish which were due to a combination of over exploitation and declining ecosystem production.

We did not attempt to fit regime specific harvesting rates for shellfish since reliable time series of benthos production were not available. We did however compare the equilibrium production of carnivorous benthos for each regime obtained with the fitted demersal and pelagic harvesting rates and the long-term average benthos harvesting, with the tentative estimate of benthic carnivore production derived from CPR data by Heath (2005) (Fig.18). The model and CPR-derived estimates were at least around the same level, although the trends were different. Similarly, the regime specific landings from the model (assuming constant long-term average harvesting rates) were at an equivalent level to the observational data but did not replicate the differences between regimes.

After fitting of fish harvesting rates for each regime period, regime specific nutrient and plankton concentrations were compared with regime averaged observations. Monthly averaged simulated surface and deep nitrate and ammonia concentrations were within the 17th and 83rd quantiles of monthly averaged concentrations during 1960-2000 derived from the observational dataset (Fig. 19). Similarly, monthly averaged chlorophyll derived from the simulated biomasses of micri- and meso-phytoplankton were within the 5th and 95th quantiles of observations.

Meso- and carnivorous zooplankton biomasses in the regime-specific equilibrium model results were compared with measured North Sea estimates of meso-zooplankton and carnivorous zooplankton averaged temporally over each of the regime periods. The measured estimates were derived from CPR data according to Heath (2005). Monthly averaged values for each regime were within the 5th and 95th quantiles of the monthly observations between 1960 and 2000 (Fig. 20). Regime specific annual averaged simulated values showed similar trends to annual averaged CPR data, though the levels were slightly different (Fig. 21)

Ecosystem response to expected climate change

Drinkwater et al. (2009; RECLAIM deliverable 4.1) reported on scenario studies with different hydrodynamic models to assess the marine consequences of changes in air temperature (+3ºC), sort-wave radiation (+20%), and wind stress (+30%) consistent with IPCC regional predictions of the consequences of greenhouse gas emissions. The models predicted rises in sea surface and sub-surface temperatures in the North Sea of between 1 and 2ºC compared to the period 2002-2004, and a reduction in the spatial extent of stratified water in summer of 5-10%. Regarding advection, the NORWECOM model, from which the advection data were taken to develop driving data for this study, predicted an increase of 0.2 Sv across the northern boundary of the North Sea and an equivalent amount from the Skagerrak, but not clear change in inflow through the English Channel.

To assess the consequences of these predicted climate related changes in driving data for the food web fluxes in our model, we carried our runs with 1996-2005 regime conditions (boundary concentrations and fitted fish harvesting rates), with a) temperature deviation of +0.157 (equivalent to an annual average increase of 1.5ºC relative to 1996-2005), b) inflow volume deviations of +0.2024 for the surface and deep layers (equivalent to the predicted changes in inflow), c) increased vertical diffusion coefficient (+25%) during the summer months (May-September), and d) combined deviations in temperature, inflow and vertical diffusion (Fig. 22). Either the rise in temperature or increase in vertical diffusion alone produced a 7% increase in annual primary production, whilst the increase in inflow produced only a 0.6% increase. The combined changes in physical drivers produced a 10% increase in total primary production compared to the 1996-2005 regime (Fig. 23a,b).

The effects of the combined changes in physical drivers varied across the food web, so that the increase in pelagic fish production was 22% and 65% in demersal fish, whilst carnivorous zooplankton production, pelagic fish recruitment and shellfishery landings changed by +2%, -9% and -5% respectively (Fig. 23a,b).

Discussion

The four most important conclusions from this study are that:

- The North Sea is a net sink for dissolved inorganic nitrogen and a net exporter of particulate organic nitrogen.
- Fisheries for pelagic and demersal fish and benthic species cannot be considered as independent of each other. Food web interactions may cause production and landings of pelagic fish and shellfish as functional groups to vary by up to 15% in a constant environment and with constant pelagic harvesting rates, solely as a result of varying demersal harvesting rates. Similarly, demersal production and landings may vary by up to 10% solely as a result of varying pelagic harvesting rates. Hence advice on maximum fisheries yield for pelagic fish, for example, can onky be given in the context of a given level of abundance of demersal fish, and vice versa.
- Shifts in the nutrient supply to the ecosystem caused by combinations of environmental factors propagate up the food web to cause large changes in fish production and potential yield from fisheries. The difference between maximum and minimum fish production since 1960 has been a factor of 1.7, easily within the range of demersal fish annual landing rates which have been observed over the same period.
- The expected change in climate before 2100 is predicted to cause an increase in nutrient supply and primary production, but not necessarily similar increases in fish production.

Nutrient budgets

Our model suggests that the North Sea is a net sink for dissolved inorganic nitrogen and a net source of particulate organic nitrogen to the ocean. Previous studies have been inconclusive on whether the North Sea is a net source or sink for total nitrogen, and on the magnitudes of the gross fluxes. Brion et al. (2004) carried out a budget estimate, but the calculations were crude compared to our model results. We estimate approximately 2-times the advective import of total nitrogen compared to Brion et al., 30% of their atmospheric deposition, and around 10% of their estimated denitrification (Table 9).

Table 9. Import and export fluxes as estimated by Brion et al. (2004) compared to our model results).

		Brion et al. 2004 (Fluxes during 1976-1995)	Our model simulations using monthly resolved data and 1960-2005 median boundary and transport data
Total N imports $kt.y^{-1}$		8576	10816
	Advection inflow	6190	9724
	Rivers/estuaries	805	663
	Direct discharges	70	-
	Nitrogen fixation	0.000125	-
	Atmospheric	1631	429

	deposition		
Total N exports $kt.y^{-1}$		8576	10816
	Advection outflow	6476	10537
	Denitrification	2080	226
	Burial	20	-
	Fishing	-	53

Regarding the inflow estimates, closer examination of the calculations presented by Brion et al. shows that their results were based on annual average concentrations of total nitrogen throughout the water column at the northern boundary of the North Sea, the Skagerrak and the English Channel, which were higher than the average of our monthly resolved data (Brion et al., northern 13.0 $mMN.m^{-3}$, Skagerrak 11.7 $mMN.m^{-3}$, 8.9 $mMN.m^{-3}$; our data, northern 7.0 $mMN.m^{-3}$, Skagerrak 6.2 $mMN.m^{-3}$, 6.1 $mMN.m^{-3}$) but their estimates of annual volume flux were lower. Across the northern boundary the values are relatively similar (Brion et al., 1.035 Sv averaged over 1976-1995; our study 1.537 Sv). However, across the Skagerrak boundary Brion et al. state that there is only an outflow from the North Sea of 0.054 Sv, whilst our analysis of the NORWECOM data shows an inflow of 0.823 Sv. At the English Channel boundary the two studies are more in agreement (Brion et al. 0.042 Sv, our study 0.076 Sv). It is difficult to understand the basis for Brion et al.'s assumption that there is only an outflow from the North Sea across the Skagerrak boundary since this cannot be the case simply on mass balance grounds. In our study, we obtained separately the integrated inflows and outflows along each of the boundary sections from the NORWECOM model. Summed over the North Sea, we would expect the sum of all ocean inflows plus river inputs (and rainfall if this were included in the NORWECOM model) to equal the sum of all outflows. Perhaps Brion et al. mistakenly used the net transport across the Skagerrak boundary (inflow + outflow), rather than just the inflow to the North Sea to calculate the nitrogen flux.

Regarding atmospheric deposition, Brion et al. relied on a combination of wet deposition monitoring data from OSPARCOM (1998b), and relatively crude estimates of dry deposition from van Boxtel et al. (1991). We used the more recent (2003) estimates of combined wet and dry deposition from the Co-operative Programme for Monitoring and Evaluation of the Long-range Transmission of Air pollutants in Europe (EMEP) which should be more reliable. In addition, Brion et al. assumed a larger sea surface area then us (700,000 km^2, compared to our 557,428 km^2). More serious, is the discrepancy in denitrification estimates. Brion et al. cite field studies suggesting annual denitrification rates ranging from 3 - 255 $mMN.m^{-2}.y^{-1}$, and opt for a value of 201 ± 64 $mMN.m^{-2}.y^{-1}$. In contrast, our simulation results are based primarily on an assumed rate of conversion of sediment pore water nitrate to nitrogen gas of 20% of nitrate per day at the reference temperature of 10ºC. This rate coefficient was based mainly on porosity estimates and the denitrification rates and sediment pore water nitrate concentrations measured in a range of North Sea sites by Law and Owens (1990). The simulated pore water nitrate concentrations during the year were consistent with field measurements, as were the simulated estimates of total sediment nitrogen, and the simulated annual denitrification flux (29 $mMN.m^{-2}.y^{-1}$) was similar to the experimental estimates obtained by Van Raaphorst et al. (1990, 1992). However, the discrepancy between this and the choice of annual flux chosen

by Brion et al. (2004) remains unresolved and it seems that there is a great deal of uncertainty as to annual denitrification rates in the North Sea.

Overall, our simulations suggested that the North Sea was a net exporter of nitrogen across the northern boundary to the Atlantic of around 813 $kt.y^{-1}$, compared to Brion et al.'s estimate of 406 $kt.y^{-1}$. For comparison, Radach and Lenhart (1995) estimated a net export of 710 $kt.y^{-1}$ from a spatial simulation model, whilst Hydes et al. (1999) estimated the North Sea to be a net sink of 1990 $kt.y^{-1}$. Brion et al. (2004) did not resolve the proportions of DIN and PON in advection inputs and outputs from the North Sea. Our simulations indicate that 91% of the advected input is DIN, compared to 86% of the output, suggesting that the system is a net converter of DIN to PON.

Structure of the simulated ecosystem

The major flows of nutrient through the model food web were fitted to the assembled target data set, so clearly the model results conformed with our understanding of production at various strophic levels of the system. Of more interest and diagnostic value were the emergent fluxes for which there were little or no established measurements. For example, the difference between the MMIP measure of new production and the annual uptake of nitrate, relative to total annual primary production (long-term average optimized run: MMIP/TAPP = 0.30, Total NO_3 uptake/TAPP = 0.67) indicates the extent of within-year recycling activity in the system. In the open ocean we would expect these two ratios to be more similar since a high proportion of organic production is exported permanently from the photic zone to the deep ocean. The model clearly indicates that this is not the case in the shallow North Sea and that the over-turn of organic matter is much more rapid. Related to this, the simulation results implied that the majority of nutrient flux between the sediment and overlying water column was in the form of ammonia, not as nitrate, and that the bulk of nitrification occurred in the water column (Ward 2005, Yool et al 2007). Denitrification, which is concentrated in the sediment, effectively consumed the products of nitrification in the sediment.

The model systematically underestimated the available estimates of fish consumption by other fish, and no combination of parameters could be found that would resolve the difference whilst maintaining consistency with the other observational target data. There is clearly a need to reconsider the estimates of piscivory in the food web (Heath, 2005), which were based on stomach contents data for a subset of species, and extrapolated to the whole demersal community. The overall diet composition of demersal fish in the model contained <20% other fish, which seems small but may well be reasonable bearing in mind that the functional group includes all truly benthivourous fish, such as flatfish, as well as the more piscivorous species such as cod. However, even cod do not develop piscivory until around age 1, so on a population biomass basis the extent of piscivory may be less than appears to be the case on a per capita basis.

In addition to fishing, the top-level of the model food web was represented by a predation term representing seabirds and marine mammals. However, unlike fishing which was a sink for nutrient i.e. there was no closed return of nutrient to the ecosystem from the fish that were landed, the predation by birds and mammals was

returned to the system as detritus and ammonia. The magnitude of predation by birds and mammals in the North Sea is somewhat uncertain since population census estimates are difficult to obtain and the diets of some species are uncertain. Bryant and Doyle (1992) reviewed the available data and derived maximum and minimum likely estimates of the consumption rate of fish which, for birds and mammals combined were in the range 0.082 – 0.122 $gC.m^{-2}.y^{-1}$. For comparison, our long-term averaged optimized model results with initial 'expert opinion' values for the various uptake parameters indicated an annual consumption of 0.045 $gC.m^{-2}.y^{-1}$. We made no attempt to fit this flux to the Bryant and Doyle estimates by parameter adjustment since the impact of such adjustments on the rest o fthe model ecosystem would have been negligible.

It proved impossible to simultaneously fit both the measured landing rates of demersal and pelagic fish and the estimates of fish production (Heath, 2005) solely through the application of biomass harvesting rates in the model. To achieve convergence it was necessary to assume a discarding rate applied to the catch, with discarded material being consigned to sediment detritus. The fitted discarding rates were surprisingly high (70% for pelagic fish, 88% for demersal fish). For comparison, Mackinson and Daskalov (2007) estimated that 20% of catch is discarded, based on North Sea observer data. However, the discarding rate term in the model cover the difference between the biomass of fish which is killed by the fishing process and that which is landed officially at the quayside, including the mortality inflicted on fish which escape or are ejected through the meshes of fishing nets, loss from nets during gear handling, rejection of non-commercial species and under-size commercial species, slippage of over-quota catch, gutting at sea, and high-grading (discarding of legal-sized but low value fish), the fitted discard rates are perhaps not so unfeasible as they may seem. Unfortunately, there are few data with which to attempt corroboration the whole process. Observer data collection aboard commercial fishing vessels, such as used by Mackinson and Daskalov (2007) have largely been focused on estimating the discard rates of commercial target species which are successfully brought aboard, to support the existing single-species assessment effort, and not on answering more ecological questions about the extent of mortality inflicted on the community as a whole by the whole fishing process.

Food web interactions

The original premise for the study was that predator-prey relationships in the food web must lead to trade-offs between pelagic, demersal and benthos fisheries, since the maximum production of higher trophic levels is ultimately dictated by primary production. Ultimately, we aim to address the question of whether the sum of North Sea species-specific maximum sustainable yields (MSY's) assessed on a species by species basis, could be accommodated within the maximum sustainable fisheries yield from the ecosystem, the latter being ultimately set by primary production. The same question has been asked for the eastern Bering Sea, and the conclusion was that the ecosystem could not support the sum of all the maximum yields predicted by single-species assessments (Mueter and Megrey 2006). Our work has shown that even for a fixed level of primary production, food web interactions are such that MSY for pelagic fish is only meaningful in the context of a given abundance of demersal fish, and vice versa. Since demersal fish have apparently been consistently exploited at

harvesting rates well above F_{MSY} since 1960, all of the historical data on which single species MSY's might be based come from the system in a condition of depleted demersal fish abundance. We conclude that single species estimates of, for example herring MSY based on historical data can never be compatible with a state in which the major demersal species such as cod and whiting are also being harvested at their respective F_{MSY} values.

To determine how the trade-offs between pelagic, demersal and shellfisheries might work, it was necessary to account for the supply of material from lower levels in the food web to fish, and the interactions between fish groups. The demography of fish means that the predator-prey relationships are complicated since, for example, pelagic fish are on the one hand potential predators on the eggs and larvae of demersal fish (e.g. herring consume cod eggs), and on the other hand prey for adult demersal fish. Similarly, carnivorous zooplankton prey on fish eggs and larvae, but are food for adult fish. The conclusion of the experiments conducted to analyses these aspects of the model were that carnivorous zooplankton and benthos are an integral part of the trade-off between pelagic and demersal fisheries. Harvesting of either pelagic or demersal fish, but especially demersal fish, leads to increased production of carnivorous zooplankton due to the reduced predation, and in turn to increased predation on fish eggs and larvae. Key signatures of these food web interactions were the recruitment responses of pelagic fish under different scenarios of demersal harvesting, and vice versa, the recruitment response of demersal fish under different scenarios of pelagic harvesting. In the former case, pelagic fish recruitment was suppressed as a result of depleting demersal fish abundance by harvesting, the mechanism being increased predation on pelagic larvae by carnivorous zooplankton which were in turn released from predation by demersal fish. Conversely, demersal fish recruitment was more than doubled as a result of depleting pelagic fish by high harvesting rates. The mechanism in this case was relaxation of predation on demersal fish eggs and larvae by adult pelagic fish. There is evidence of the latter recruitment response signature in North Sea cod. Heath et al. (2008; Fig.8 therein) derived a time-series of residuals of cod recruitment from a Ricker stock-recruitment relationship incorporating a temperature term, fitted to the past records of cod spawning biomass, recruitment and North Sea temperature. A loess smoother through the residuals showed a strong inverse relation to the total stock biomass of herring (r^2 0.51, n = 41), tending to support the interpretation of demersal fish recruitment responses seen in the ecosystem model.

The food web interactions between fish and carnivorous zooplankton also cascaded down the food web through increased predation on mesozooplankton by carnivores and reduced predation on phytoplankton by mesozooplankton. The impact on benthos of changing fish harvesting rates was less complicated, since in this model benthic groups were not predators on fish life stages. Reducing the production of demersal fish led to straightforward increases in benthic production due to the relaxation of predation.

Effect of physical regime shifts on ecosystem production

Numerous authors have presented evidence of several more-or-less abrupt changes in the ecological the state of the North Sea since 1960 (e.g. Reid et al. 2001a, Weijerman

et al. 2005). Evidence of regime changes having taken place are most notable from the Continuous Plankton Recorder (CPR) data which indicate step-changes in zooplankton community composition and abundance on a number of occasions. Convergent results have also been obtained from analyses of time series data on a range of other taxonomic and functional groups, all suggesting that something happened during the 1976-1979, 1988-1989, and less clearly during 1997-1999 to cause step-changes in the organization of the biological system. There have been several attempts at relating these step-changes to oceanographic variables as possible explanatory driving factors, with evidence for the role of warming sea temperatures and inflow from the North Atlantic (Beaugrand 2004, Beaugrand et al. 2008, Edwards et al. 1999, Holliday and Reid 2001, Reid et al. 2001b).

Our principal components analysis of time series of physical drivers in the North Sea was extremely convergent with the published evidence of step change in the biological composition. We were able to identify four regimes based on advective inflow, temperature and freshwater discharge from river catchments to the North Sea, and the start and end points these regimes coincided with the biological step-changes reported in the literature (1975-76, 1988-89, and 1995-1996). However, there were several important physical drivers of the model for which we were unable to obtain time series data, in particular the vertical diffusion coefficient and length scale, and sea surface irradiance. In addition, the results clearly show that the model was sensitive to the concentrations of nutrients and PON at the inflow boundaries, as well as the volume transport rates. Unfortunately, the observational data are largely inadequate for resolving annual variability in boundary concentrations. We were able to use the data to estimate deviations in boundary concentrations during each of the regimes, but the data were not adequate for use in the process of identifying the regime periods.

Given constant advective conditions, the model clearly showed that changes in nitrogen input generated by the combination of boundary concentrations, river discharge and atmospheric deposition, translate proportionally into changes in primary production which propagate up the food web to fish. However, the introduction of variability in advection changes this dramatically. Given constant boundary concentrations, increased advection increases the import of nutrient, but also increases the export of detritus and living particulate matter. Hence, advection depresses the ratio of annual primary production to annual nitrogen import and has a detrimental effect on the flux of nutrient from DIN to fish. Thus, we found very different ecosystem responses to annual nitrogen import between the four regimes, depending on the combination of boundary concentrations, advection, river discharges and atmospheric deposition. The 1989-1995 regime in particular was characterized by extreme inflow of water from the Atlantic, but the resulting high nutrient influx did not cause the rise in production in the North Sea that might have been expected. Instead, the 1976-1988 regime was the most productive of the study period.

Pelagic and demersal fish did not necessarily respond proportionally to the changes in primary production induced by the different physical regime conditions. This was partly because the flushing effects of advection impacted on the planktonic and benthic parts of the food web differently (benthos was anchored within the model and not subject to advection), and partly because the changes in production did not only affect the maximum sustainable yields from the stocks, but also the harvesting rates at

which MSY was achieved. So, with fixed harvesting the effect of regime changes was to move F_{MSY} relative to the actual harvesting rate with strongly non-linear effects on yields.

The simulated differences in fish production and yields during the four physical forcing regimes highlighted the history of over exploitation of the demersal assemblage in the North Sea. It was possible to match pelagic fish production and landings with harvesting rates that were close to F_{MSY} thoughout most of the time series. However this was not the case at all for the demersal assemblage which appears to have been harvested at rates well above F_{MSY}. The consequence of this is that demersal fish production and abundance is currently well below the potential of the system. For the pelagic fish, the most productive regime was during 1976-1988, but harvesting was apparently in excess of F_{MSY} during this period. These years coincide with severe depletion of herring stocks and the closure of herring fisheries, so it may seem strange to suggest that pelagic fish were over-exploited during this period. However, the landings data show that whilst herring yield was severely depleted, landings of sprat and industrial fisheries for sandeel and Norway pout were explanding, so that as a functional group it may well have been the case that harvesting was exceeding the sustainable limits set by the productivity of the regime. The lowest rates of recruitment and maximum sustainable yield for pelagic fish were predicted to be during the most recent regime (1996-2005). This result is in accordance with recent observations (since 2001) of a step-change downwards in the recruitment performance of herring and sandeels in the North Sea. However, it remains the case that despite the demonstable effects of physical regime changes on fish production and yield, the greatest and most direct impact on fish is the harvesting rate. As harvesting rates begin to exceed F_{MSY}, the sensitivity of of the system increases and small increases in harvesting can lead to large and catastrophic declines in yield, in excess of those likely to be caused by regime change.

Impact of future Climate

The predicted effects of climate change on the key physical drivers of the model seem to indicate that we can expect an increase in primary production. However, since one of the predicted changes in physical drivers is an enhancement of advective input, the effect is likely to be less extensive than the change in nutrient input alone would imply. In addition, the expected changes seem to be towards further declines in pelagic fish recruitment, but increases in demersal fish recruitment, although overall fish production rates should increase assuming 1966-2005 status-quo harvesting rates. However, the future state of the North Sea ecosystem could be transformed is demersal harvesting rates can be reduced. At the level of resolution provided by this model, reductions in harvesting have as much or greater potential to affect the state of the system than the changes in climate.

Further modeling work

The approach taken in this study was to run the model to a stationary state with a repeating annual cycle of environmental forcing data. The time taken to attain the stationary state was variable, depending on the prescribed initial conditions, the

concentrations of nutrient at the boundaries and the modeled advection rates. However in most cases the simulations were tolerably close to stationary within 4-6 years. This practice is an accepted modeling approach, and the only effective way to estimate maximum sustainable yields, but there is a question about whether it is appropriate to fit the model to observed values of the various components under these circumstances. The key issue is the extent to which the observed system represents a steady state, or whether in fact the system is more usually in a transient state as a result of variability in the environmental forcing. One of the next stage of our work will be to run the model with multi-annual time series of environmental forcing and attempt to fit the time series of results to observations.

Finally, it is important to emphasise that these model results should not be over-interpreted. Inherent in this type of functional group modeling is the assumption that the characteristics of the group, as represented by the uptake and physiological parameters remain constant over all conditions. Changes in speciation would be expected to violate this assumption. In reality, some of the simulations were extreme situations, for example where pelagic fish were exploited to extinction in the model, and although the model predicted that demersal fish continue to exist with a diet composed almost exclusively of benthos and zooplankton, there is no suggestion that this could happen in reality without catastrophic consequences for the species composition of the demersal fish functional group. Essentially, all the major piscivirous fish in the group which rely on small pelagic fish in their adult diet would disappear and be replaced by benthivores, or have to undergo massive changes in behaviour. In these extremes, the representation of all piscivorous and benthivorous fish as a demersal functional group with a constant parameterization is too crude. But, the purpose of the model was to diagnose gross patterns in the ecosystem and how overall levels of production are set by nutrient budgets and primary production, not detail at any functional level in the food web. Resolving details would require a different modeling approach allowing representation of more finely resolved functionality, probably at the expense of other parts of the system. A likely way forward is to combine the end-to-end ecosystem, functional group approach taken here, with a multi-species partial food web modeling approach, in which the focus is on a subset of key species of interest, and the production rates of groups of species more trophically remote from the central focus is derived from the sort of model we describe here.

Acknowledgements

This work was partly supported by EU-RECLAIM project (Framework 6, 044133 (SSP8)), and Scottish Government project MF0758. Our thanks to Morten Skogen for providing volume transport data from NORWECOM model outputs. Thanks also to Jens Rasmussen for assembling the relationship between vertical attenualtion coefficient and turbidity.

References

Beaugrand G (2004) The North Sea regime shift: evidence, causes, mechanisms and consequences. Prog Oceanogr 60:245-262
Beaugrand G, Edwards M, Brander K, Loczak C, Ibanez F (2008) Causes and projections of abrupt climate-driven ecosystem shifts in the North Atlantic. Ecol Lett 11: 1157-1168
Bisagni JJ (2003) Seasonal variability of nitrate supply and potential new primary production in the Gulf of Maine and Georges Bank regions. J Geophys Res 108 C11: 8015, doi:10.1029/2001JC001136
Brion N, Baeyens W, de Galani S, Elskens M, Laane RWPM (2004) The North Sea: source or sink for nitrogen and phosphorus to the Atlantic Ocean? Biogeochemistry 68: 277–296
Broekhuizen, N., Heath, M.R., Hay, S.J. and Gurney, W.S.C. 1995. Modelling the dynamics of the North Sea's zooplankton. Neth. J. Sea Res. 33(3/4) 381-406.
Bryant AD, Doyle P (1992) Static predation loading estimation for North Sea top predators. ERSEM Progress Report January 1992, Annex 6: 1–16 (EU MAST I project CT90–0021)
Bryant, A.D., Heath, M.R., Broezhuizen, J.G., Ollason, J.G., Gurney, W.S.C. and Greenstreet, S.P.R. 1995. Modelling the predation, growth and population dynamics of fish within a spatially-resolved shelf-sea ecosystem model. Neth. J. Sea Res. 33 (3/4), 407-421.
Chassot E, Mélin F, Le Pape O, Gascuel D (2007) Bottom-up control regulates fisheries production at the scale of eco-regions in European seas. Mar Ecol Prog Ser 343: 45–55
Drinkwater K, Skogen M, Hjøllo S, Schrum C, Alekseeva I, Huret M, Léger F (2009) The effects of future climate change on the physical oceanography and comparisons of the mean and variability of the future physical properties with present day conditions. RECLAIM Deliverable 4.1
Dugdale RC, Goering J J (1967) Uptake of new and regenerated forms of nitrogen in primary productivity. Limnol Oceanogr 12: 196–206
Edwards M, John AWG, Hunt HG, Lindley JA (1999) Exceptional influx of oceanic species into the North Sea late 1997. J Mar Biol Ass UK 79: 737-739
Eppley RW, Peterson BJ (1979) Particulate organic matter flux and planktonic new production in the deep ocean. Nature 282: 677–680
Falkowski PG, Barber RT, Smetacek V (1998) Biogeochemical controls and feedbacks on ocean primary production. Science 281: 200-206
Garside C, Garside JC (1993) The f-ratio on 20 degrees W during the North Atlantic Bloom Experiment. Deep Sea Res 40 (1-2): 75-90
Goes JI, Saino T, Oaku H, Ishizaka J, Wong CS, Nojiri Y (2000) Basin scale estimates of sea surface nitrate and new production from remotely sensed seas surface temperature and chlorophyll. Geophys Res Lett 27: 1263-1266
Heath MR (2005) Changes in the structure and function of the North Sea fish food web, 1973-2000, and the impacts of fishing and climate. ICES J Mar Sci 62: 847-868
Heath MR (2007) Spatially resolved monthly riverine fluxes of oxidised nitrogen (nitrate and nitrite) to the European shelf seas, 1960-2005. FRS Internal Report 02/07: 59p www.frs-scotland.gov.uk/FRS.Web/Uploads/Documents/0207.pdf accessed 17 Oct 2007.
Heath, M.R., Adams, R.D., Brown, F., Dunn, J., Fraser, S., Hay, S.J., Kelly, M.C., MacDonald, E.M., Robertson, M.R., Robinson, S., Wilson, C. (1999).

Plankton monitoring off the east coast of Scotland in 1997 and 1998. *Fisheries Research Services Report* 13/99.
Heath, M.R. and Beare, D.J. (2008). New primary production in northwest European shelf seas, 1960-2003. Marine Ecology Progress Series 363, 183-203.
Heath, M.R., Edwards, A.C., Pätsch, J. and Turrell, W.R. (2002). Modelling the behaviour of nutrients in the coastal waters of Scotland. *Fisheries Research Services Report 10/02. 107pp*. http://www.frs-scotland.gov.uk/FRS.Web/Uploads/Documents/ersem_report_final.pdf
Heath, M.R., Kunzlik, P.A., Gallego, A., Holmes, S.J. and Wright, P.J. (2008). A model of meta-population dynamics for northern European cod - the dynamic consequences of natal fidelity. Fish. Res. 93, 92-116.
Holliday P, Reid PC (2001) Is there a connection between high transport of water through the Rockall Trough and ecological changes in the North Sea? ICES J Mar Sci 58: 270 - 274
Horne EPW, Loder JW, Harrison WG, Mohn R, Lewis MR, Irwin B, Platt T (1989) Nitrate supply and demand at the Georges Bank tidal front. Scient Mar 53: 145-158
Huisman G, de Boer RJ (1997) A Formal Derivation of the "Beddington" Functional Response J Theor Biol 185: 278-399
Hydes DJ, Kelly-Gerreyn BA, Le Gall AC, Proctor R (1999) The balance of supply of nutrients and demands of biological production and denitrification in a temperate latitude shelf sea – a treatment of the southern North Sea as an extended estuary. Mar Chem 68: 117–131
Kelly-Gerreyn1 BA, Trimmer M, Hydes DJ (2001) A diagenetic model discriminating denitrification and dissimilatory nitrate reduction to ammonium in a temperate estuarine sediment. Mar Ecol Prog Ser 220: 33–46
Law CS, Owens NJP (1990) Denitrification and nitrous oxide in the North Sea. Neth J Sea Res 25: 65–74
Laws EA, Falkowski PG, Smith WO Jr, Ducklow H, McCarthy JJ (2000) Temperature effects on export production in the open ocean. Global Biogeochem Cycles 14: 1231–1246
Lenhart HJ, Pätsch J, Kühn W, Moll A, Pohlmann T (2004) Investigation on the trophic state of the North Sea for three years (1994–1996) simulated with the ecosystem model ERSEM – the role of a sharp NAOI decline. Biogeosciences Discussions 1: 725–754
Lenhart HJ, Radach G, Backhaus JO, Pohlmann T (1995) Simulations o fthe North Sea circulation, its variability, and its implementation as hydrodynamical forcing in ERSEM. Neth J Sea Res 33 (3/4) 271-299
Lenhart, H.J., Radach, G. and Ruardij, P. 1997. The effects of river input on the ecosystem dynamics in the continental coastal zone of the North Sea using ERSEM. J. Sea Res. 38, 249-274
Lipshultz F, Owens NJP (1996) An assessment of nitrogen fixation as a source of nitrogen to the North Atlantic Ocean. Biogeochemistry 35: 261–274
Lohse L, Kloosterhuis HT, Van Raaphorst W, Helder W (1996) Denitrification rates as measured by the isotope pairing method and by the acetylene inhibition technique in continental shelf sediments of the North Sea. Mar Ecol Prog Ser 132: 169–179
Mackinson S, Daskalov G (2007) An ecosystem model of the North Sea to support an ecosystem approach to fisheries management: description and parameterisation. Sci. Ser. Tech Rep., Cefas Lowestoft, 142: 195pp.

Moll A. (1997) Modelling primary production in the North Sea. Oceanogr 10: 24-26
Morin PJ (1999) Community ecology. Wiley-Blackwell 424pp.
Mueter FJ, Megrey BA (2006) Using multi-species surplus production models to estimate ecosystem-level maximum sustainable yields. Fish Res 81: 189–201
Nixon SW (1988) Physical energy inputs and the comparative ecology of lake and marine ecosystems, *Limnol Oceanog* 33: 1005–1025
R Development Core Team (2005) R: A language and environment for statistical computing. R Foundation for Statistical Computing, Vienna, Austria. ISBN 3-900051-07-0, URL http://www.R-project.org.
Negi K, Gakkhar S (2007) Dynamics in a Beddington–DeAngelis prey–predator system with impulsive harvesting. Ecological Modelling 2 0 6: 421–430
Pauly D, Christensen V, Walters C (2000) Ecopath, Ecosim and Ecospace as tools for evaluating ecosystem impact of fisheries. ICES J Mar Sci, 57: 697-706
Pauly D (Ed) (1998). Use of Ecopath with Ecosim to evaluate strategies for sustainable exploitation of multispecies resources. Fisheries Centre Research Reports, 6(2): 49pp.
Perry RI, Schweigert JF (2008) Primary productivity and the carrying capacity for herring in NE Pacific marine ecosystems. Prog Oceanogr. 77: 241–251
Pitcher TJ, Cochrane K (Eds) (2002) The use of ecosystem models to investigate multi-species management strategies for capture fisheries. Workshop 17th-20th July 2000, Vancouver. FCRR 2002, Vol. 10(2): 156pp.
Pohlmann T (1996) Calculating the annual cycle of the vertical eddy viscosity in the North Sea with a three-dimensional baroclinic shelf sea circulation model. Cont Shelf res 16: 147-161
Pohlmann, T. and Puls, W. 1994. Currents and transport in water. In: Sundermann, J. (Ed.), Circulation and contaminant fluxes in the North Sea. Springer Verlag, Berlin, pp. 345-402.
Puls, W. and Sundermann, J. 1990. Simulation of suspended sediment dispersion in the North Sea. In: Cheng R.T. (Ed.), Residual currents and long-term transport. Coast. Estuar. Stud. 38, 356-372.
Radach G, Lenhart HJ (1995) Nutrient dynamics in the North Sea: Fluxes and budgets in the water column derived from ERSEM. Neth J Sea Res 33 (3/4): 301-335
Radach G, Moll A (2006) Review of three-dimensional ecological modelling related to the North Sea shelf system - Part 2: Model validation and data needs. Oceanogr Mar Biol Ann Rev 44: 1-60
Radach G, Pätsch J (2007) Variability of continental riverine freshwater and nutrient inputs into the North Sea for the years 1977-2000 and its consequences for the assessment of eutrophication. Est Coasts 30(1): 66-81
Redfield AC, Ketchum BH, Pritchard FA (1963) The influence of organisms on the composition of seawater. In: The Sea, vol 2 [Hill, N., ed.]. Interscience, New York
Reid PC, De Borges MF, Svendsen E (2001a) A regime shift in the North Sea circa 1988 linked to changes in the North Sea horse mackerel fishery. Fish Res 50:163-171
Reid PC, Holliday NP, Smyth TJ (2001b) Pulses in the eastern margin current and warmer water off the north west European shelf linked to North Sea ecosystem changes. Mar Ecol Prog Ser 215: 283-287
Richardson K, Pedersen B (1998) Estimation of new production in the North Sea: consequences for temporal and spatial variability in phytoplankton. ICES J Mar Sci 55: 574–580

Ruardij, P. and van Raaphorst, W. 1995. Benthic nutrient regeneration in the ERSEM ecosystem model of the North Sea. Netherlands Journal of Sea Research. Vol.33(3-4): 453-483.

Simpson D, Fagerli HJ, Jonson JE, Tsyro S, Wind P, Tuovinen J-P (2003) Transboundary Acidification, Eutrophication and Ground Level Ozone in Europe. EMEP Status Report 1/2003 PART I Unified EMEP Model Description., Norwegian Meteorological Institute, Oslo, Norway. 104pp

Skogen MD, Moll A (2005) Importance of ocean circulation in ecological modelling: An example from the North Sea. J Mar Syst 57: 289-300

Skogen MD, Søiland H (1988) A User's guide to NORWECOM v2.0. The NORWegian ECOlogicalModel system. Tech rept Fisken og Havet 18/98. Institute of Marine Research. Pb 1970, N-5024 Bergen. 42pp

Skogen M, Svendsen E, Berntsen J, Aksnes D, Ulvestad K (1995) Modelling the primary production in the North Sea using a coupled 3 dimensional physical chemical biological oceanmodel. Est Coast Shelf Sci 41: 545–565

Skogen M, Svendsen E, Ostrowski M (1997) Quantifying volume transports during SKAGEX with the Norwegian Ecological Model system. Contl Shelf Res 17: 1817–1837

Soetaert S, Herman PMJ (2008) A Practical Guide to Ecological Modelling. Springer 372pp.

Tarrasón L (2003) Transboundary Acidification, Eutrophication and Ground Level Ozone in Europe. EMEP Status Report 1/2003 Part II, Unified EMEP Model Performance, Norwegian Meteorological Institute, Oslo, Norway. 170pp

van Boxtel AMJV, von Koningslow M, Tossings FM (1991) Atmospheric deposition of nutrients into the North Sea: assessment of possible effects on algae growth. Geosense B.V. by order of the Ministry of Public Works and Transport. North Sea Directorate, The Netherlands, 60 p.

van Raaphorst W, Kloosterhuis HT, Cramer A, Bakker KJM (1990) Nutrient early diagenesis in the sediments of the Dogger Bank area, North Sea: pore water results. Netherlands J Sea Res 26: 25–52

van Raaphorst W, Kloosterhuis HT, Berghuis EM, Gieles AJM, Malschaert JFP, Van Noort GJ (1992) Nitrogen cycling in two types of sediments of the Southern North Sea (Frisian Front, Broadfourteens): field data and mesocosm results. Neth J Sea Res. 28: 293–316

Walters CJ, Christensen V, Pauly D (1997) Structuring dynamic models of exploited ecosystems from trophic mass-balance assessments. Rev Fish Biol Fisheries, 7: 139-172

Walters CJ, Kitchell JF , Christensen V, Pauly D (2000) Representing density dependent consequences of life history strategies in aquatic ecosystems: Ecosim II. Ecosyst, 3: 70-83

Ward BB (2005) Temporal variability in nitrification rates and related biogeochemical factors in Monterey Bay, California, USA. Mar Ecol Prog Ser 292: 97–109

Weijerman M, Lindeboom H, Zuur AF (2005) Regime shifts in marine ecosystems of the North Sea and Wadden Sea. Mar Ecol Prog Ser 298: 21-39

Williams PJ leB, Thomas DN, Reynolds CS (Eds.) (2002) Phytoplankton Productivity: Carbon Assimilation in Marine and Freshwater Ecosystems. Blackwell, Oxford, UK 386pp.

Yool A,. Martin AP, Fernández C, Clark DR (2007) The significance of nitrification for oceanic new production. *Nature* 447: 999-1002 (doi:10.1038/nature05885)

Appendix 1. Model description

Physical setup

Parameter	**Symbol**	**Description**
Thicknesses of the surface and deep layers	T_s and T_d	Vertical distance between surface and base of mixed layer, and base of mixed layer to the seabed
Thickness of benthic feeding layer	T_x	Layer in which benthos have access to phytoplankton and suspended detritus (must be less than t_d).

Driving variables

Term	**Symbol**	**Description**
Sea surface light	L(t)	A daily resolution time series cosine function varying between a winter minimum (L_w) on day 0 and 360, and a summer maximum (L_s) on day 180
Vertical attenuation coefficient of light (base e)	Kvert(t)	A daily resolution time series of the log-e coefficient of vertical attenuation. The proportion of surface irradiance representing the mean light intensity in the surface layer is then derived from the integral of the light profile ($L_{depth} = L.e^{-kvert.depth}$) ie. (((1/kvert)*$e^{-kvert.0}$) - ((1/kvert)*$e^{-kvert.thick\_s}$))/thick_s
Vertical diffusion coefficient per unit length	V(t)	A daily resolution time series of either a constant value or a cosine function representing the seasonal variation of vertical diffusion coefficient. The material flux across the diffusion interface is given by the concentration gradient of the substance, multipled by the diffusion coefficient i.e. (((molesN m^{-3}) m^{-1}) m^2 d^{-1}) = molesN m^{-2} d^{-1}. However, since in the model all we have is the difference in concentration between the two layers, and not the gradient across the interface, we transfer the length term into the diffusion coefficient and express the coefficient with units m^2 d^{-1} m^{-1} = m d^{-1}.
External source of nitrogen from rivers and atmosphere	R(t)	A daily resolution time series of the mass of nitrogen introduced to the system from an external source
Horizontal advection inflow from the ocean to the surface layer	I_s(t)	A daily resolution time series or constant value of the inflow volume to the surface layer as a proportion of surface layer volume per day
Horizontal advection	I_d(t)	A daily resolution time series or constant

inflow from the ocean to the deep layer		value of the inflow volume to the deep layer as a proportion of deep layer volume per day
Vertical upwelling volume from deep layer to surface layer	I_d (t)	Proportion of deep layer volume upwelled into the surface layer per day = the horizontal inflow volume $I_d(t)$
Horizontal outflow volume from the surface layer to the ocean	$O_s(t)$	Proportion of surface layer advected horizontally out of the system each day = $I_s(t) + (t_d * I_d(t))/t_s$
Ocean concentrations of horizontally advected components in the surface and deep layers	$[]_{bs}(t)$ and $[]_{bd}(t)$	Nitrate, ammonia, detritus, micro-phytoplankton, meso-phytoplankton, and microzooplankton are susceptible to horizontal advection and ocean boundary concentrations (molesN m^{-3}) of each are required as a constant or time series
Pelagic fish spawning pattern	Pspn(t)	A daily resolution time series of the proportion of adult pelagic fish biomass shed as eggs per day
Demersal fish spawning pattern	Dspn(t)	A daily resolution time series of the proportion of adult demersal fish biomass shed as eggs per day
Pelagic fish recruitment pattern	Prec(t)	A daily resolution time series of the proportion of larval pelagic fish biomass recruiting to the adult pelagic stock per day
Demersal fish recruitment pattern	Drec(t)	A daily resolution time series of the proportion of larval demersal fish biomass recruiting to the adult demersal stock per day

State variables (mass of nitrogen in a given layer)

Term	**Symbol**
Surface detritus	D_s
Deep detritus	D_d
Sediment detritus	D_x
Surface ammonia	A_s
Deep ammonia	A_d
Surface nitrate	N_s
Deep nitrate	N_d
Surface micro-phytoplankton	U_s
Deep micro-phytoplankton	U_d
Surface large-phytoplankton	P_s
Deep large-phytoplankton	P_d
Surface micro-zooplankton	Z_s
Deep micro-zooplankton	Z_d
Mesozooplankton	H
Carnivores	C
Benthos-suspension feeders	Bs
Benthos-deposit feeders	Bd

Benthos-carnivores	Bc
Fish pelagic larvae	FLp
Fish demersal larvae	FLd
Fish pelagic	Fp
Fish demersal	Fd
Birds/mammals	J
Humans (sink term)	M

The generalised function for the daily uptake of nutrient by phytoplankton ($\Omega_{nutrient\text{-}phytoplankton}$, mMN m^{-2} d^{-1}) is :

$$Min\left\{1.0\ ,\ \frac{L}{L_{\max}}\right\} * nutrient * \mu_{nutrient-phytoplankton} * Min\left\{1.0\ ,\ \frac{phytoplankton}{T * h_{nutrient-phytoplankton}}\right\}$$

Nutrient refers to the mass of either ammonia (A) or nitrate (N; mMN m^{-2}) in a given layer of thickness T (m). Phytoplankton refers to the mass (mMN m^{-2}) of either micro-phytoplankton (U) or meso-phytoplankton (P) in a given layer. The parameter $\mu_{nutrient\text{-}phytoplankton}$ is the maximum rate of uptake of nutrient per unit phytoplankton (d^{-1}), whilst $h_{nutrient\text{-}phytoplankton}$ is the threshold concentration of phytoplankton (mMN m^{-3}) below which uptake per unit phytoplankton is maximal.

The proportion of nutrient concentration taken up per day is controlled by the combination of phytoplankton concentration and irradiance. L_{max} is the irradiance (E m^{-2} s^{-1}) at which the proportion of nutrient concentration taken up per day maximal. Below this irradiance proportion of nutrient concentration taken up per day scales lineally with irradiance. The value of L_{max} is assumed to be the same for both micro-phytoplankton and meso-phytoplankton.

The generalised uptake function for prey by heterotrophs is :

The generalised function for the daily uptake of prey by heterotrophic predators ($\Omega_{prey\text{-}predator}$, molesN m^{-2} d^{-1}) is :

$$prey * \mu_{prey-predator} * Min\left\{1.0\ ,\ \frac{predator}{T * h_{prey-predator}}\right\}$$

Prey refers to the mass (mMN m^{-2}) of a given prey group in a given layer of thickness T (m), whilst predator refers to the mass (mMN m^{-2}) of a predator. $\mu_{prey\text{-}predator}$ is the maximum proportion of prey concentration consumed per day per unit predator biomass (d^{-1}), whilst $h_{prey\text{-}predator}$ is the threshold of predator concentration (mM N m^{-3}) below which proportion of prey concentration consumed per day is maximal.

For heterotrophs, the assimilation efficiency (proportion of ingestate converted into body mass) is denoted by a_x, where x is the predator class. The background metabolic

rate is represented by the coefficient e_x, which is the proportion of nitrogen biomass which is converted to ammonia per day by predator class x.

Other parameters

Parameter	**Symbol**
Remineralisation of suspended detritus in the surface and deep layers to ammonia, expressed as the proportion of suspended detritus nitrogen converted to ammonia per day	m
Remineralisation of sediment detritus to ammonia, expressed as the proportion of sediment detritus nitrogen converted to ammonia per day	m_x
Nitrification rate of ammonia to nitrate, expressed as the proportion of ammonia converted to nitrate per day	n
Death rate of phytoplankton in the surface layer, expressed as the proportion of surface phytoplankton (mico and large alike) exported to detritus per day	x_s
Death rate of phytoplankton in the surface layer, expressed as the proportion of deep phytoplankton (mico and large alike) exported to detritus per day	x_d
Sinking rate of phytodetritus in the surface layer, expressed as the proportion of surface layer detritus exported per day to the deep layer	x_{sink_s}
Sinking rate of detritus in the deep layer, expressed as the proportion of deep layer detritus exported per day to the sediment	x_{sink_d}
Sink term for nitrate representing denitrification, expressed as the proportion of nitrate lost from the system to nitrogen gas per day	d
Fraction of pelagic fish catch which is not landed	$disc_p$
Fraction of demersal fish catch which is not landed	$disc_d$
Fraction of carnivorous benthos fish catch which is not landed	$disc_{Bc}$
Fraction of suspension feeding benthos fish catch which is not landed	$disc_{Bs}$

Uptake rates

Uptake term	**Description**
Uptake of ammonia by microphyto	$\Omega_{As\text{-}Us} = Min\{1.0,L(t)/L_{max}\}.A_s.\ \mu_{A\text{-}U}.\ Min\{1.0,U_s/\ (h_{A\text{-}U}.\ T_s)\}$
Uptake of ammonia by largephyto	$\Omega_{As\text{-}Ps} = Min\{1.0,L(t)/L_{max}\}.A_s.\ \mu_{A\text{-}P}\ .\ Min\{1.0,P_s/\ (h_{A\text{-}P}.\ T_s)\}$
Uptake of nitrate by largephyto	$\Omega_{Ns\text{-}Ps} = Min\{1.0,L(t)/L_{max}\}.N_s.\ \mu_{N\text{-}P}\ .Min\{1.0,P_s/\ (h_{N\text{-}P}.\ T_s)\}$
Uptake of surface microphyto by microzoo	$\Omega_{Us\text{-}Zs} = U_s.\ \mu_{U\text{-}Z}\ .Min\{1.0,Z_s/\ (h_{U\text{-}Z}.\ T_s)\}$
Uptake of deep microphyto by microzoo	$\Omega_{Ud\text{-}Zd} = U_d.\ \mu_{U\text{-}Z}\ .Min\{1.0,Z_d/\ (h_{U\text{-}Z}.\ T_d)\}$
Uptake of surface microzoo by mesozoo	$\Omega_{Zs\text{-}H} = Z_s.\ \mu_{Z\text{-}H}\ .Min\{1.0,H.((Z_s+P_s)/(Z_s+P_s+Z_d+P_d))/\ (h_{Z\text{-}H}.\ T_s)\}$
Uptake of deep	$\Omega_{Zd\text{-}H} = Z_d.\ \mu_{Z\text{-}H}\ .Min\{1.0,H((Z_d+P_d)/(Z_s+P_s+Z_d+P_d))/\ (h_{Z\text{-}H}.$

microzoo by mesozoo	$T_d)\}$
Uptake of surface large phyto by mesozoo	$\Omega_{Ps\text{-}H} = P_s.\ \mu_{P\text{-}H}\ .Min\{1.0,H((Z_s+P_s)/(Z_s+P_s+Z_d+P_d))/\ (h_{P\text{-}H}.\ T_s)\}$
Uptake of deep large phyto by mesozoo	$\Omega_{Pd\text{-}H} = P_d.\ \mu_{P\text{-}H}\ .Min\{1.0,H((Z_d+P_d)/(Z_s+P_s+Z_d+P_d))/\ (h_{P\text{-}H}.\ T_d)\}$
Uptake of deep largephyto by benthos suspension feeders	$\Omega_{Pd\text{-}Bs} = (T_x/T_d).P_d.\ \mu_{P\text{-}Bs}\ .Min\{1.0,Bs/\ h_{P\text{-}Bs}\}$
Uptake of suspended detritus by benthos suspension feeders	$\Omega_{Dd\text{-}Bs} = (T_x/T_d).D_d.\ \mu_{D\text{-}Bs}\ .Min\{1.0,Bs/\ h_{D\text{-}Bs}\}$
Uptake of sediment detritus by benthos deposit feeders	$\Omega_{Dx\text{-}Bd} =D_x.\ \mu_{X\text{-}Bd}\ .Min\{1.0,Bd/\ h_{X\text{-}Bd}\}$
Uptake of suspension feeders by benthic carnivores	$\Omega_{Bs\text{-}Bc} =Bs.\ \mu_{Bs\text{-}Bc}\ .Min\{1.0,Bc/\ h_{Bs\text{-}Bc}\}$
Uptake of deposit feeders by benthic carnivores	$\Omega_{Bd\text{-}Bc} =Bd.\ \mu_{Bd\text{-}Bc}\ .Min\{1.0,Bc/\ h_{Bd\text{-}Bc}\}$
Uptake of mesozoo by carniv zoo	$\Omega_{H\text{-}C} =H.\ \mu_{H\text{-}C}\ .Min\{1.0,C/\ (h_{H\text{-}C}.\ (T_s+T_d))\}$
Uptake of pelagic fish larvae by carniv zoo	$\Omega_{FLp\text{-}C} =FLp.\ \mu_{FLp\text{-}C}\ .Min\{1.0,C/\ (h_{FLp\text{-}C}.\ (T_s+T_d))\}$
Uptake of demersal fish larvae by carniv zoo	$\Omega_{FLd\text{-}C} =FLd.\ \mu_{FLd\text{-}C}\ .Min\{1.0,C/\ (h_{FLd\text{-}C}.\ (T_s+T_d))\}$
Uptake of mesozoo by pelagic fish larvae	$\Omega_{H\text{-}FLp} =H.\ \mu_{H\text{-}FLp}\ .Min\{1.0,Fp/\ (h_{H\text{-}FLp}.\ (T_s+T_d))\}$
Uptake of mesozoo by pelagic fish	$\Omega_{H\text{-}Fp} =H.\ \mu_{H\text{-}Fp}\ .Min\{1.0,Fp/\ (h_{H\text{-}Fp}.\ (T_s+T_d))\}$
Uptake of carnivzoo by pelagic fish	$\Omega_{C\text{-}Fp} =C.\ \mu_{C\text{-}Fp}\ .Min\{1.0,Fp/\ (h_{C\text{-}Fp}.\ (T_s+T_d))\}$
Uptake of pelagicl fish larvae by pelagic fish	$\Omega_{FLp\text{-}Fp} =FLd.\ \mu_{FLpd\text{-}Fp}\ .Min\{1.0,Fp/\ (h_{FLp\text{-}Fp}.\ (T_s+T_d))\}$
Uptake of demersal fish larvae by pelagic fish	$\Omega_{FLd\text{-}Fp} =FLd.\ \mu_{FLd\text{-}Fp}\ .Min\{1.0,Fp/\ (h_{FLd\text{-}Fp}.\ (T_s+T_d))\}$
Uptake of mesozoo	$\Omega_{H\text{-}FLd} =H.\ \mu_{H\text{-}FLd}\ .Min\{1.0,Fd/\ (h_{H\text{-}FLd}.\ (T_s+T_d))\}$

by demersal fish larvae	
Uptake of carnivzoo by demersal fish	$\Omega_{C\text{-}Fd} = C.\ \mu_{C\text{-}Fd}\ .Min\{1.0, Fd/\ (h_{C\text{-}Fd}.\ (T_s+T_d))\}$
Uptake of benthos suspension feeders by demersal fish	$\Omega_{Bs\text{-}Fd} = Bs.\ \mu_{Bs\text{-}Fd}\ .Min\{1.0, Fd/\ (h_{Bs\text{-}Fd}.\ (T_s+T_d))\}$
Uptake of benthos deposit feeders by demersal fish	$\Omega_{Bd\text{-}Fd} = Bd.\ \mu_{Bd\text{-}Fd}\ .Min\{1.0, Fd/\ (h_{Bd\text{-}Fd}.\ (T_s+T_d))\}$
Uptake of benthos carnivores by demersal fish	$\Omega_{Bc\text{-}Fd} = Bc.\ \mu_{Bc\text{-}Fd}\ .Min\{1.0, Fd/\ (h_{Bc\text{-}Fd}.\ (T_s+T_d))\}$
Uptake of pelagic fish larvae by demersal fish	$\Omega_{FLp\text{-}Fd} = FLp.\ \mu_{FLp\text{-}Fd}\ .Min\{1.0, Fd/\ (h_{FLp\text{-}Fd}.\ (T_s+T_d))\}$
Uptake of demersal fish larvae by demersal fish	$\Omega_{FLd\text{-}Fd} = FLp.\ \mu_{FLd\text{-}Fd}\ .Min\{1.0, Fd/\ (h_{FLd\text{-}Fd}.\ (T_s+T_d))\}$
Uptake of pelagic fish by demersal fish	$\Omega_{Fp\text{-}Fd} = Fp.\ \mu_{Fp\text{-}Fd}\ .Min\{1.0, Fd/\ (h_{Fp\text{-}Fd}.\ (T_s+T_d))\}$
Uptake of pelagic fish by birds/mammals	$\Omega_{Fp\text{-}J} = Fp.\ \mu_{Fp\text{-}J}\ .Min\{1.0, J/\ (h_{Fp\text{-}J})\}$
Catch of benthos suspension feeders	$\Omega_{Bs\text{-}M} = Bs.\ \mu_{Bs\text{-}M}$
Catch of benthos carnivores	$\Omega_{Bc\text{-}M} = Bc.\ \mu_{Bc\text{-}M}$
Catch of pelagic fish	$\Omega_{Fp\text{-}M} = Fp.\ \mu_{Fp\text{-}M}$
Catch of demersal fish	$\Omega_{Fd\text{-}M} = Fd.\ \mu_{Fd\text{-}M}$

Rate equations

Rate term	**Description**
Rate of change of surface detritus (formed from faeces of microzoo and death of surface micro- and large phyto).	$dD_s/dt = ((1\text{-}a_Z)/2).\ \Omega_{Us\text{-}Zs} + x_s.U_s + x_s.P_s - m.D_s - x_{sink\_s}.D_s + V(t).((D_d/T_d)\text{-}(D_s/T_s)) + I_s(t)*T_s*[D]_{bs}(t) + I_d(t)*D_d - (I_s(t)*T_s+I_d(t)*T_d)*D_s/T_s$
Rate of change in deep detritus	$dD_d/dt = ((1\text{-}a_Z)/2).\ \Omega_{Ud\text{-}Zd} + ((1\text{-}a_H)/2).\ (\Omega_{Zs\text{-}H} + \Omega_{Zd\text{-}H} + \Omega_{Ps\text{-}H} + \Omega_{Pds\text{-}H})$

(formed from death of deep large phyto, death of deep micro-phyto and the faeces of deep microzoo, plus sinking of the same from the surface layer) .	$+ ((1-a_C)/2).(\Omega_{H-C} + \Omega_{FLp-C} + \Omega_{FLd-C})$ $+ ((1-a_{FLp})/2). (\Omega_{H-FLp})$ $+ ((1-a_{FLd})/2). (\Omega_{H-FLd})$ $+ ((1-a_{Fp})/2). (\Omega_{H-Fp} + \Omega_{C-Fp} + \Omega_{FLp-Fp} + \Omega_{FLd-Fp})$ $+ ((1-a_{Fd})/2). (\Omega_{C-Fd} + \Omega_{FLp-Fd} + \Omega_{FLd-Fd} + \Omega_{Fp-Fd} + \Omega_{Bs-Fd} + \Omega_{Bd-Fd} + \Omega_{Bc-Fd})$ $+ ((1-a_J)/2). \Omega_{Fp-J}$ $+ x_d.U_d + x_d.P_d + x_{sink}.D_s - m.D_d - x_{sink\_d}.D_d$ $- \Omega_{Dd-Bs} - V(t).((D_d/T_d)-(D_s/T_s)) + I_d(t)*T_d*[D]_{bd}(t) - I_d(t)*D_d$
Rate of change in sediment detritus (formed from the faeces of mesozoo, carnivzoo,, fish and benthos) .	$dD_x/dt =$ $+ ((1-a_{Bs})/2). (\Omega_{Dd-Bs} + \Omega_{Pd-Bs})$ $+ ((1-a_{Bd})/2). \Omega_{Dx-Bd}$ $+ ((1-a_{Bc})/2). (\Omega_{Bs-Bc} + \Omega_{Bd-Bc})$ $+ x_{sink\_d}.D_d$ $+ disc_p.\Omega_{Fp-M} + disc_d.\Omega_{Fd-M} + disc_{Bs}.\Omega_{Bc-M} + disc_{Bc}.\Omega_{Bs-M}$ $- m_x.D_x - \Omega_{Dx-Bd}$
Rate of change in surface ammonia	$dA_s/dt = m.D_s + e_Z.Z_s$ $+ (T_s/(T_s+T_d))(e_H.H + e_C.C + e_{FLp}.FLp + e_{FLd}.FLd + e_{Fp}.Fp)$ $+ (T_s/(T_s+T_d))(((1-a_{Fp})/2). (\Omega_{H-Fp} + \Omega_{C-Fp} + \Omega_{FLp-Fp} + \Omega_{FLd-Fp}))$ $+ (T_s/(T_s+T_d))(((1-a_{FLp})/2).(\Omega_{H-FLp})$ $+ (T_s/(T_s+T_d))(((1-a_{FLd})/2).(\Omega_{H-FLd})$ $+ (T_s/(T_s+T_d))(((1-a_C)/2).(\Omega_{H-C} + \Omega_{FLp-C} + \Omega_{FLd-C}))$ $+ ((1-a_H)/2).(\Omega_{Zs-H} + \Omega_{Ps-H})$ $+ ((1-a_Z)/2). \Omega_{Us-Zs}$ $+ ((1-a_J)/2). \Omega_{Fp-J}$ $+ e_J.J$ $- n.A_s - \Omega_{As-Us} - \Omega_{As-Ps} + V(t).((A_d/T_d)-(A_s/T_s))$ $+ I_s(t)*T_s*[A]_{bs}(t) + I_d(t)*A_d - (I_s(t)*T_s+I_d(t)*T_d)*A_s/T_s$
Rate of change in deep ammonia	$dA_d/dt = m.D_d + m_x.D_x + e_Z.Z_d$ $+ (T_d/(T_s+T_d))(e_H.H + e_C.C + e_{Fp}.Fp)$ $+ e_{Bs}.Bs + e_{Bd}.Bd + e_{Bc}.Bc + e_{Fd}.Fd$ $+ (T_d/(T_s+T_d))(((1-a_{FLp})/2).(\Omega_{H-FLp})$ $+ (T_d/(T_s+T_d))(((1-a_{FLd})/2).(\Omega_{H-FLd})$ $+ (T_d/(T_s+T_d))(((1-a_{Fp})/2). (\Omega_{H-Fp} + \Omega_{C-Fp} + \Omega_{Fd-Fp}))$ $+ (((1-a_{Fd})/2). (\Omega_{C-Fd} + \Omega_{FLp-Fd} + \Omega_{FLd-Fd} + \Omega_{Fp-Fd} + \Omega_{Bs-Fd} + \Omega_{Bd-Fd} + \Omega_{Bc-Fd}))$ $+ (T_d/(T_s+T_d))(((1-a_C)/2).(\Omega_{H-C} + \Omega_{FLp-C} + \Omega_{FLd-C}))$ $+ ((1-a_H)/2).(\Omega_{Zd-H} + \Omega_{Pd-H})$ $+ ((1-a_{Bs})/2). (\Omega_{Dd-Bs} + \Omega_{Pd-Bs})$ $+ ((1-a_{Bd})/2). \Omega_{Dx-Bd}$ $+ ((1-a_{Bc})/2). (\Omega_{Bs-Bc} + \Omega_{Bd-Bc})$ $+ ((1-a_Z)/2). \Omega_{Ud-Zd}$ $- n.A_d - V(t).((A_d/T_d)-(A_s/T_s)) + I_d(t)*T_d*[A]_{bd}(t) - I_d(t)*A_d$
Rate of change in surface nitrate	$dN_s/dt = n.A_s - \Omega_{Ns-Ps} - d.N_s + V(t).((N_d/T_d)-(N_s/T_s)) + R(t)$ $+ I_s(t)*T_s*[N]_{bs}(t) + I_d(t)*N_d - (I_s(t)*T_s+I_d(t)*T_d)*N_s/T_s$
Rate of change in deep nitrate	$dN_d/dt = n.A_d - d.N_d - V(t).((N_d/T_d)-(N_s/T_s)) + I_d(t)*T_d*[N]_{bd}(t) - I_d(t)*N_d$
Rate of change in surface micro-phytoplankton	$dU_s/dt = \Omega_{As-Us} - x_s.U_s - \Omega_{Us-Zs} + V(t).((U_d/T_d)-(U_s/T_s))$ $+ I_s(t)*T_s*[U]_{bs}(t) + I_d(t)*U_d - (I_s(t)*T_s+I_d(t)*T_d)*U_s/T_s$

Rate of change in deep micro-phytoplankton	$dU_d/dt = – x_d.U_d - \Omega_{Ud-Zd} - V(t).((U_d/T_d)-(U_s/T_s)) + I_d(t)*T_d*[U]_{bd}(t) - I_d(t)*U_d$
Rate of change in surface large-phytoplankton	$dP_s/dt = \Omega_{As-Ps} + \Omega_{Ns-Ps} – x_s.P_s – \Omega_{Ps-H} + V(t).((P_d/T_d)-(P_s/T_s)) + I_s(t)*T_s*[P]_{bs}(t) + I_d(t)*P_d – (I_s(t)*T_s+I_d(t)*T_d)*P_s/T_s$
Rate of change in deep large-phytoplankton	$dP_s/dt = – x_d.P_d – \Omega_{Pd-H} - \Omega_{Pd-Bs} - V(t).((P_d/T_d)-(P_s/T_s)) + I_d(t)*T_d*[P]_{bd}(t) - I_d(t)*P_d$
Rate of change in surface microzooplankton	$dZ_s/dt = a_Z.\ \Omega_{Us-Zs} – e_Z.Z_s – \Omega_{Zs-H} + V(t).((Z_d/T_d)-(Z_s/T_s)) + I_s(t)*T_s*[Z]_{bs}(t) + I_d(t)*Z_d – (I_s(t)*T_s+I_d(t)*T_d)*Z_s/T_s$
Rate of change in deep microzooplankton	$dZ_s/dt = a_Z.\ \Omega_{Ud-Zd} – e_Z.Z_d - \Omega_{Zd-H} - V(t).((Z_d/T_d)-(Z_s/T_s)) + I_d(t)*T_d*[Z]_{bd}(t) - I_d(t)*Z_d$
Rate of change in herbivores	$dH/dt = a_H.\ (\Omega_{Zs-H} + \Omega_{Ps-H}) – e_H.H – \Omega_{H-C} - \Omega_{H-FLp} - \Omega_{H-FLd} - \Omega_{H-Fp}$
Rate of change in carnivores	$dC/dt = a_C.\ (\Omega_{H-C} + \Omega_{FLp-C} + \Omega_{FLd-C}) – e_C.C – \Omega_{C-Fd} – \Omega_{C-Fp}$
Rate of change in suspension feeding benthos	$dBs/dt = a_{Bs}.\ (\Omega_{Pd-Bs} + \Omega_{Dd-Bs}) – e_{Bs}.Bs - \Omega_{Bs-Bc} - \Omega_{Bs-Fd} - \Omega_{Bs-M}$
Rate of change in deposit feeding benthos	$dBd/dt = a_{Bd}.\ (\Omega_{Dx-Bd}) – e_{Bd}.Bd - \Omega_{Bd-Bc} - \Omega_{Bd-Fd}$
Rate of change in carnivorous benthos	$dBc/dt = a_{Bc}.\ (\Omega_{Bs-Bc} + \Omega_{Bd-Bc}) – e_{Bc}.Bc - \Omega_{Bc-Fd} - \Omega_{Bc-M}$
Rate of change in pelagic fish larvae	$dFLp/dt = a_{FLp}.(\ \Omega_{H-FLp}) – e_{FLp}.FLp - \Omega_{FLp-C} – \Omega_{FLp-Fp} – \Omega_{FLp-Fd} + Pspn(t) * F_p - Prec(t) * FL_p$
Rate of change in demersal fish larvae	$dFLd/dt = a_{FLd}.(\ \Omega_{H-FLd}) – e_{FLd}.FLd - \Omega_{FLd-C} – \Omega_{FLd-Fp} – \Omega_{FLd-Fd} + Dspn(t) * F_d - Drec(t) * FL_d$
Rate of change in pelagic fish	$dFp/dt = a_{Fp}.(\ \Omega_{C-Fp} + \Omega_{H-Fp} + \Omega_{FLp-Fp} + \Omega_{FLd-Fp}) – e_{Fp}.Fp - \Omega_{Fp-Fd} – \Omega_{Fp-M} – \Omega_{Fp-J} – Pspn(t) * F_p + Prec(t) * FL_p$
Rate of change in demersal fish	$dFd/dt = a_{Fd}.(\ \Omega_{Bs-Fd} + \Omega_{Bd-Fd} + \Omega_{Bc-Fd} + \Omega_{C-Fd} + \Omega_{FLp-Fd} + \Omega_{FLd-Fd} + \Omega_{Fp-Fd}) – e_{Fd}.Fd – \Omega_{Fd-M} – Dspn(t) * F_d + Drec(t) * FL_d$
Rate of change in birds/mammals	$dJ/dt = aJ.\ \Omega_{Fp-J} – e_J.J$

Derived properties

Property	**Description**
Total annual primary production	$T = \sum_{day\,0}^{day\,360} \left(\Omega_{As-Us} + \Omega_{As-Us} + \Omega_{Ns-Ps} \right)$
Annual MMP	$\tau = \max_{day\,0}^{day\,360} (N_s + N_d) - \min_{day\,0}^{day\,360} (N_s + N_d)$

Annual PNP	$\tau p_N = \sum_{day\,0}^{day\,360} \left(\Omega_{Ns-Ps} + d.N_s - n.A_s \right)$
Annual MMIP	$\tau i_N = \tau \quad + \quad \sum_{day\,90}^{day\,270} \left(R(t) + I_s(t) * T_s * ([N]_{bs} + [A]_{bs}) + I_d(t) * (N_d + A_d) \right)$
Annual vertical nitrate flux	$Vf_N = \sum_{day\,0}^{day\,360} \left(\mathrm{V(t).((N_d/T_d) - (N_s/T_s)) + I_d(t) * N_d} \right)$
Annual horizontal nitrate flux in the surface layer	$Hf_N = \sum_{day\,0}^{day\,360} \left((\mathrm{I_s(t) * T_s * [N]_{bs}}) - (\mathrm{I_s(t) * T_s + I_d(t) * T_d}) * \mathrm{N_s/T_s} \right)$
Total annual nitrate uptake	$T_N = \sum_{day\,0}^{day\,360} \left(\Omega_{Ns-Ps} \right)$
Annual f-ratio	$f = \tau p / T$
Annual microzooplankton gross production	$\psi = \sum_{day\,0}^{day\,360} \left(\mathrm{a_Z} . (\Omega_{Us-Zs} + \Omega_{Ud-Zd}) \right)$
Annual mesozooplankton gross production	$\gamma = \sum_{day\,0}^{day\,360} \left(\mathrm{a_H} . (\Omega_{Zs-H} + \Omega_{Ps-H} + \Omega_{Zd-H} + \Omega_{Pd-H}) \right)$
Annual carnivorous zooplankton gross production	$\chi = \sum_{day\,0}^{day\,360} \left(\mathrm{a_C} . (\Omega_{H-C} + \Omega_{FLp-C} + \Omega_{FLd-C} \right)$
Annual benthos gross production	$\beta = \sum_{day\,0}^{day\,360} \left(\mathrm{a_B} . (\Omega_{Pd-Bs} + \Omega_{Dd-Bs} + \Omega_{Dx-Bd} + \Omega_{Bs-Bc} + \Omega_{Bd-Bc}) \right)$
Annual demersal fish gross production	$\phi d = \sum_{day\,0}^{day\,360} \left(\mathrm{a_{Fd}} . (\Omega_{C-Fd} + \Omega_{Bs-Fd} + \Omega_{Bd-Fd} + \Omega_{Bc-Fd} + \Omega_{Fp-Fd} + \Omega_{FLp-Fd} + \Omega_{FLd-Fd}) \right)$
Annual pelagic fish gross production	$\phi p = \sum_{day\,0}^{day\,360} \left(\mathrm{a_{Fp}} . (\Omega_{H-Fp} + \Omega_{C-Fp} + \Omega_{FLp-Fp} + \Omega_{FLd-Fp}) \right)$
Annual demersal fish larvae gross production	$\phi Ld = \sum_{day\,0}^{day\,360} \left(\mathrm{a_{FLd}} . (\Omega_{H-FLd}) \right)$
Annual pelagic fish larvae gross production	$\phi Lp = \sum_{day\,0}^{day\,360} \left(\mathrm{a_{FLp}} . (\Omega_{H-FLp}) \right)$
Annual bird/mammal gross production	$\Pi = \sum_{day\,0}^{day\,360} \left(\mathrm{a_J} . \Omega_{Fp-J} \right)$
Pelagic fish annual egg production	$Pel\_eggP = \sum_{day\,0}^{day\,360} \left(\mathrm{Pspn(t) . Fp} \right)$
Pelagic fish annual recruitment	$Pel\_rec = \sum_{day\,0}^{day\,360} \left(\mathrm{Prec(t) . FLp} \right)$
Demersal fish annual egg	$Dem\_eggP = \sum_{day\,0}^{day\,360} \left(\mathrm{Dspn(t) . Fd} \right)$

production	
Demersal fish annual recruitment	$Dem\_rec = \sum_{day\,0}^{day\,360} (\mathrm{Drec(t)} . \mathrm{FLd})$
Total export from secondary producers	$\sum_{day\,0}^{day\,360} \left(\Omega_{\mathrm{H\text{-}C}} + \Omega_{\mathrm{H\text{-}FLp}} + \Omega_{\mathrm{H\text{-}Fld}} + \Omega_{\mathrm{H\text{-}Fp}} + \Omega_{\mathrm{Bs\text{-}Bc}} + \Omega_{\mathrm{B}d-Bc} + \Omega_{\mathrm{Bs\text{-}Fd}} + \Omega_{\mathrm{Bd\text{-}Fd}} \right)$
Total animal production	$\Psi + \gamma + \chi + \beta + \phi Lp + \phi Ld + \phi p + \phi d + \Pi$
Fishery catch	$catch = \sum_{day\,0}^{day\,360} \Omega_{Fp-M} + \Omega_{Fd-M} + \Omega_{Bs-M} + \Omega_{Bc-M}$
Total annual water column mineralization flux	$\mathrm{wc\_min}eral = \sum_{day\,0}^{day\,360} m \left(\mathrm{D_s} + \mathrm{D_d} \right)$
Total annual sediment mineralization flux	$sed\_\mathrm{min}eral = \sum_{day\,0}^{day\,360} m_x . \mathrm{D_x}$
Total annual denitrification flux	$denitrif = \sum_{day\,0}^{day\,360} d \left(\mathrm{N_s} + \mathrm{N_d} \right)$
Total annual nitrification flux	$nitrif = \sum_{day\,0}^{day\,360} n \left(\mathrm{A_s} + \mathrm{A_d} \right)$
Total mass of nitrogen	$D_s + D_d + D_x + A_s + A_d + N_s + N_d + U_s + U_d + P_s + P_d + H + C + Bs + Bd + Bc + FLp + FLd + Fp + Fd + J$

Table A1. Uptake function parameter $\mu_{prey\text{-}predator}$ (d^{-1}) at the reference temperature of 10ºC for all predator prey links in the model

Predators → / **Prey ↓**	**micro-phyto**	**meso-phyto**	**micro-zoo**	**meso-zoo**	**carniv. zoo**	**susp feeding benthos**	**deposit feeding benthos**	**carniv benthos**	**pelagic fish larvae**	**demersal fish larvae**	**pelagic fish adults**	**demersal fish adults**	**birds/ mammals**
DIN	0.1	0.14											
micro-phyto			0.2										
meso-phyto				0.25		0.05							
micro-zoo				0.1									
meso-zoo					0.0185				0.02	0.01	0.006		
carniv. zoo											0.005	0.005	
sediment detritus							0.005						
deep detritus						0.02							
susp feeding benthos								0.003				0.003	
deposit feeding benthos								0.003				0.003	
carniv benthos												0.0015	0.001
pelagic fish larvae					0.0075						0.01	0.0025	
demersal fish larvae					0.0075						0.02	0.0025	
pelagic fish adults												0.003	
demersal fish adults													
birds/ mammals													

Table A2. Uptake function parameter $h_{prey\text{-}predator}$ (mMN.m^{-3}) for all predator prey links in the model

Predators →													
Prey ↓	**micro-phyto**	**meso-phyto**	**micro-zoo**	**meso-zoo**	**carniv. zoo**	**susp feeding benthos**	**deposit feeding benthos**	**carniv benthos**	**pelagic fish larvae**	**demersal fish larvae**	**pelagic fish adults**	**demersal fish adults**	**birds/ mammals**
DIN	2	1											
micro-phyto			0.2										
meso-phyto				1.5		0.1							
micro-zoo				1.5									
meso-zoo					0.15				0.075	0.05	0.015		
carniv. zoo											0.015	0.015	
sediment detritus							0.01						
deep detritus						0.01							
susp feeding benthos								0.1				0.015	
deposit feeding benthos								0.1				0.015	
carniv benthos												0.015	0.001
pelagic fish larvae					0.15						0.015	0.015	
demersal fish larvae					0.15						0.015	0.015	
pelagic fish adults												0.015	
demersal fish adults													
birds/mammals													

Table A3. Metabolic parameters for all living components of the model

Predator	Q_{10} for uptake rates	Proportion of uptake converted to growth (a_x)	Background proportion of biomass converted to ammonia (e_x, d^{-1}) at reference temperature of 10ºC	Q_{10} for background excretion rates
micro-phyto	2.0	0.34	n/a	n/a
meso-phyto	2.0	0.34	n/a	n/a
micro-zoo	2.2	0.34	0.03	2.4
meso-zoo	2.2	0.34	0.01	2.4
carniv. zoo	2.2	0.34	0.01	2.4
susp feeding benthos	2.2	0.34	0.01	2.4
deposit feeding benthos	2.2	0.34	0.01	2.4
carniv benthos	2.2	0.34	0.005	2.4
pelagic fish larvae	2.2	0.34	0.01	2.4
demersal fish larvae	2.2	0.34	0.025	2.4
pelagic fish adults	2.2	0.34	0.0075	2.4
demersal fish adults	2.2	0.34	0.02	2.4
birds/mammals	2.2	0.34	0.0075	2.4

Table A4. Layer dependent parameters

Parameter	**Surface layer**	**Deep layer**	**Sediment layer**
Death rate of phytoplankton d^{-1}	0.05	0.1	n/a
Sinking rate of detritus d^{-1}	0.2	0.3 at $\log_{10}$ vertical diffusion (V(t)) = -6 0.02 at $\log_{10}$ vertical diffusion (V(t)) = -3.4	n/a
Mineralization rate of detritus at the reference temperature of 10ºC, d^{-1}	0.01	0.01	0.005
Nitrification rate of ammonia at the reference temperature of 10ºC, d^{-1}	0.005	0.0387	0.1
Denitrification rate of nitrate at the reference temperature of 10ºC, d^{-1}	0.00006	0.00006	0.2
Q_{10} for mineralization, nitrification and denitrification	2.4	2.4	2.4

Table A5. Other parameters of the model

Parameter	**Value**	**Units**
Surface layer thickness	28	m
Deep layer thickness	42	m
Bottom boundary layer thickness (for feeding by suspension feeding benthos)	20	m
Sediment layer thickness	0.1	m
Sediment porosity	0.45	$m^3.m^{-3}$
Sediment-water diffusion coefficient	10^{-8}	$m^2.s^{-1}$
Length scale for sediment-water difusion	0.01	m
Irradiance at maximum nutrient uptake by phytoplankton	5	$E.m^{-2}.d^{-1}$
Pelagic fish: date of onset of spawning	100	Day of the year
Pelagic fish: duration of spawning	250	d
Pelagic fish: date of onset of recruitment	1	Day of the year
Pelagic fish: duration of recruitment	150	d
Pelagic fish: annual potential fecundity	0.25	$g.g^{-1}$
Demersal fish: date of onset of spawning	60	Day of the year
Demersal fish: duration of spawning	90	d
Demersal fish: date of onset of recruitment	200	Day of the year
Demersal fish: duration of recruitment	150	d
Demersal fish: annual potential fecundity	0.4	$g.g^{-1}$

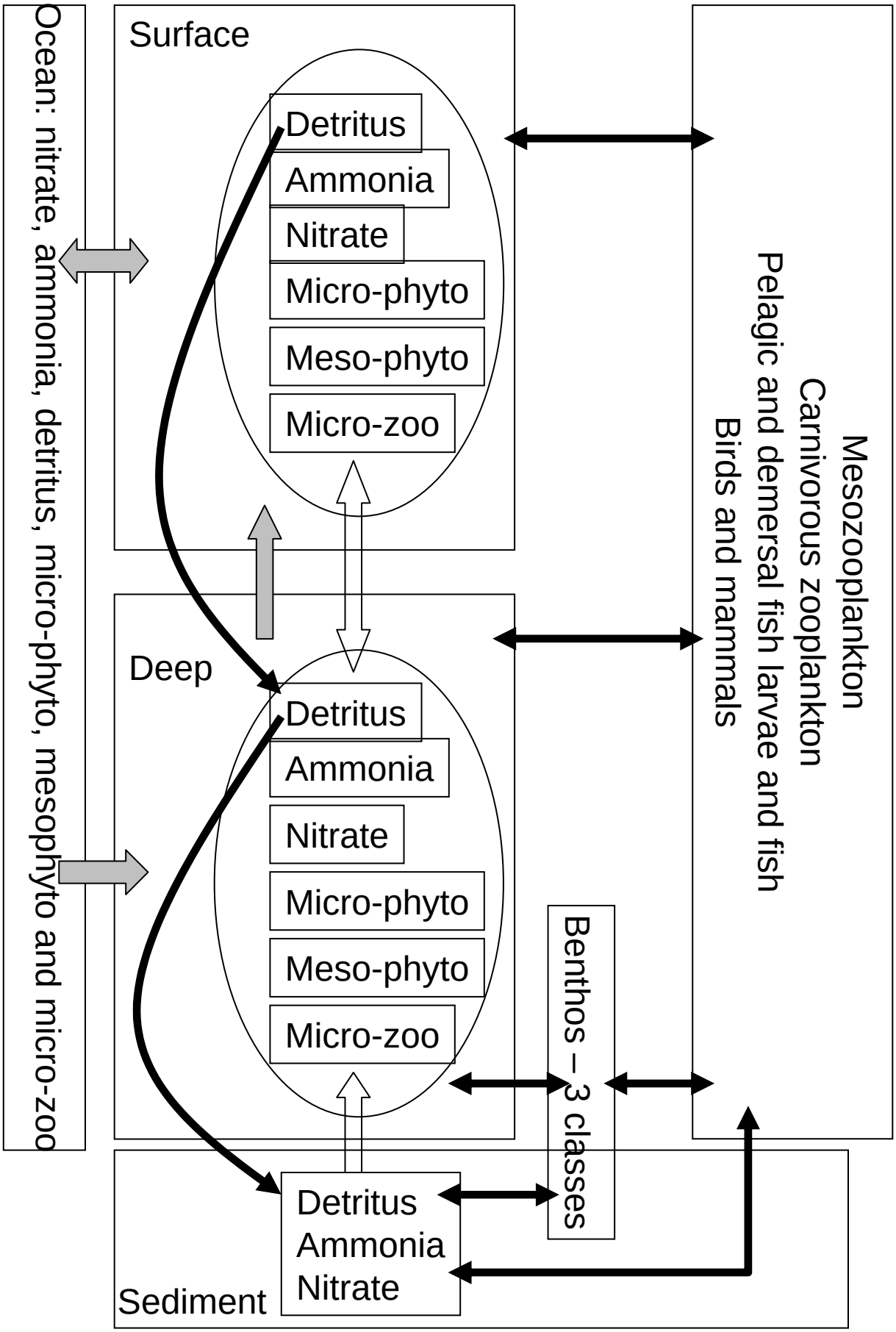

Fig.1. Schematic of the basic structure of the ecosystem model

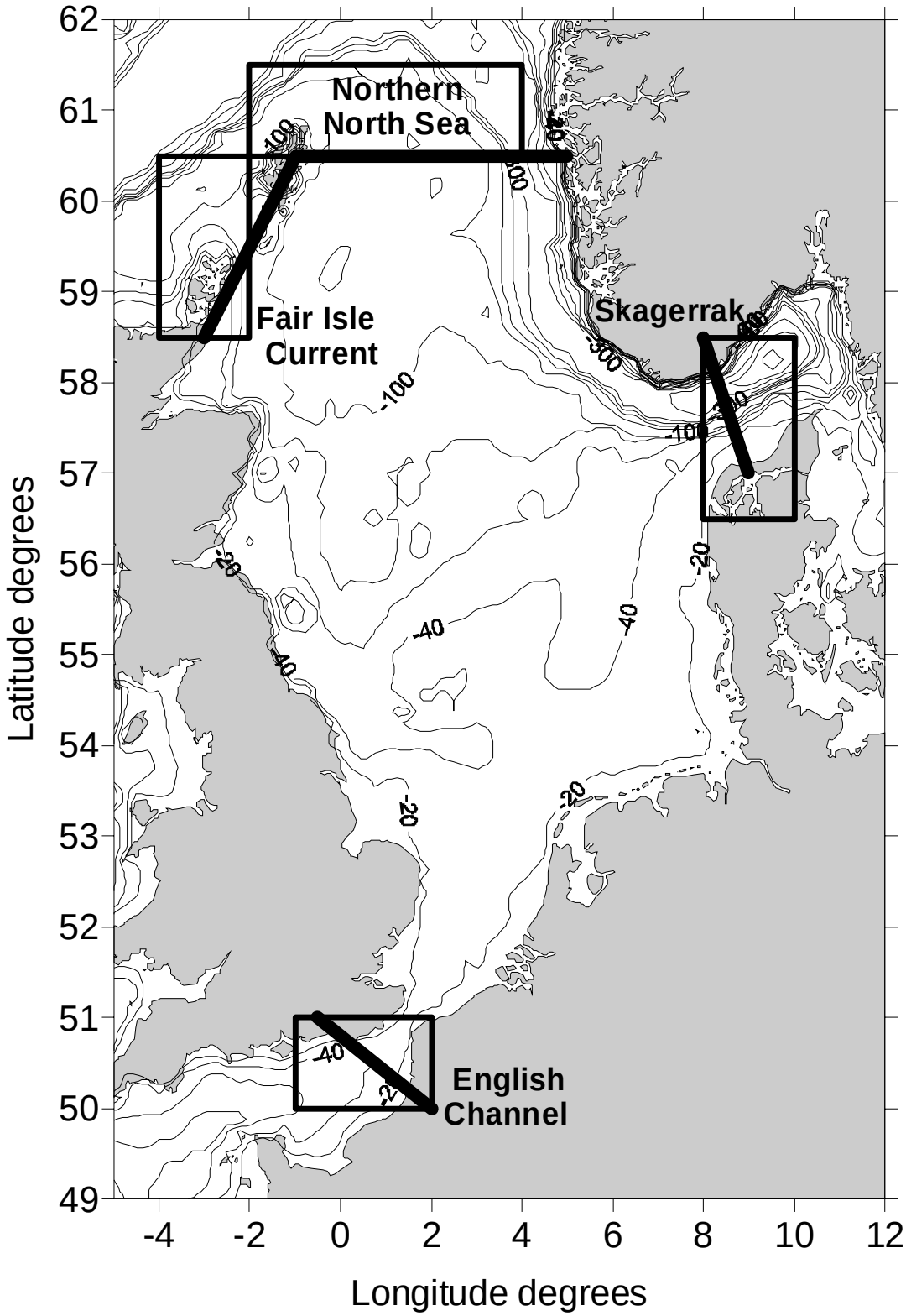

Fig.2. Spatial domain of the model and boundary zones. For each of the four inflows we defined a rectangular cell for averaging observational data to define boundary concentrations for the model.

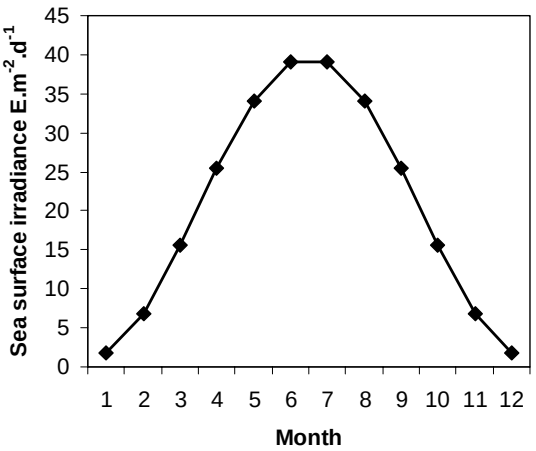

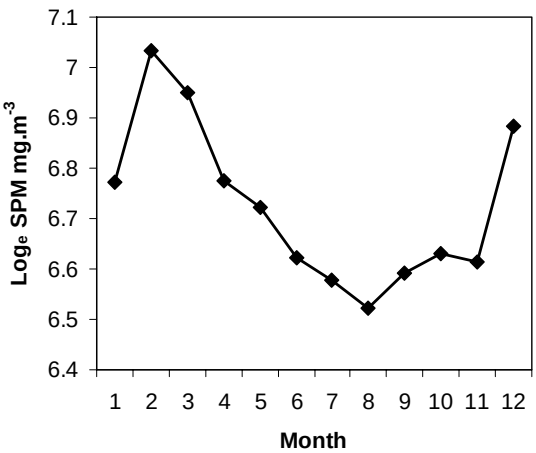

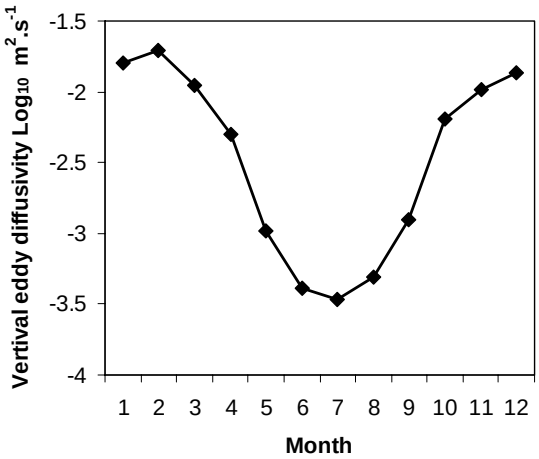

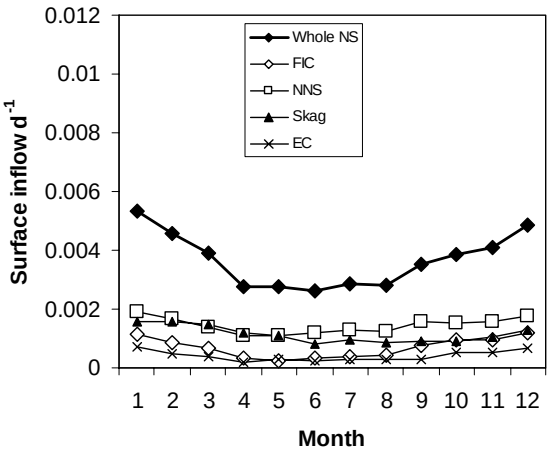

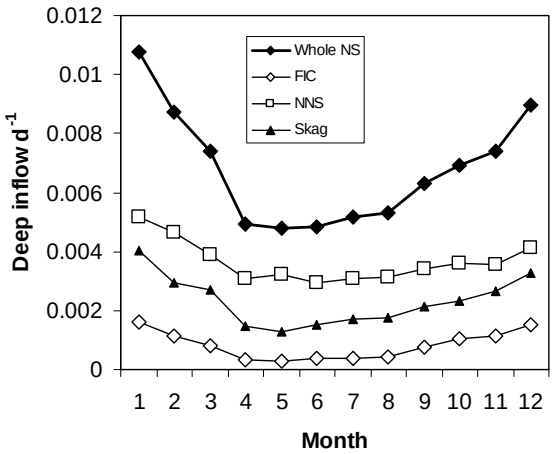

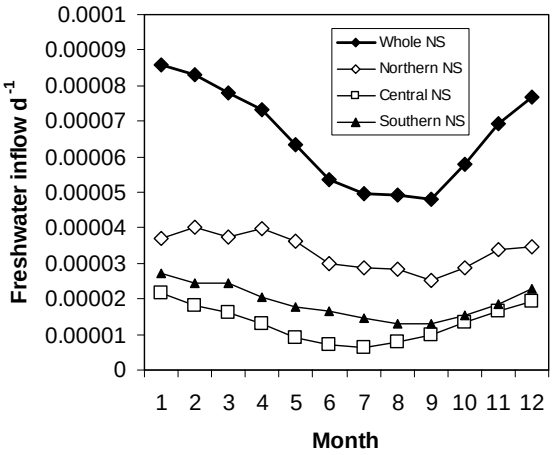

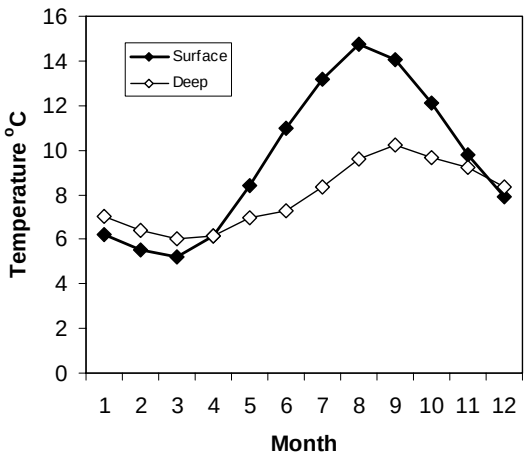

Fig.3. Long-term median physical diving data for the model. Data shown for each of the four boundaries for advection inflow, and for sub-regions of the model domain for freshwater input.

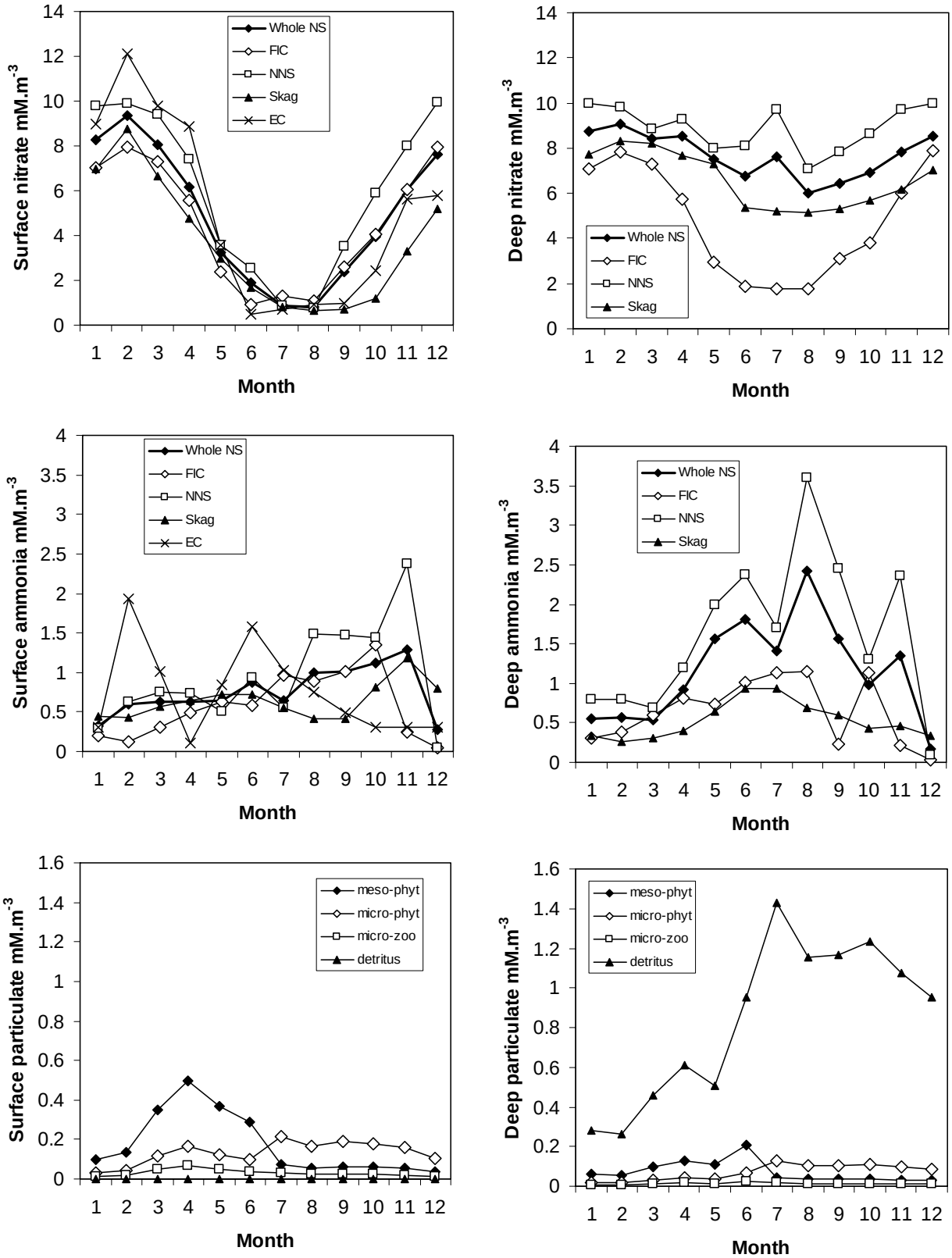

Fig.4. Long-term median concentrations of nitrate and ammonia at each of the boundaries, and the composite for the model as a whole (upper four panels). Lower two panels, North Sea composite boundary concentrations of particulate boundary components.

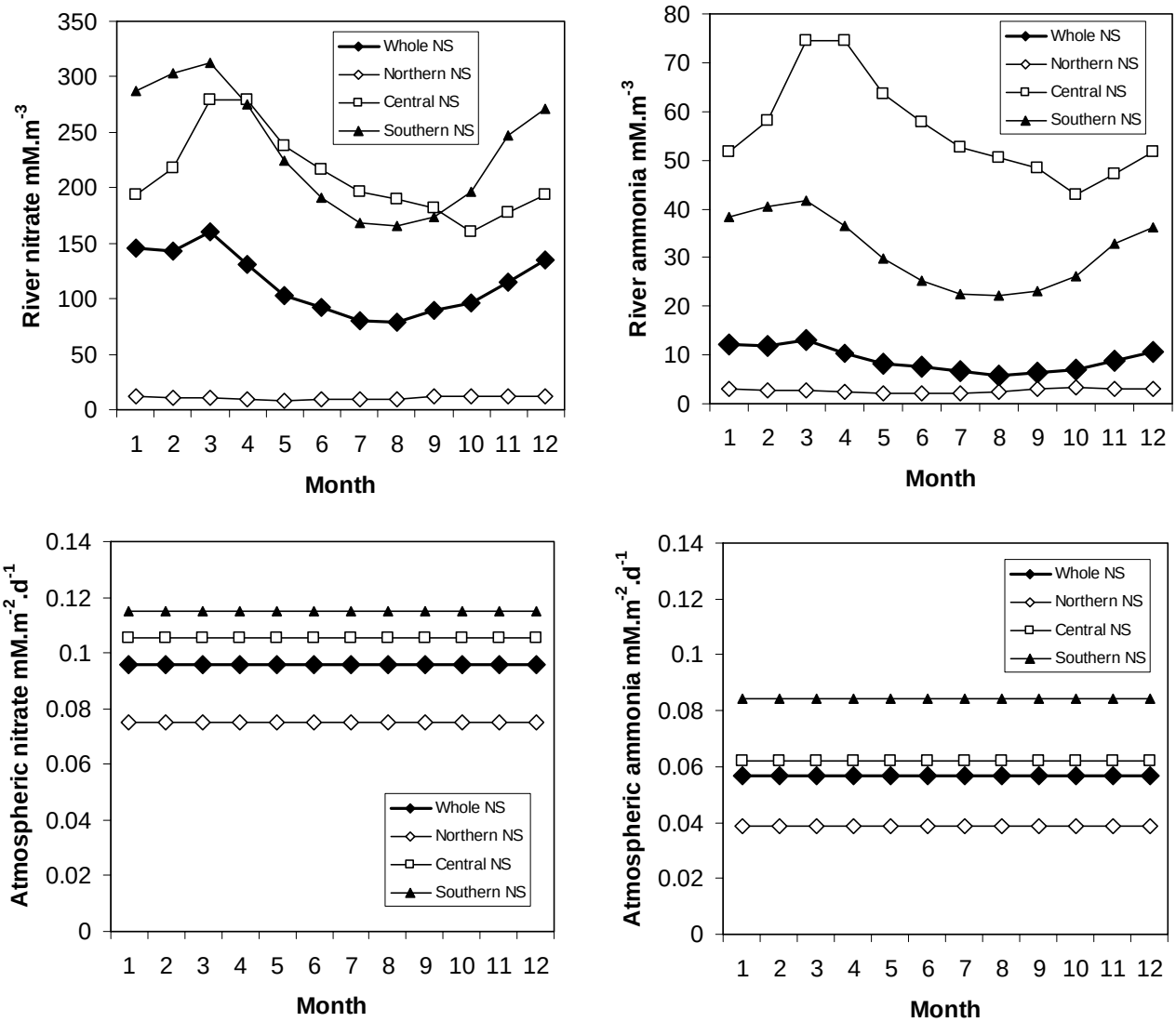

Fig.5. River nitrate and ammonia concentration, and atmospheric fluxes of nitrate and ammonia, for three sub-regions of the model domain and the composite fo rthe North Sea as a whole.

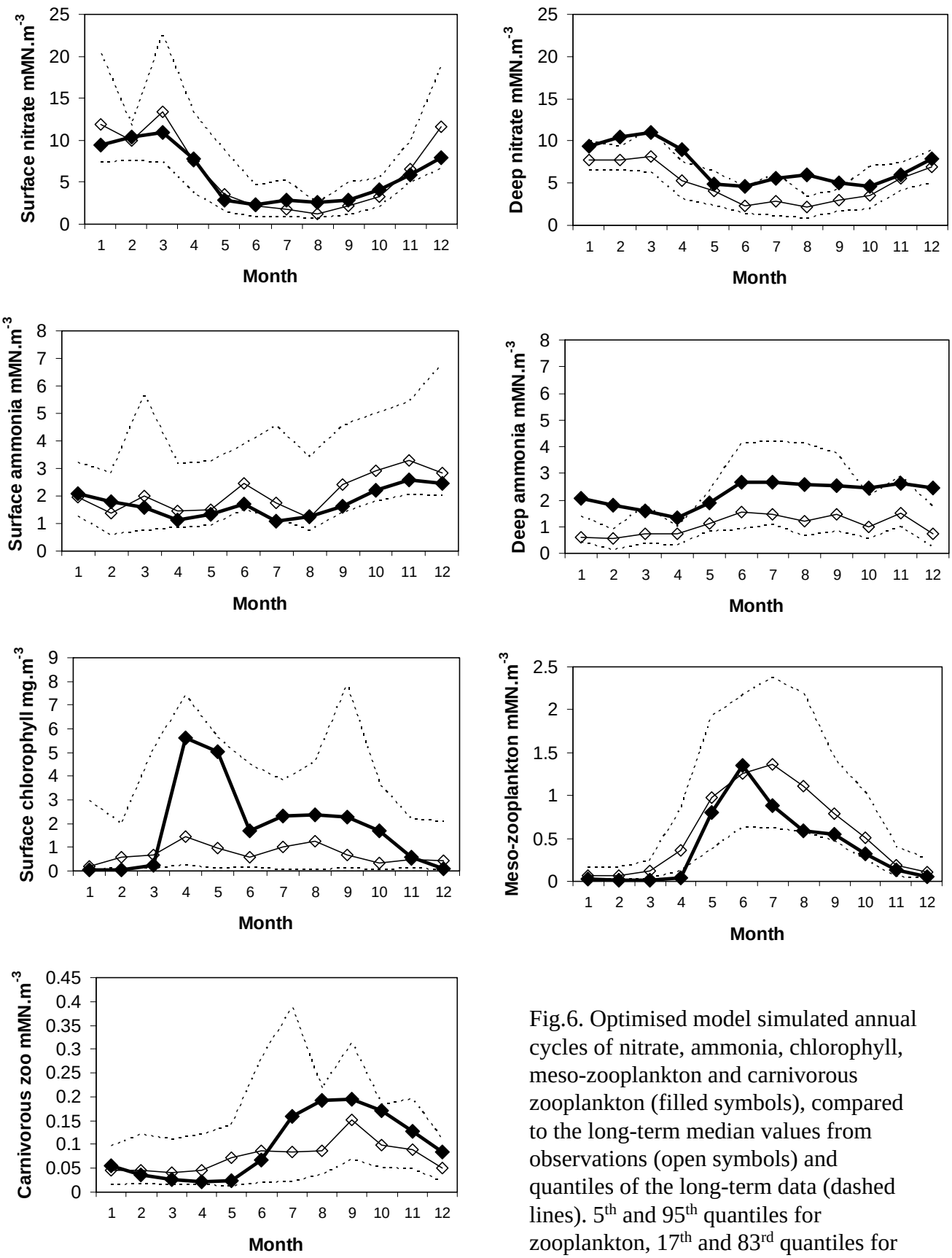

Fig.6. Optimised model simulated annual cycles of nitrate, ammonia, chlorophyll, meso-zooplankton and carnivorous zooplankton (filled symbols), compared to the long-term median values from observations (open symbols) and quantiles of the long-term data (dashed lines). 5th and 95th quantiles for zooplankton, 17th and 83rd quantiles for nitrate and ammonia.

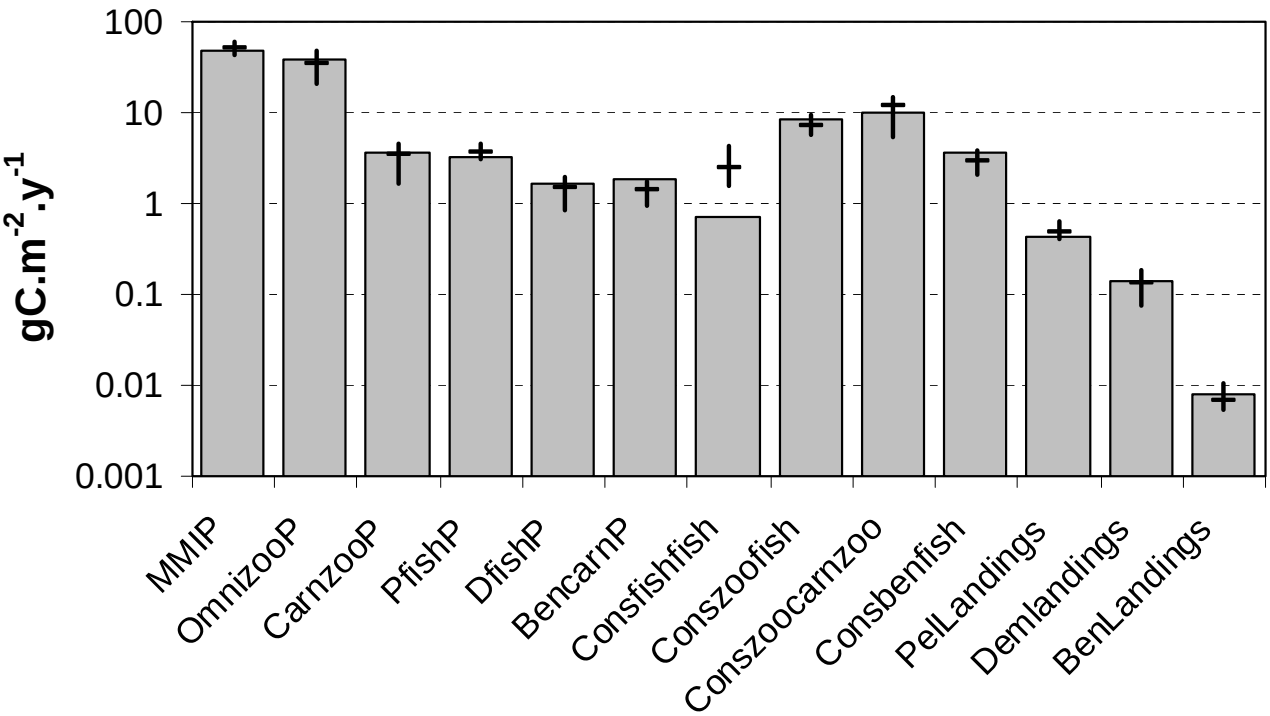

Fig.7. Optimised model simulated values of annual fluxes in the model (vertical bars), compared to values from analyses of observational data (horizontal lines represent median of observational time series, vertical lines represent 5th and 95th quantiles).

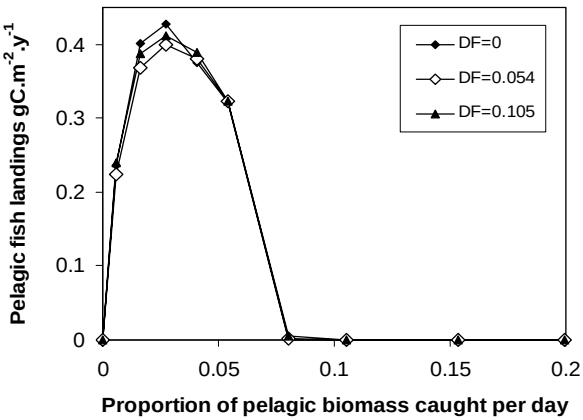

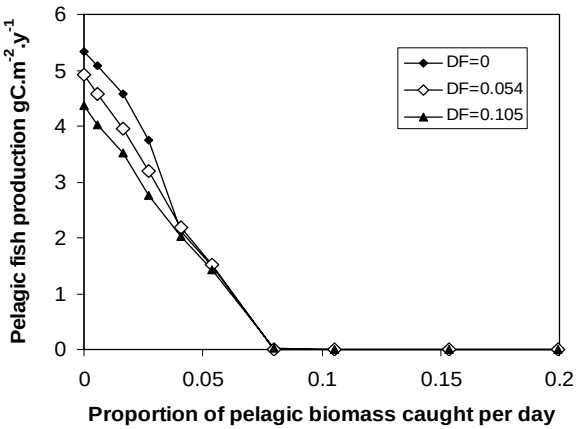

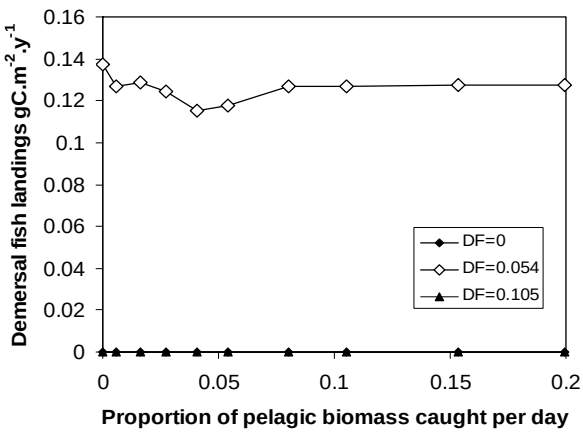

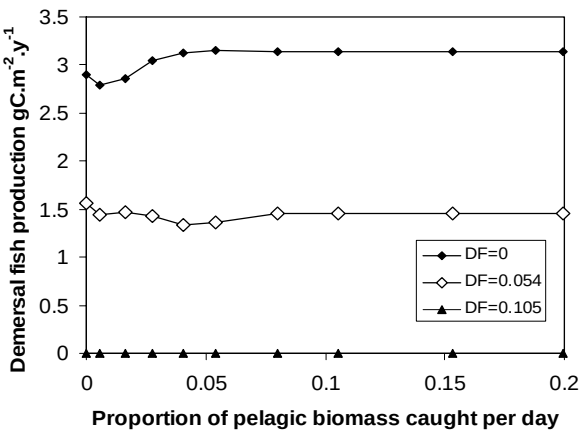

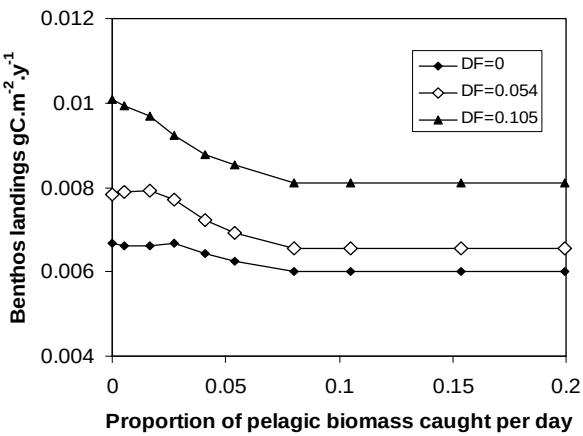

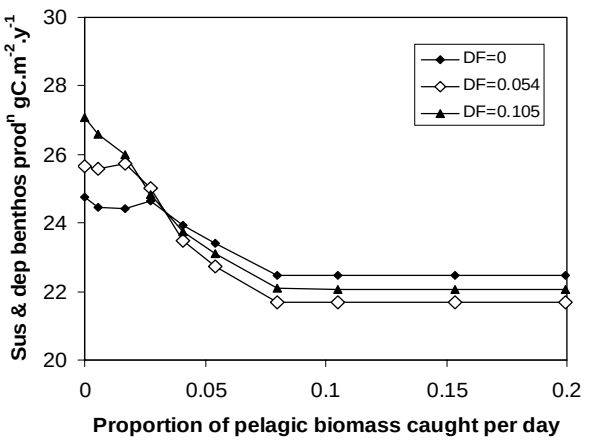

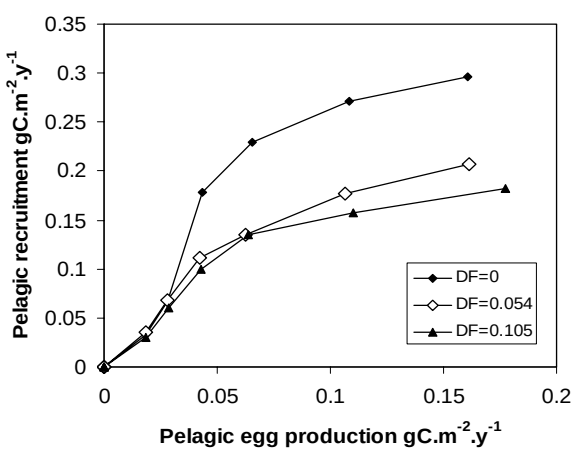

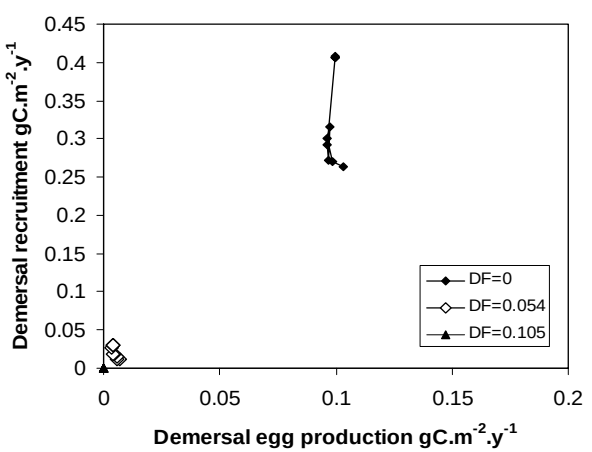

Fig.8a. Optimised model results of varying the pelagic harvesting rate, for three different levels of demersal harvesting. Shellfish harvesting was held at the optimised value and all other driving data at the long-term median.

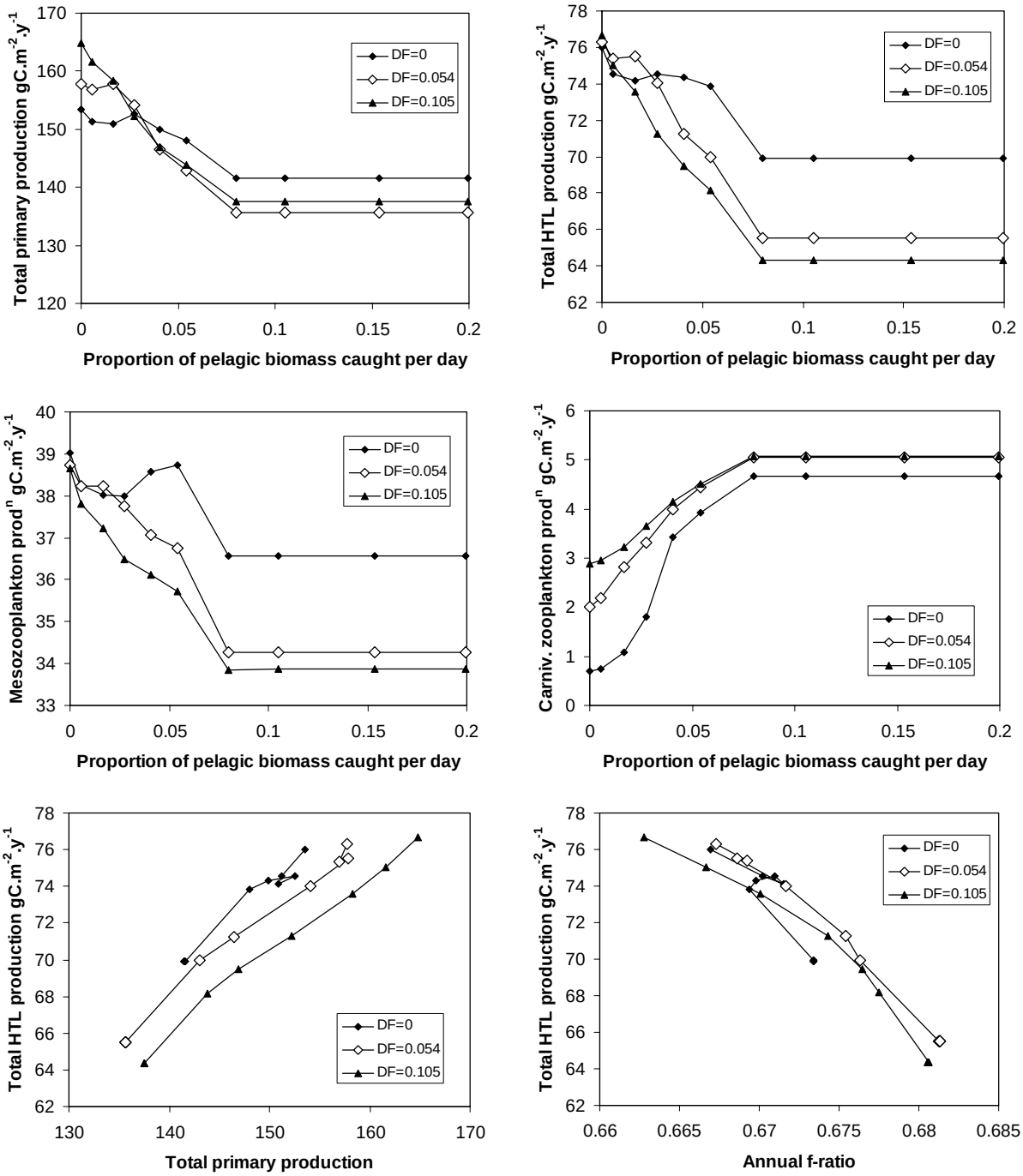

Fig.8b. Optimised model results of varying the pelagic harvesting rate, for three different levels of demersal harvesting. Shellfish harvesting was held at the optimised value and all other driving data at the long-term median.

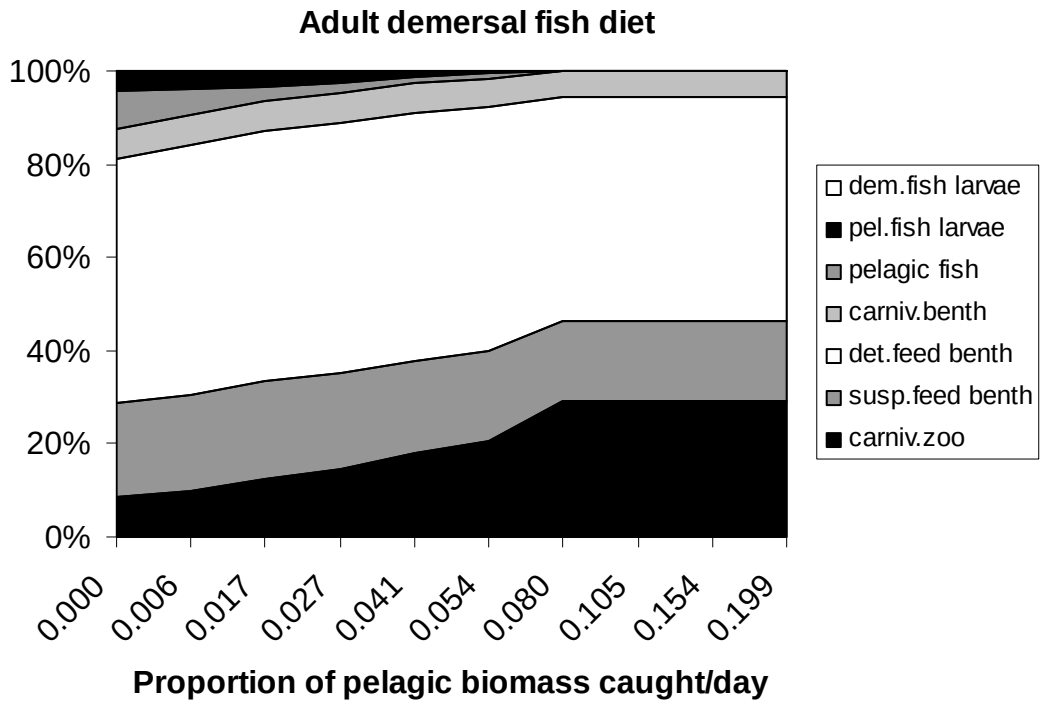

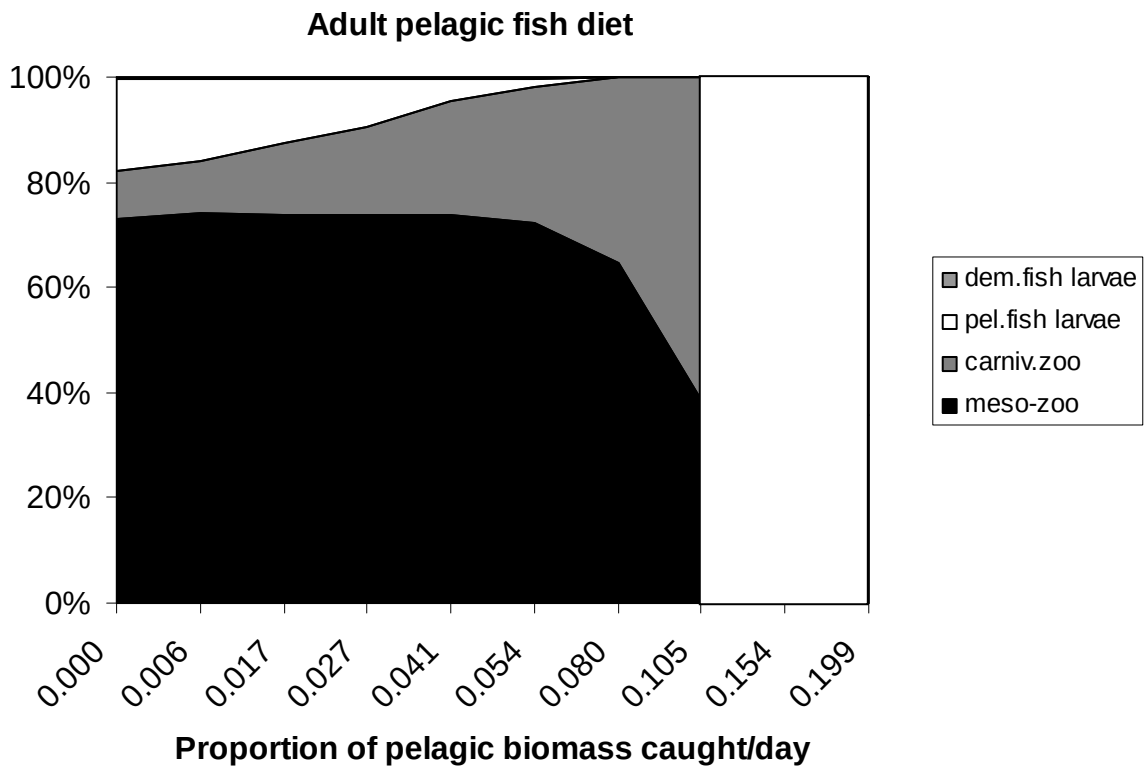

Fig.8c. Simulated proportional by weight of different diet components in the food intake by adult demersal and pelagic fish in the optimised model run with varying pelagic harvesting rate. Demersal and shellfish harvesting rates held at the optimised values. Environment driving according to the long-term median.

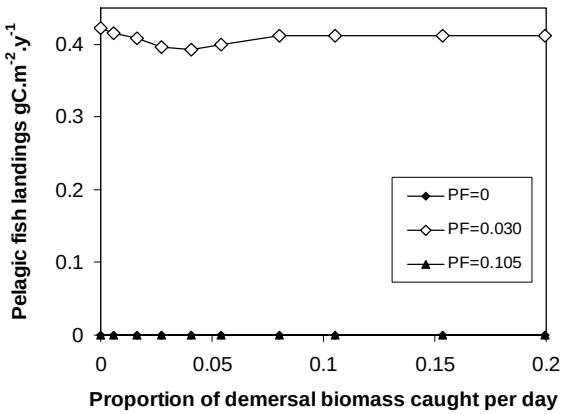

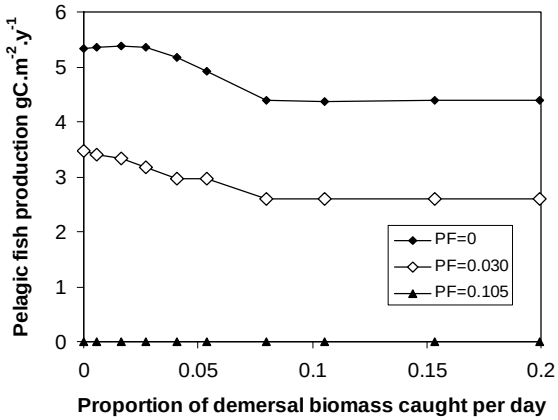

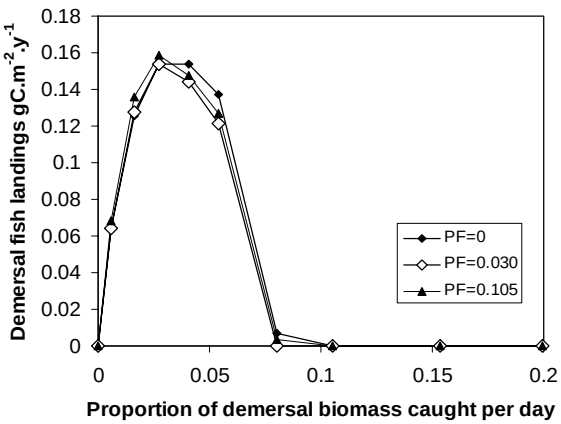

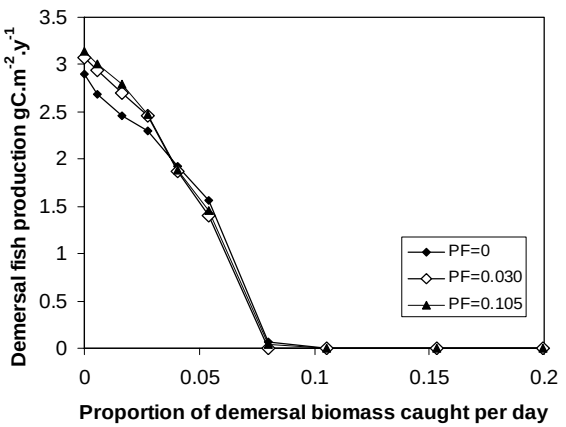

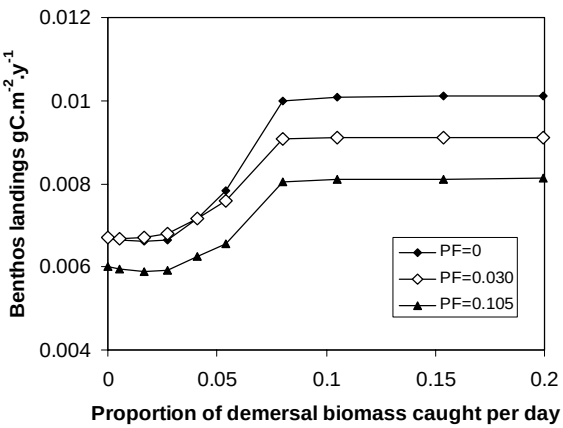

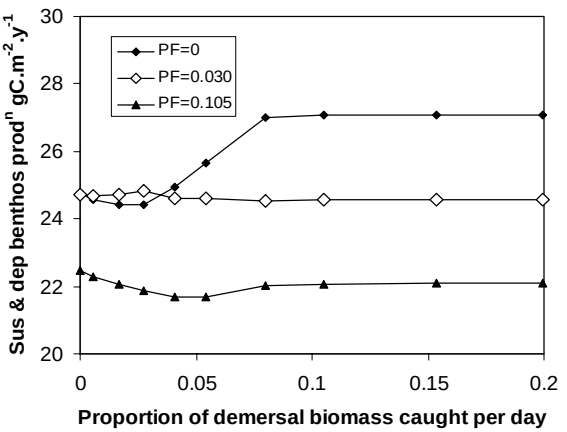

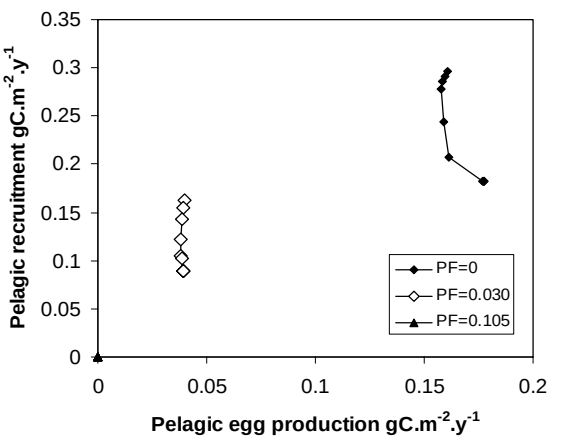

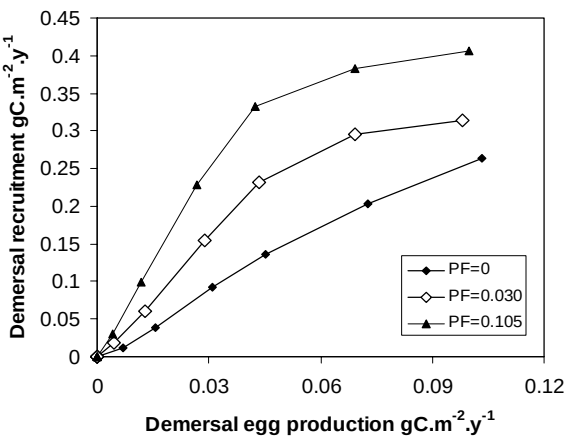

Fig.9a. Optimised model results of varying the demersal harvesting rate, for three different levels of pelagic harvesting. Shellfish harvesting was held at the optimised value and all other driving data at the long-term median.

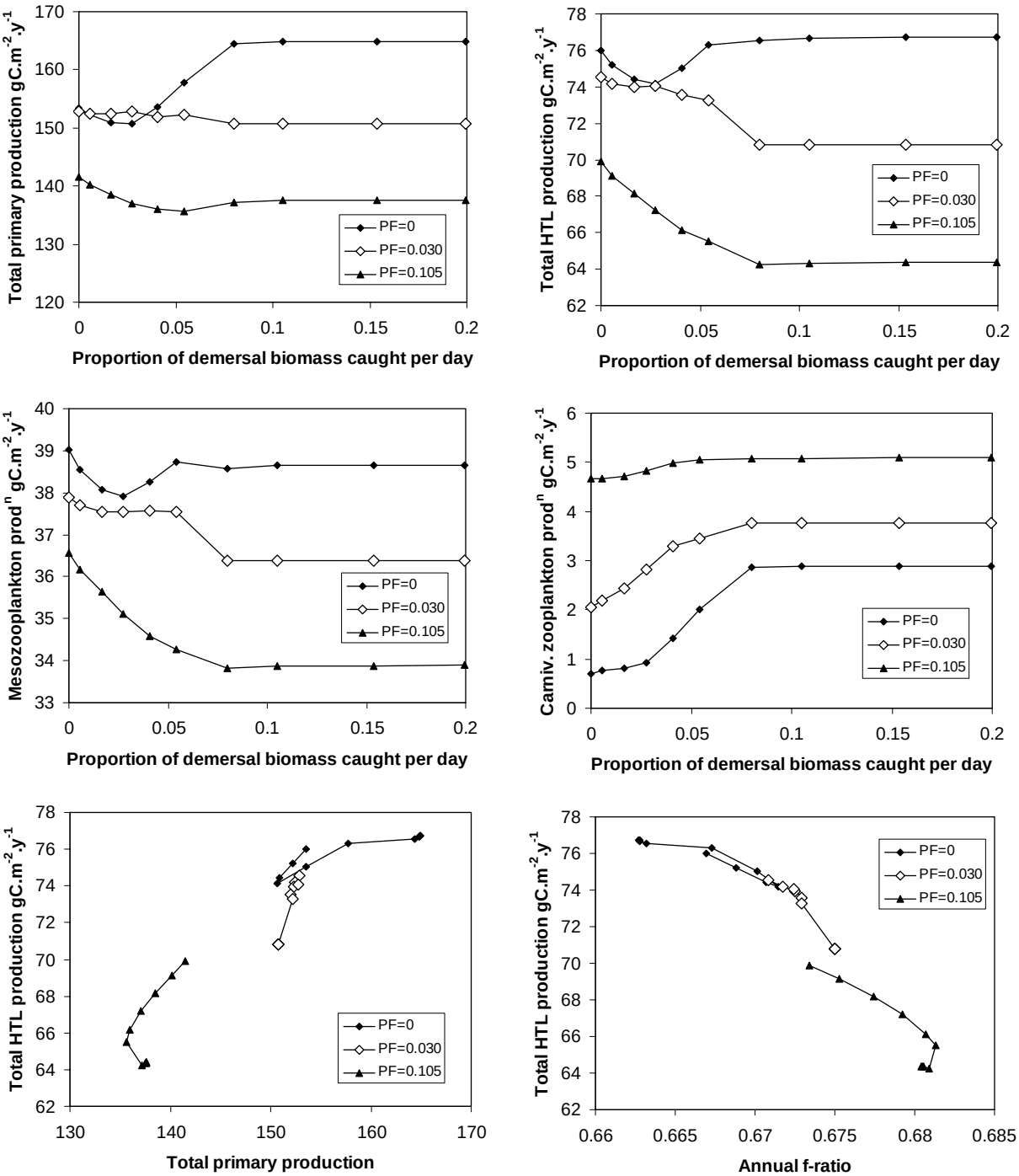

Fig.9b. Optimised model results of varying the demersal harvesting rate, for three different levels of pelagic harvesting. Shellfish harvesting was held at the optimised value and all other driving data at the long-term median.

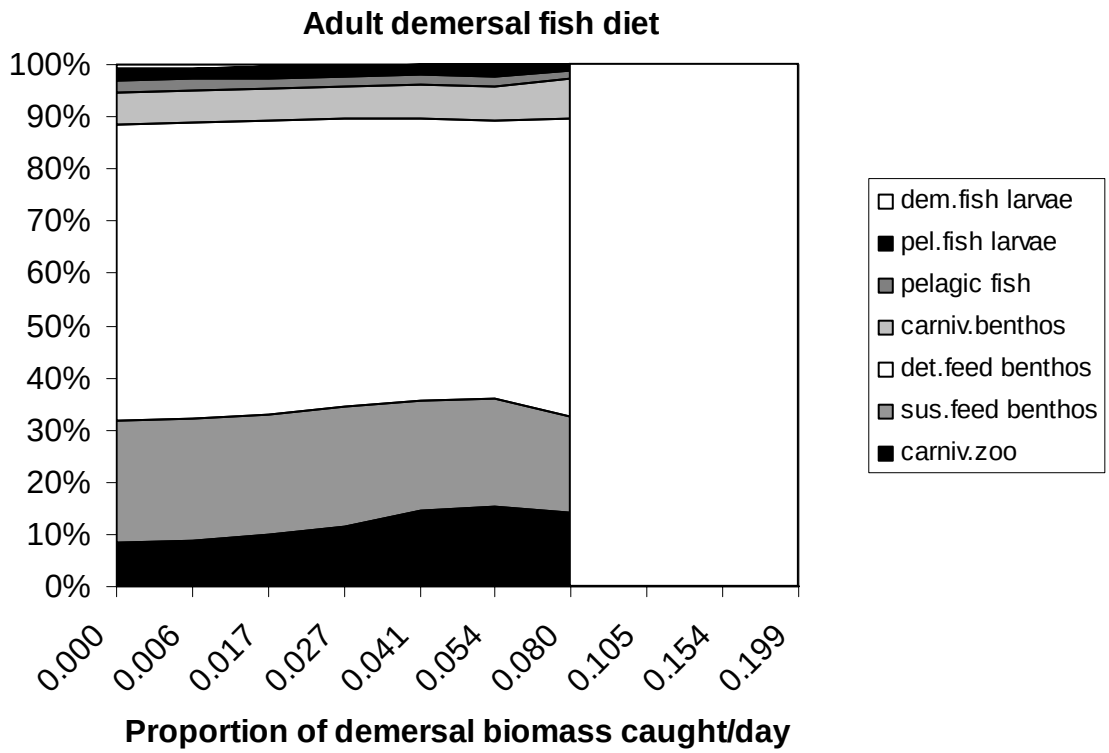

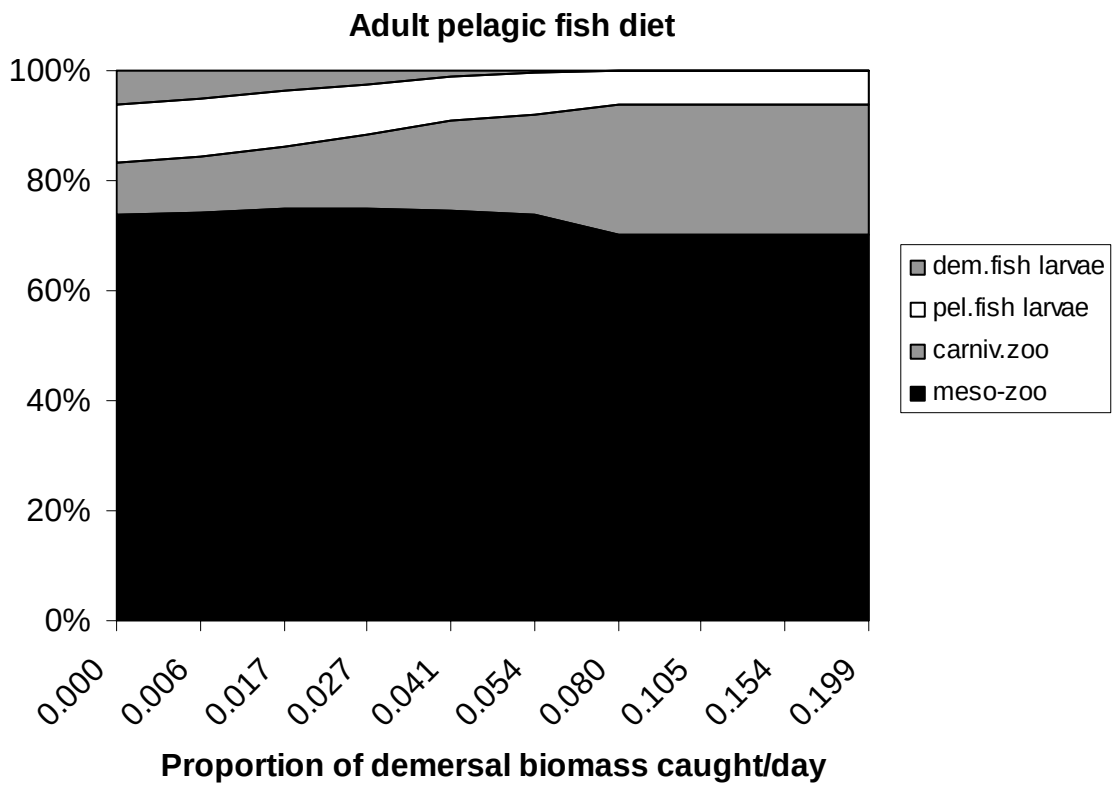

Fig.9c. Simulated proportional by weight of different diet components in the food intake by adult demersal and pelagic fish in the optimised model run with varying demersal harvesting rate. Pelagic and shellfish harvesting rates held at the optimised values. Environment driving according to the long-term median.

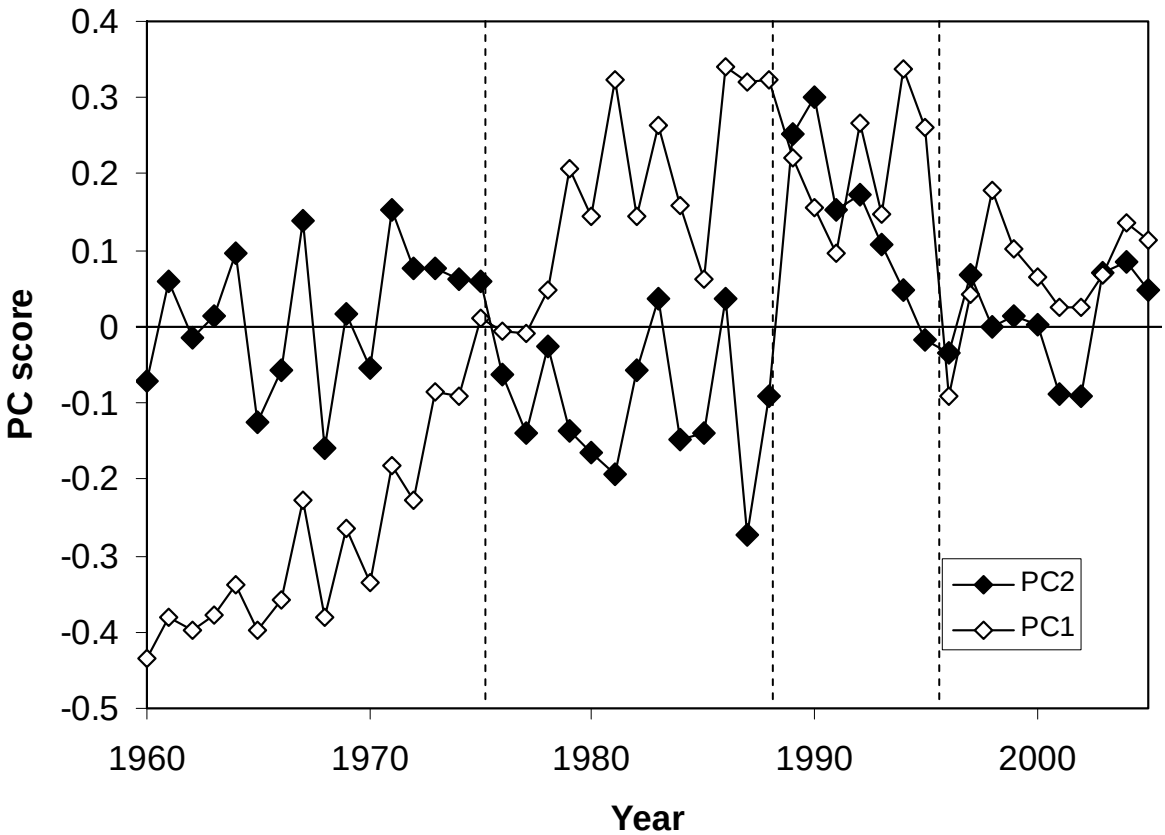

Fig.10. Time series of principal component scores from analysis of inflow, freshwater discharge, temperature and river nutrient concentrations. PC1 was highly correlated with the river nutrient concentrations, PC2 summarised the physical driving data. Vertical dashed lines show the extents of the four regime periods, 1960-1975, 1976-1988, 1989-1995 and 1996-2005.

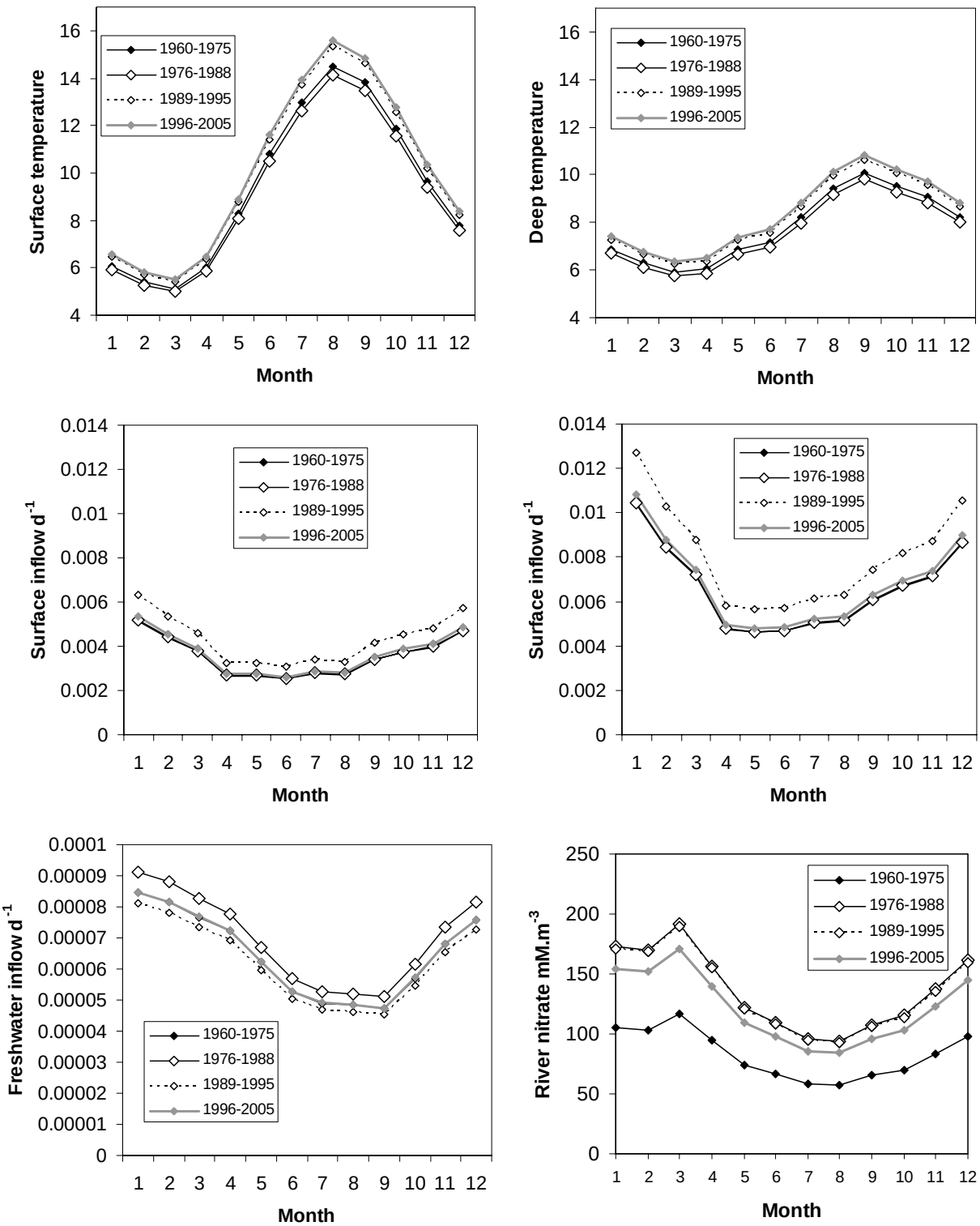

Fig.11. Time series of monthly physical drivers and river nutrient concentrations applied to the model for each of the four regime periods.

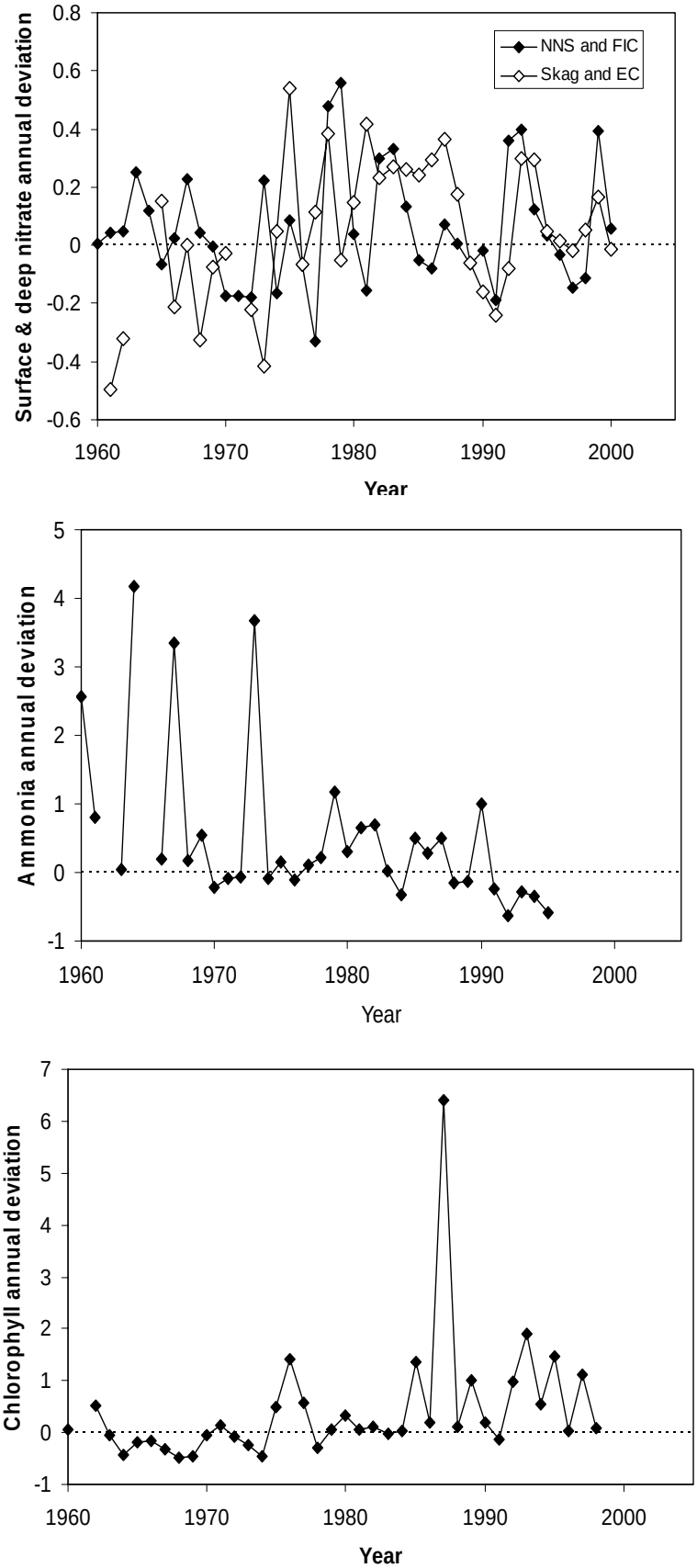

Fig.12. Time series of annual deviations from the long-term mdeian of boundary nitrate ammonia and chlorophyll concentrations from the available observations. Nitrate deviations shown separately for y the northern boundaries and the eastern and southern boundaries.

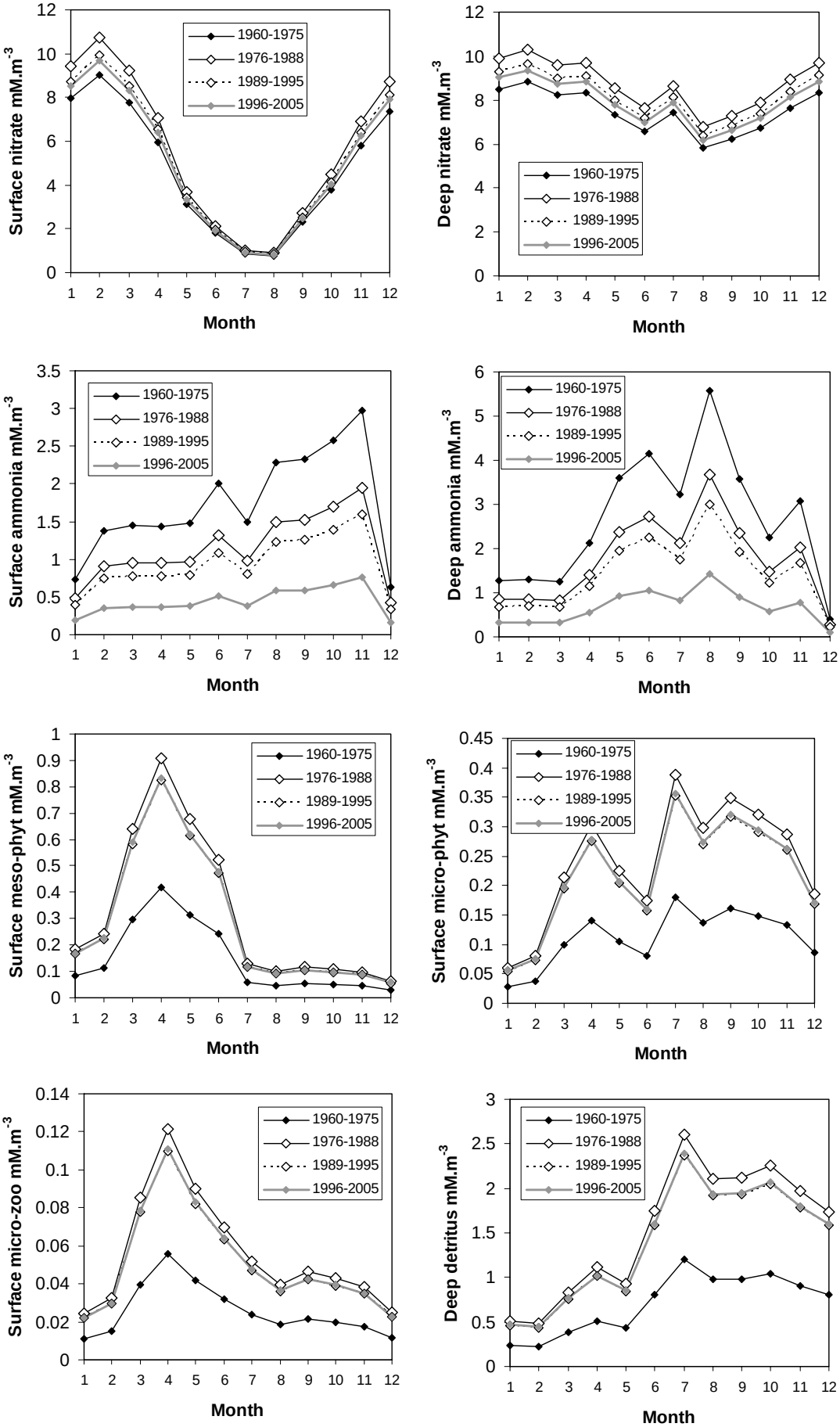

Fig.13. Time series of monthly boundary concentrations applied to the model for each of the four regime periods.

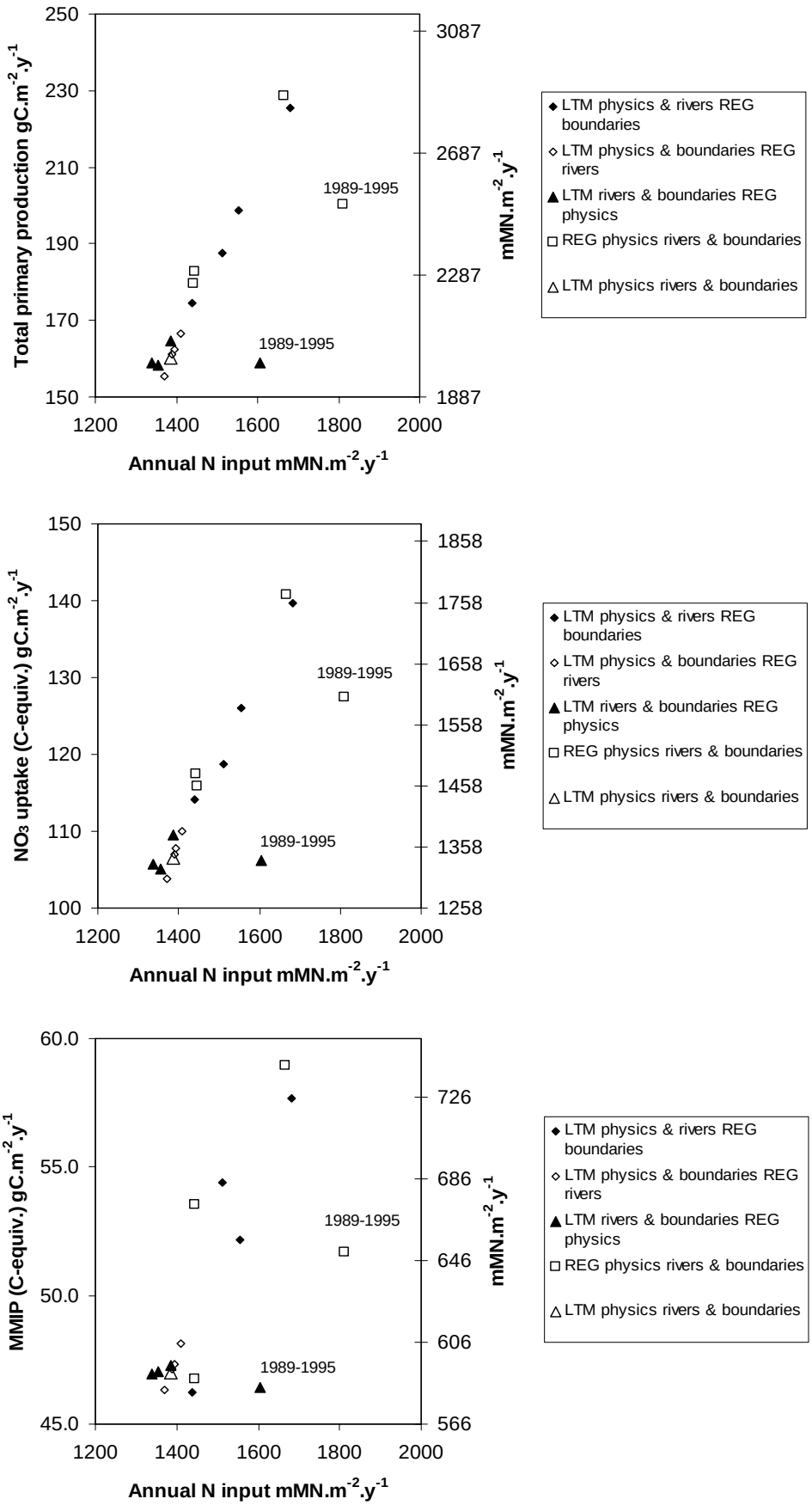

Fig.14. Equilibrium annual nitrogen influx to the model for each of the four regime periods, with different combinations of long-term median (LTM) and regime specific (REG) boundary and physical driving data, compared to simulated measures of total and new primary production. Long-term median optimised fish harvesting rates were applied in each case.

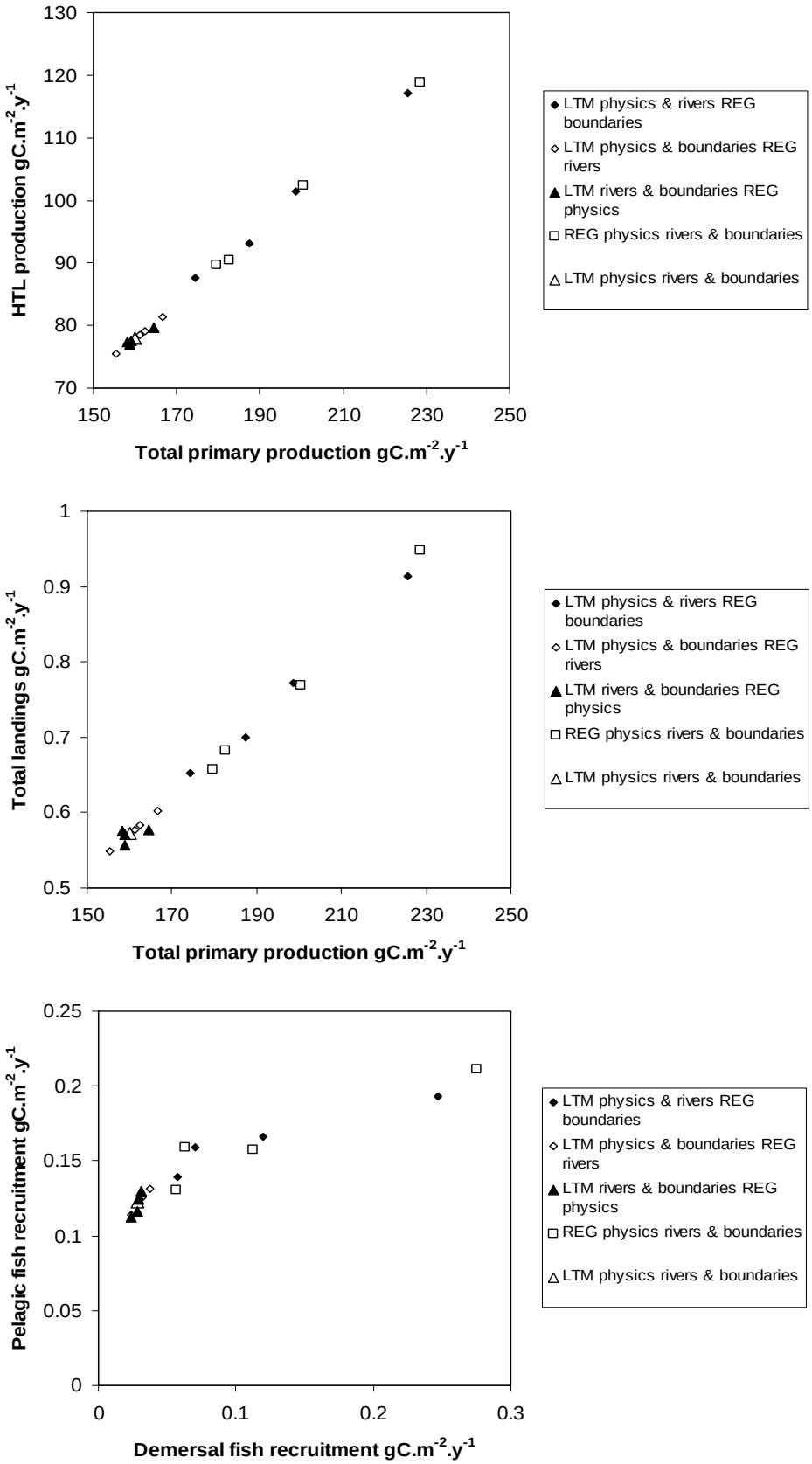

Fig.15. Equilibrium total annual primary production for each of the four regime periods, with different combinations of long-term median (LTM) and regime specific (REG) boundary and physical driving data, compared to simulated higher trophic level production (zooplankton, benthos fish and birds/mammals combined) (upper two panels). Lower panel, simulated demersal fish recruitment compared to pelagic fish recruitment for the same combinations of driving conditions. Long-term median optimised fish harvesting rates were applied in each case.

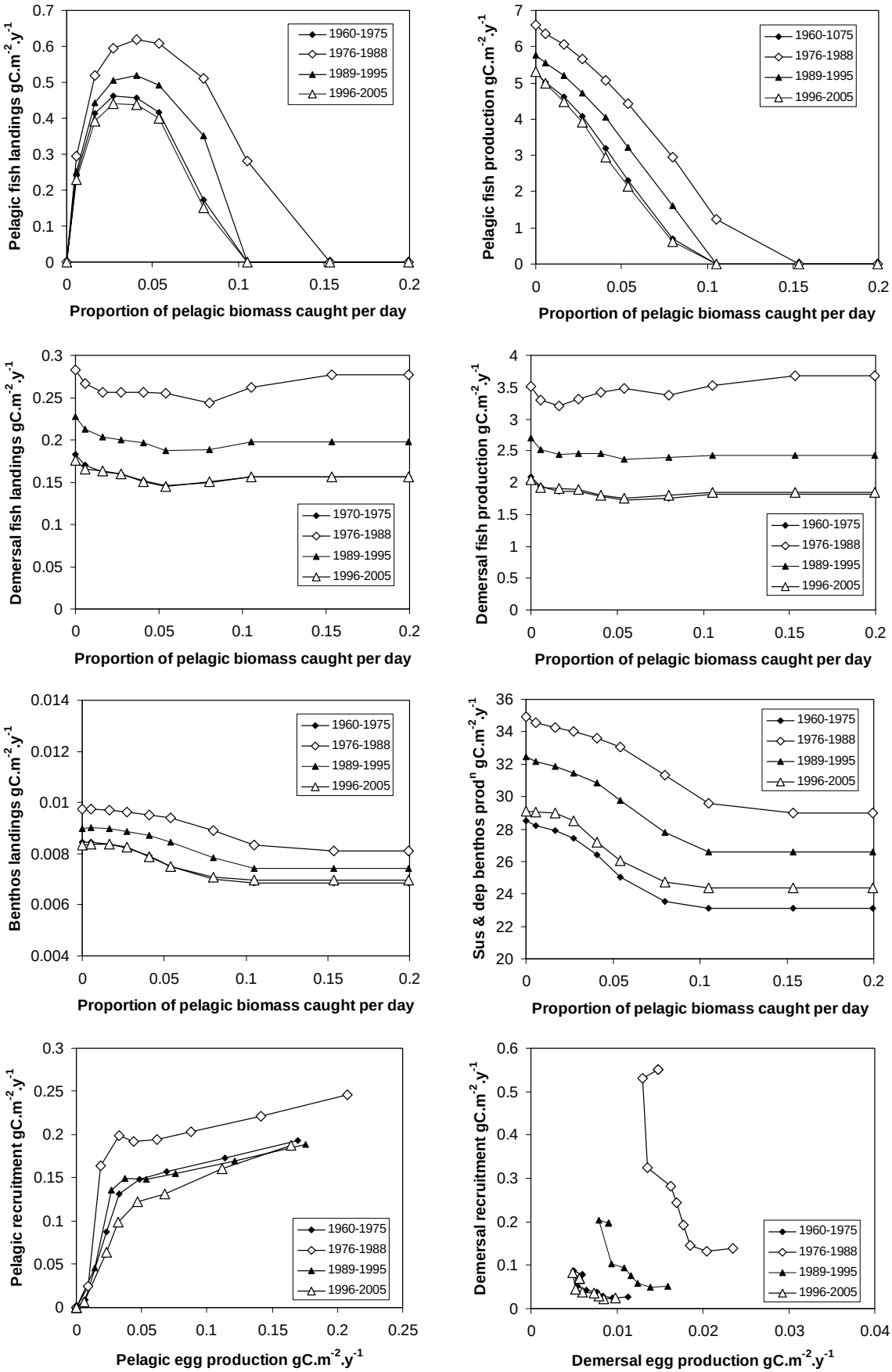

Fig.16a. Equilibrium results of varying the pelagic harvesting rate, for each of the four driving and boundary concentration regimes. Demersal and shellfish harvesting rates were held at the long-term median optimised value.

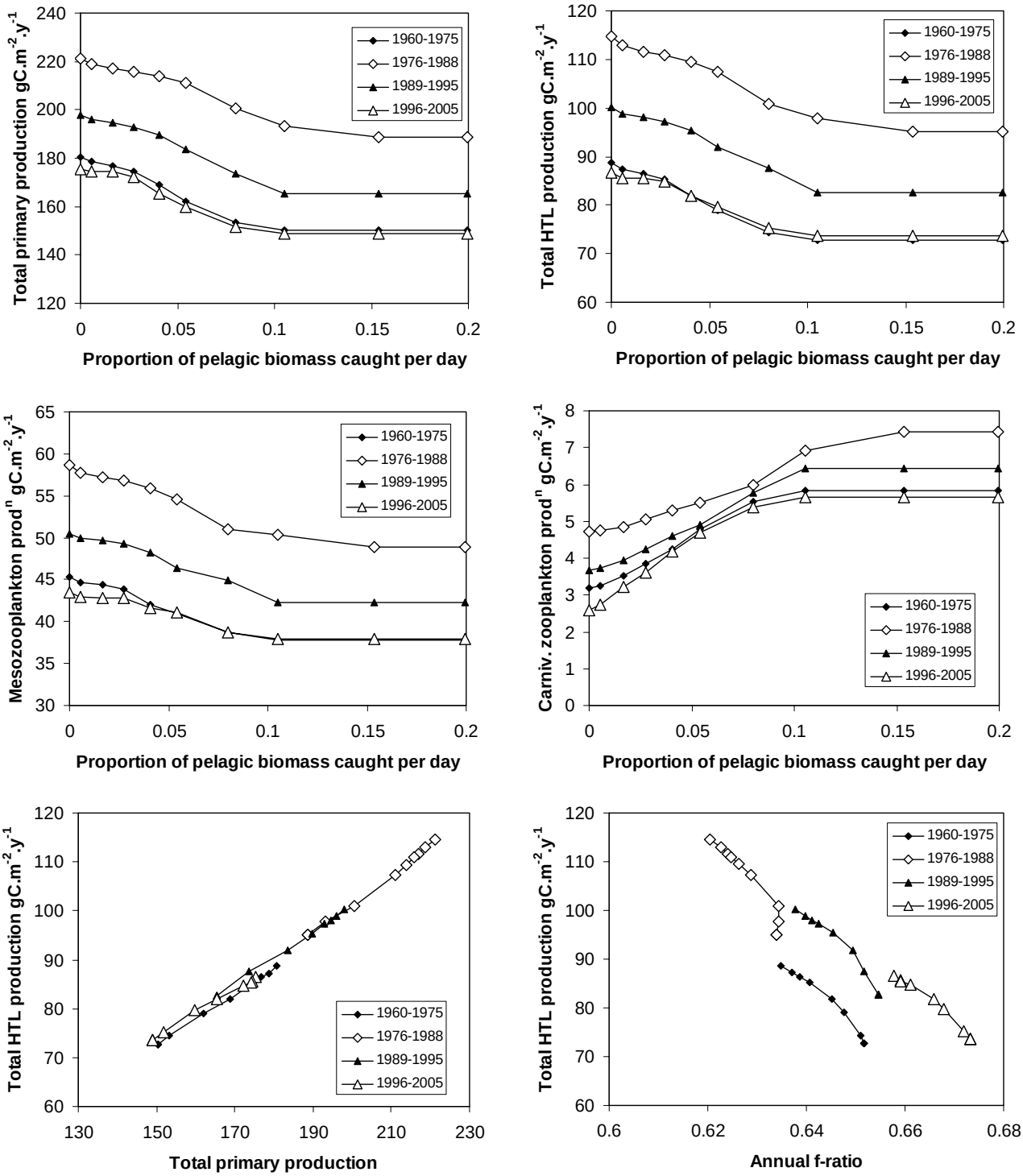

Fig.16b. Equilibrium results of varying the pelagic harvesting rate, for each of the four driving and boundary concentration regimes. Demersal and shellfish harvesting rates were held at the long-term median optimised value.

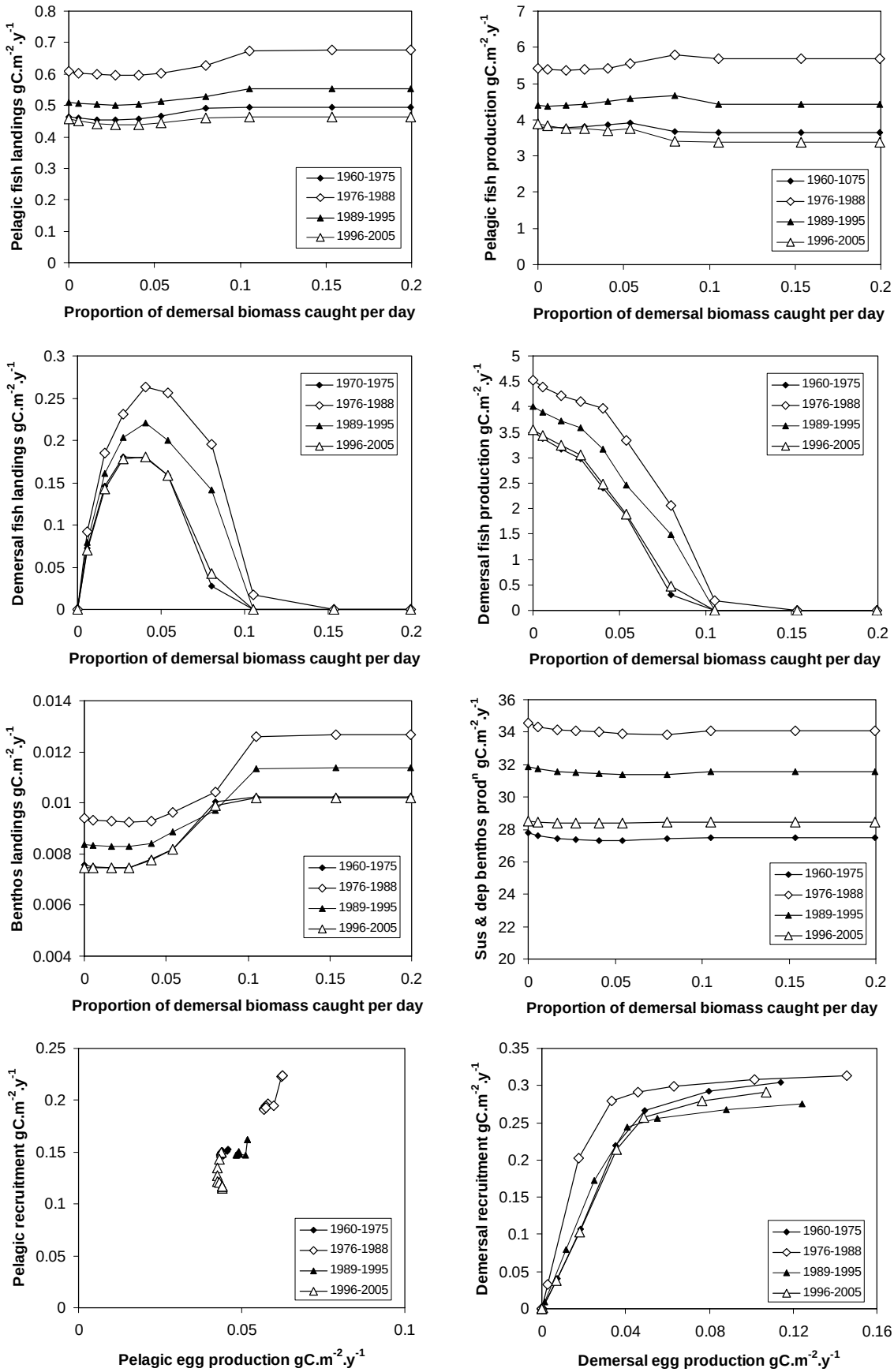

Fig.17a. Equilibrium results of varying the demersal harvesting rate, for each of the four driving and boundary concentration regimes. Pelagic and shellfish harvesting rates were held at the long-term median optimised value.

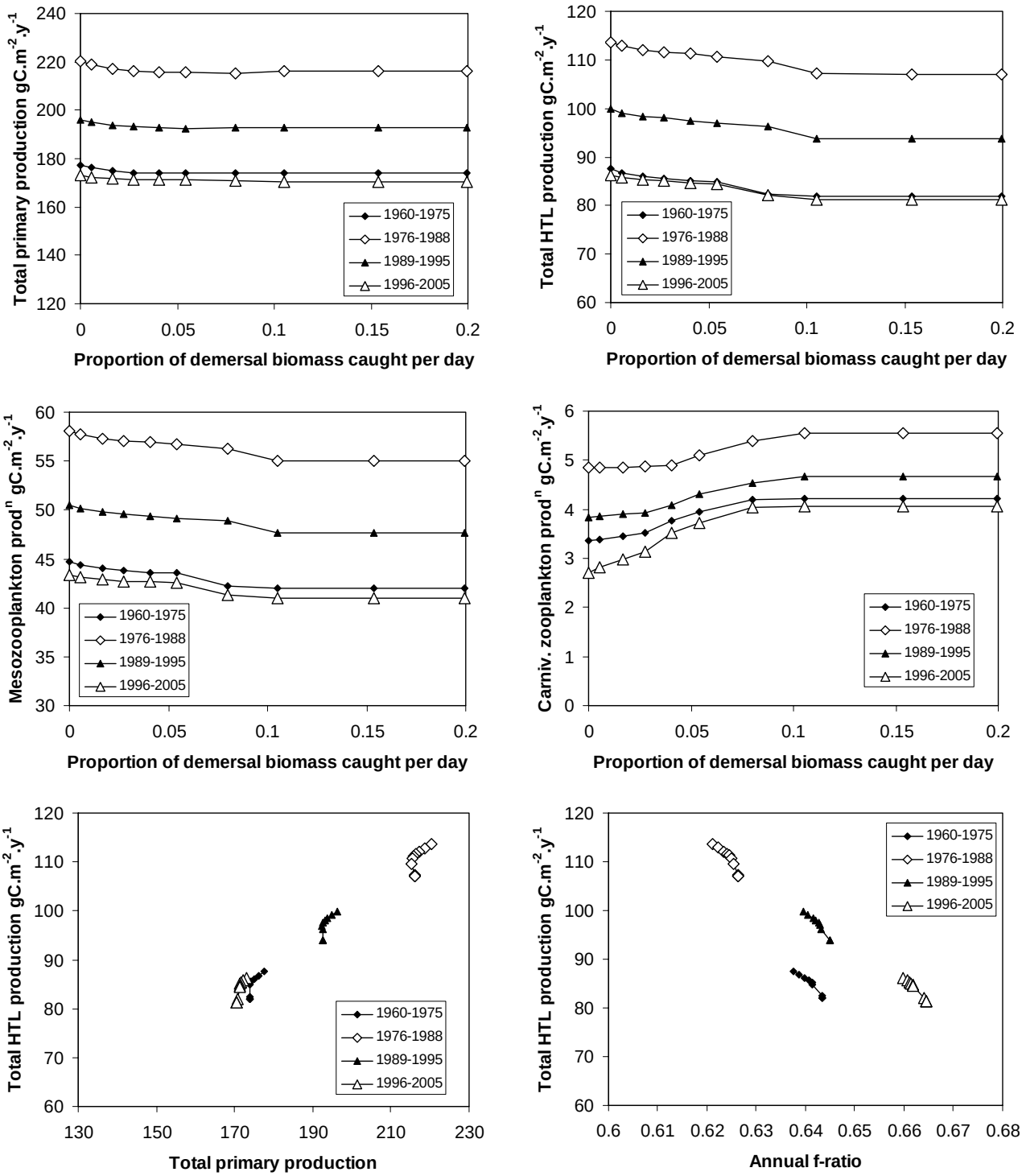

Fig.17b. Equilibrium results of varying the demersal harvesting rate, for each of the four driving and boundary concentration regimes. Pelagic and shellfish harvesting rates were held at the long-term median optimised value.

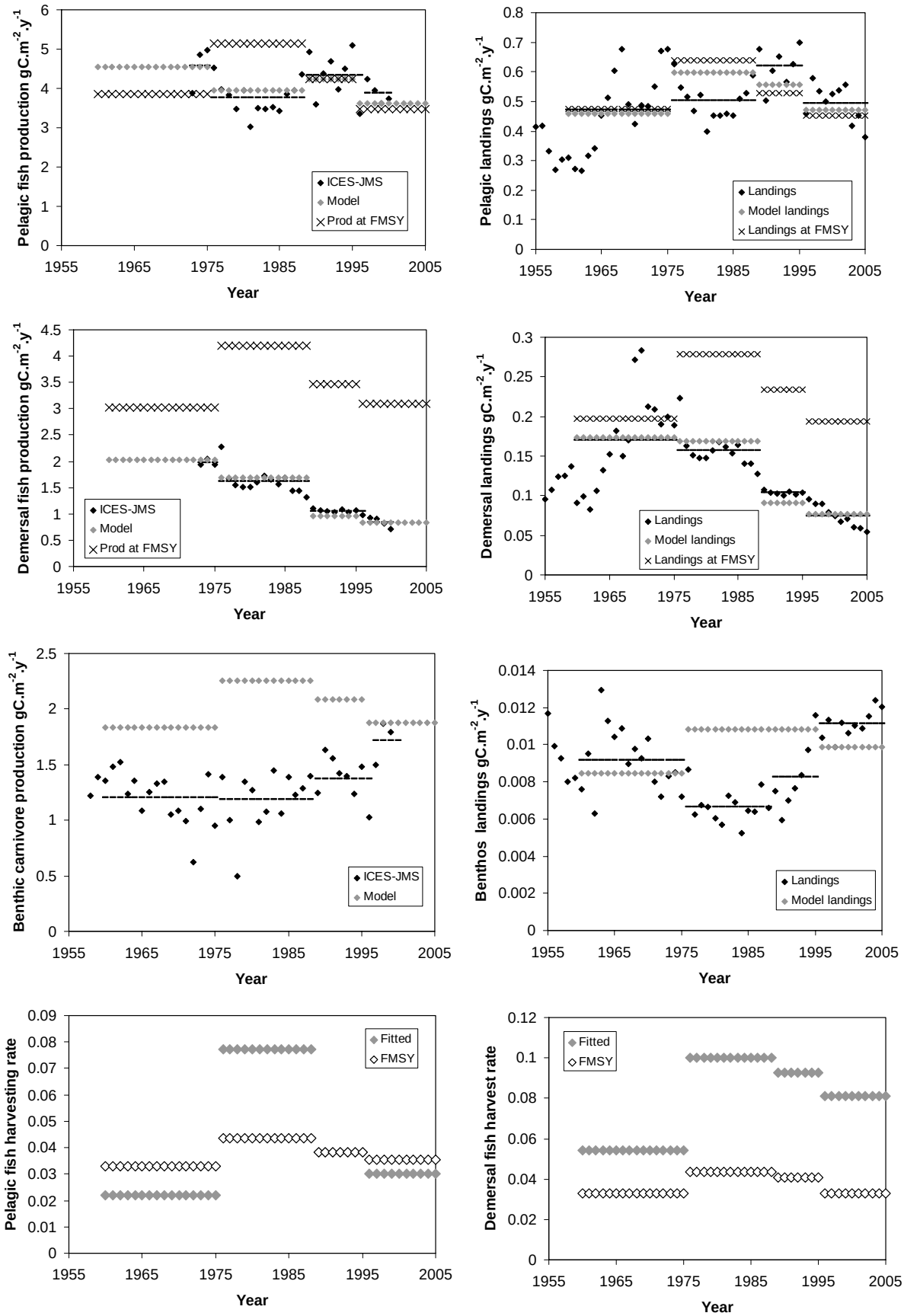

Fig.18. Top row: annual and regime averaged observed, equilibrium model maximum sustainable, and equilibrium model fitted to observations of pelagic fish production and landings. Fitted parameters were pelagic and demersal fish harvesting rates only. Second row, same for demersal fish. Third row, same for benthos. Bottom row, fitted harvesting rates and harvesting rates at maximum sustainable yield for each of the regime periods.

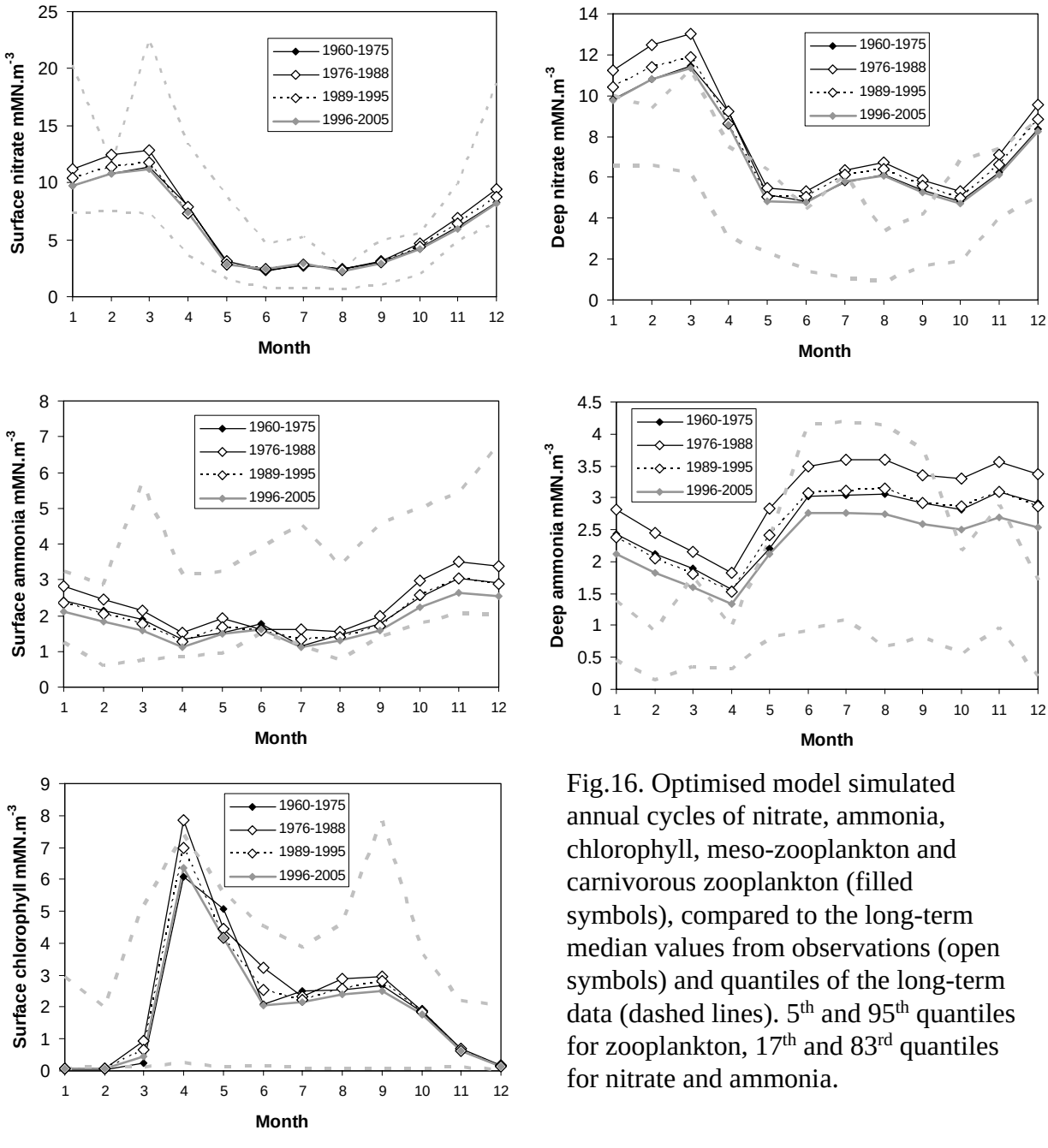

Fig.16. Optimised model simulated annual cycles of nitrate, ammonia, chlorophyll, meso-zooplankton and carnivorous zooplankton (filled symbols), compared to the long-term median values from observations (open symbols) and quantiles of the long-term data (dashed lines). 5th and 95th quantiles for zooplankton, 17th and 83rd quantiles for nitrate and ammonia.

Fig.19. Equilibrium model monthly average nitrate, ammonia and chlorophyll concentrations for each of the four regime periods, compared to quantiles of observed data over the period 1960-2000. 17th and 83rd quantiles for nitrate and ammonia, 5th and 95th quantiles for chlorophyll. Model results with the fitted fish harvesting rates for each regime as shown in Fig. 18.

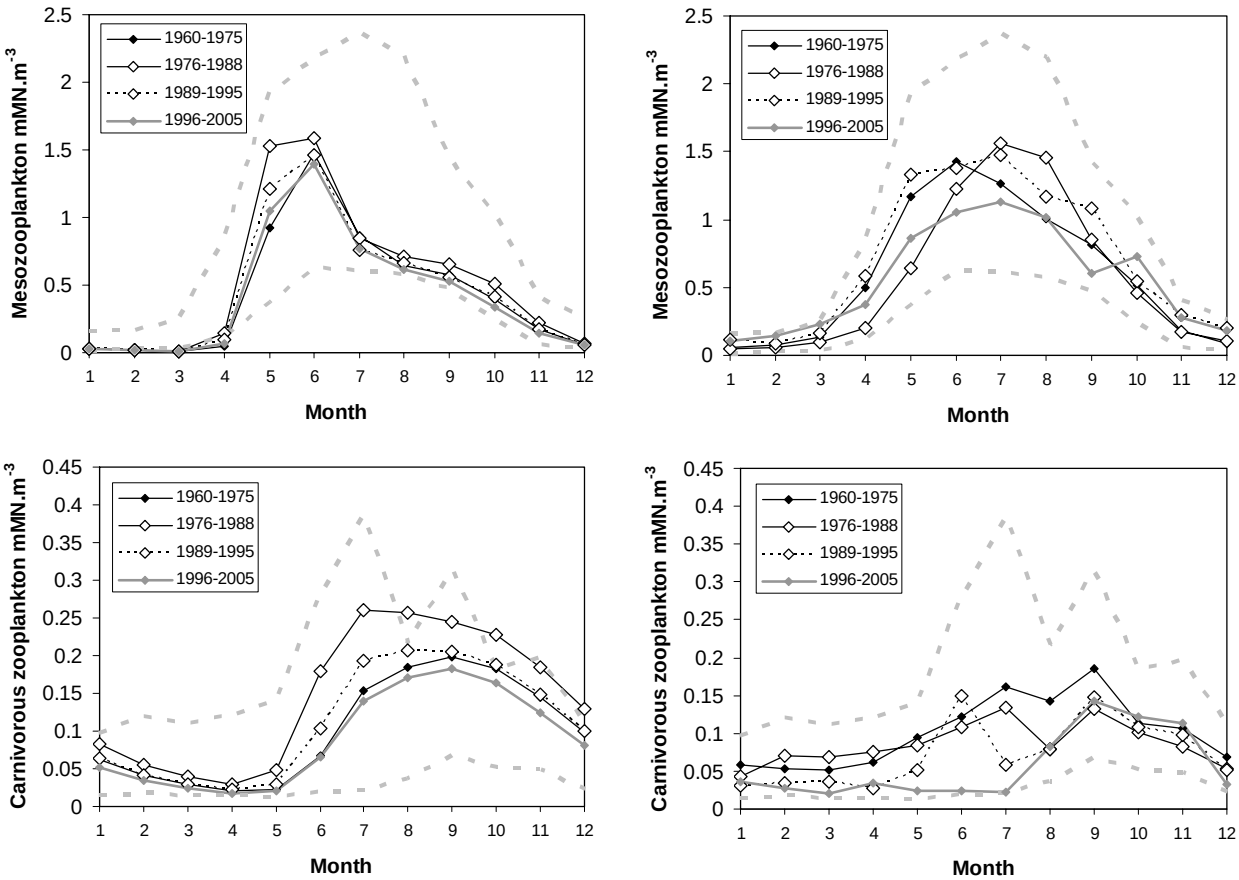

Fig.20. Left column: equilibrium model monthly average meso- and carnivorous zooplankton concentrations for each of the four regime periods, compared to 5th and 95th quantiles of observed data from CPR surveys over the period 1960-2000 (dashed grey lines). Left column: regime period averaged CPR data compared to 5th and 95th quantiles of the same data over the period 1960-2000. Model results with the fitted fish harvesting rates for each regime as shown in Fig. 18.

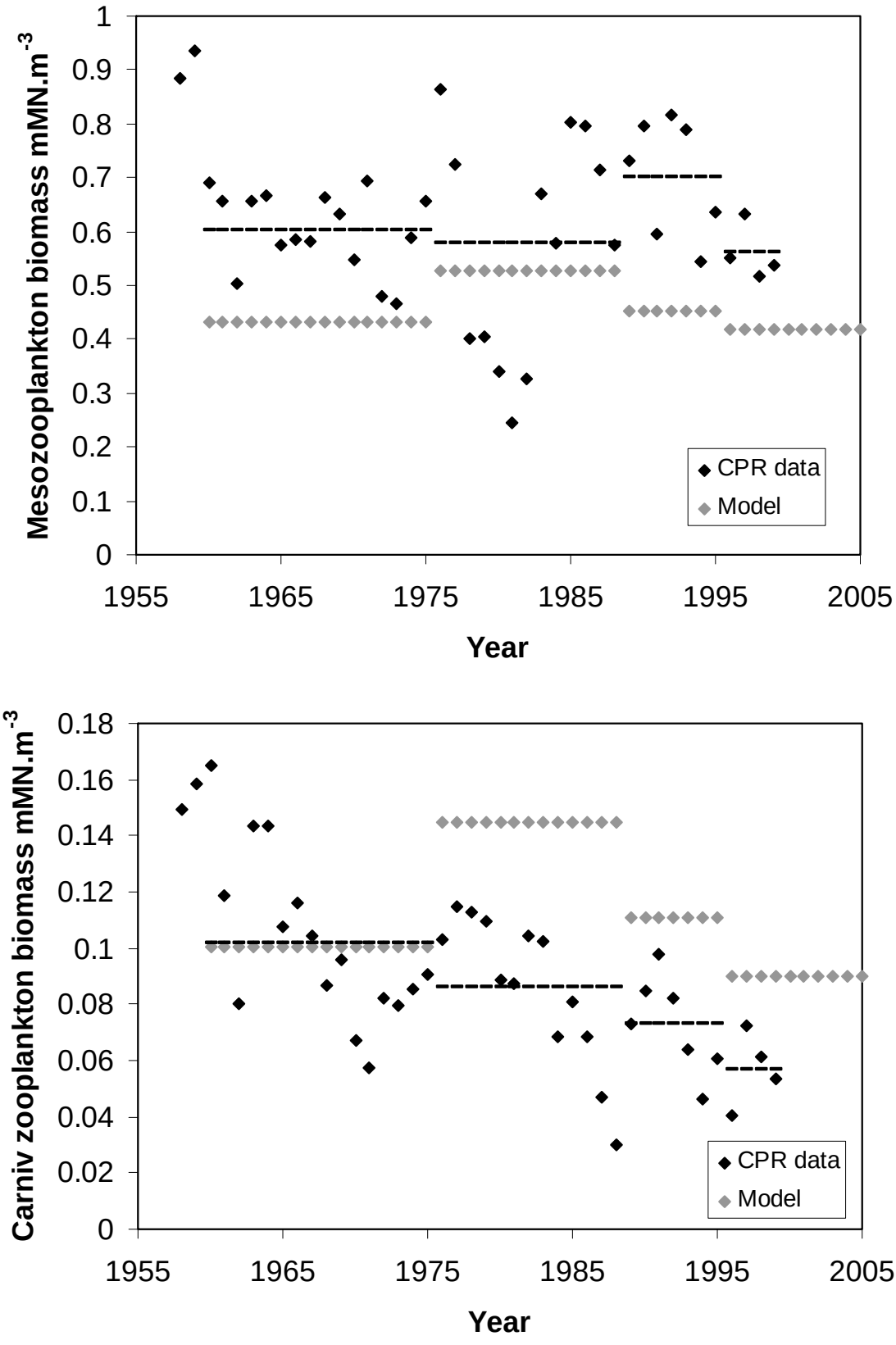

Fig.21. Equilibrium model annual average biomass of meso-zooplankton and carnivorous zooplankton for each of the four regime periods, compared to annual and regime averged biomass derived from Continuous Plankton Recorder (CPR) data. Model results with the fitted fish harvesting rates for each regime as shown in Fig. 18.

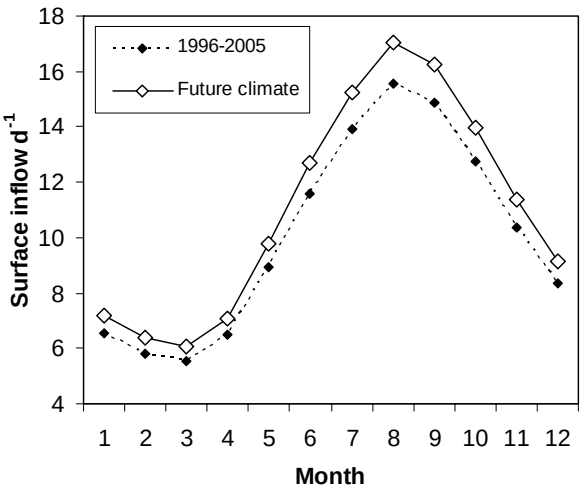

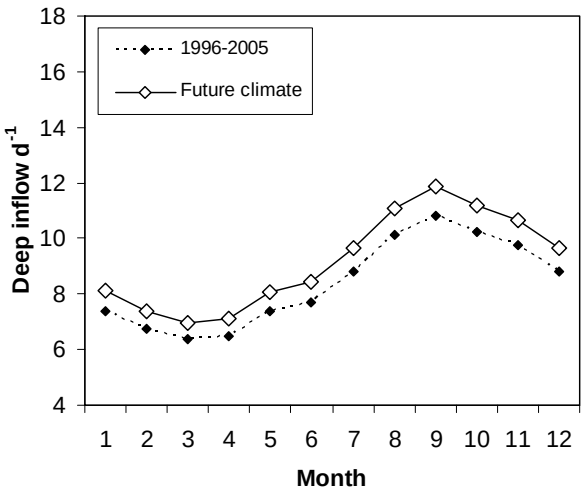

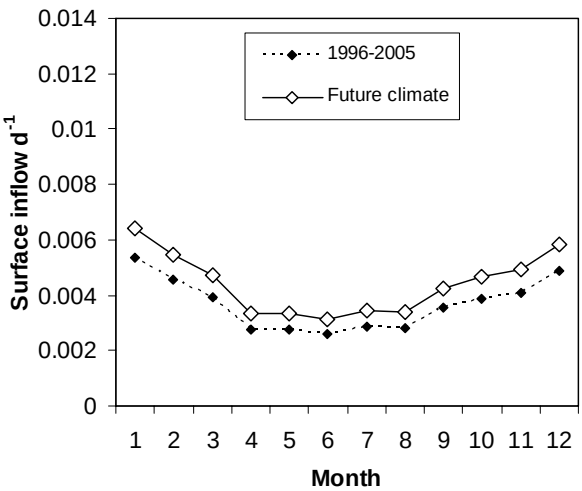

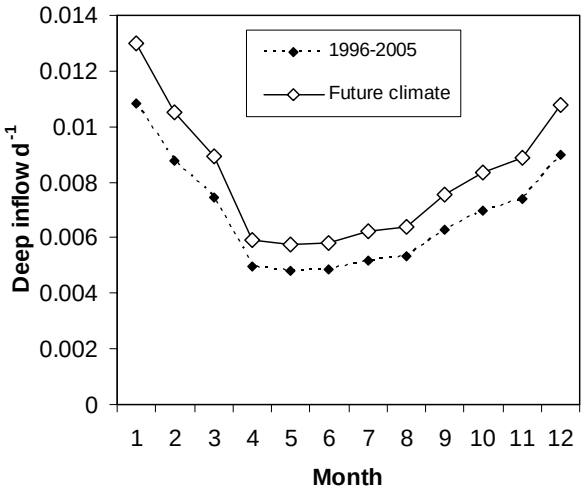

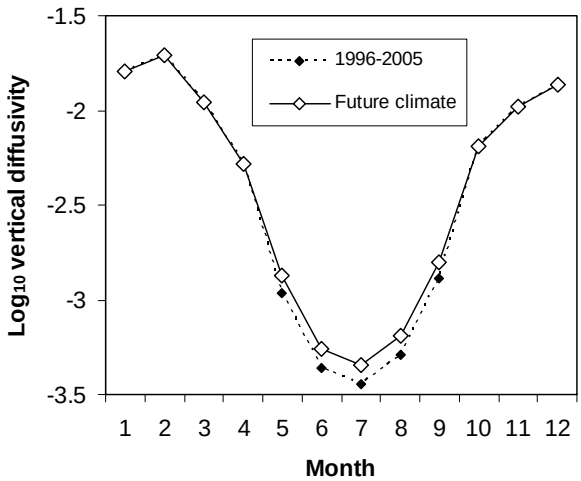

Fig.22. Monthly average values of driving data for the 1996-2005 regime, compared to the equivalent driving data for the simulated future climate conditions

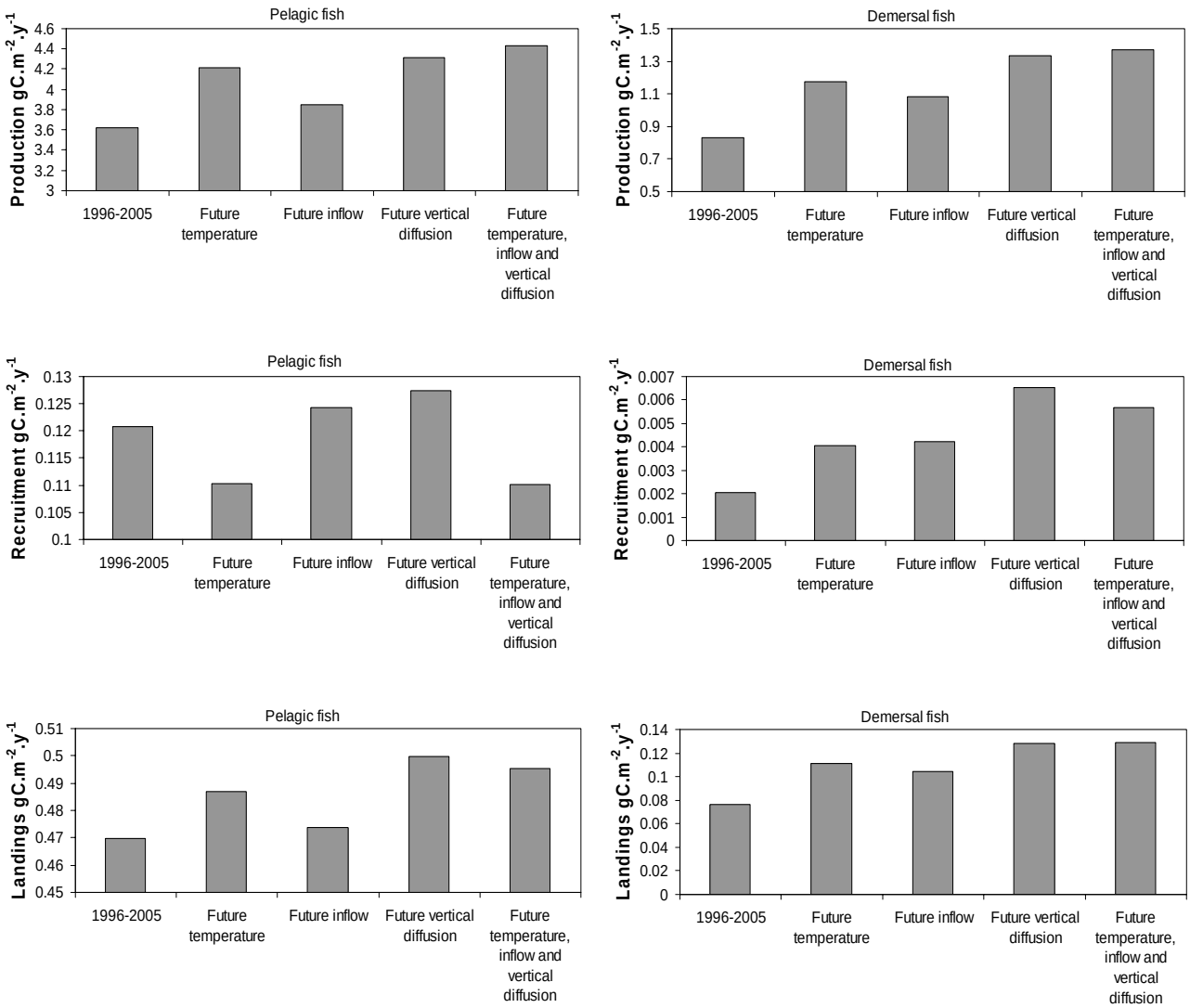

Fig.23a. Equilibrium model results for pelagic and demersal fish production, recruitment and landings, with 1996-2005 regime driving data, and with each aspect of future climate driving conditions in turn.

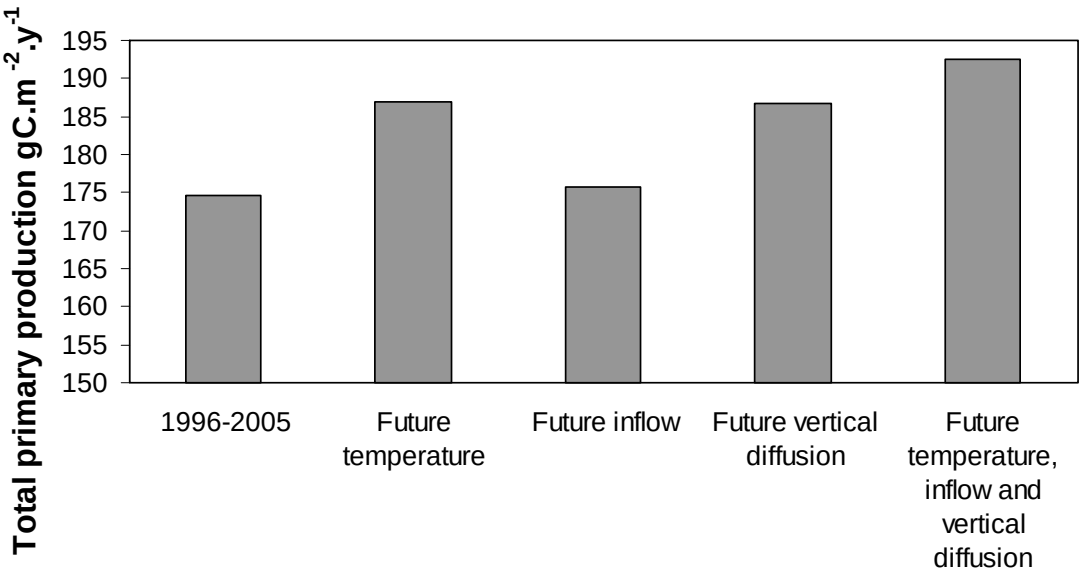

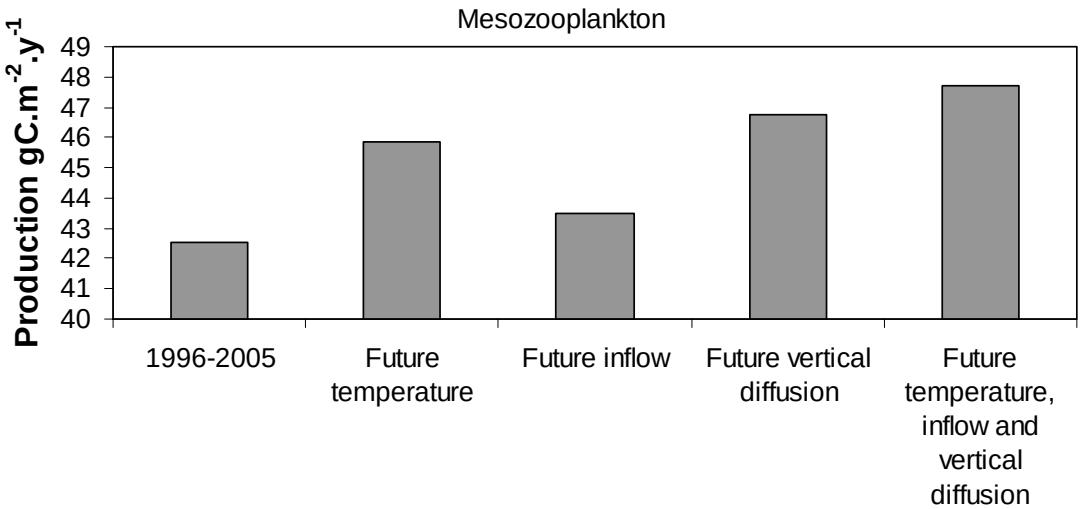

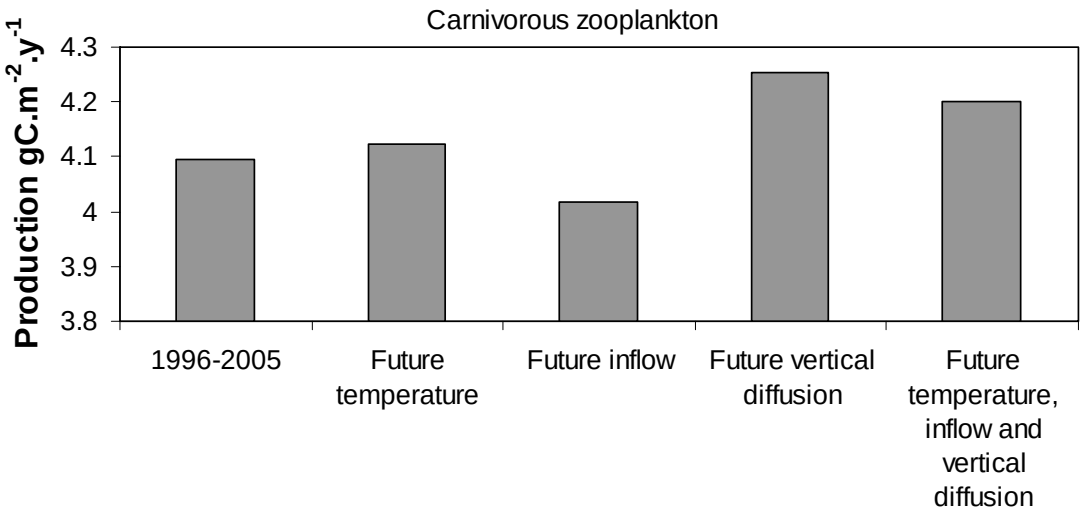

Fig.23b. Equilibrium model results for primary and zooplankton production with 1996-2005 regime driving data, and with each aspect of future climate driving conditions in turn.